2011-04-15

A Multifaceted Sedimentological Analysis on Hobble Creek

Andrew S. Dutson
Brigham Young University - Provo

A Multi-faceted Sedimentological Analysis on Hobble Creek

Andrew S. Dutson

A thesis submitted to the faculty of
Brigham Young University
in partial fulfillment of the requirements for the degree of

Master of Science

Rollin H. Hotchkiss, Chair
Russell B. Rader
Alan K. Zundel
E. James Nelson

Department of Civil and Environmental Engineering

Brigham Young University

August 2011

ABSTRACT

A Multi-faceted Sedimentological
Analysis on Hobble Creek

Andrew S. Dutson
Department of Civil and Environmental Engineering
Master of Science

Due to the endangerment of the June sucker (*Chasmistes liorus*), the lower two miles of Hobble Creek, Utah has been the focus of several restoration efforts. The portion of the creek between Interstate 15 and Utah Lake has been moved into a more "natural" channel and efforts are now being made to expand restoration to the east side of the freeway. This thesis reports on three different parts of a sedimentological analysis performed on Hobble Creek. The first part is a data set that contains information about the particle size distribution on the bed of Hobble Creek between 400 W and Interstate 15 in Springville, Utah. Particle size distributions were obtained for eleven sub-reaches within the study section. Particle size parameters such as D_{50} were observed to decrease from an average of 72 mm to 24 mm downstream from the 1650 W crossing and Packard Dam. Streambed armoring was observed along most of the reach. This data set can be used as input for PHABSIM software to determine the location and availability of existing spawning material for June sucker during a range of flows. The second part of this thesis compares predictions from four bed-load transport models to bed-load transport data measured on Hobble Creek. In general, the Meyer-Peter, Müller and Bathurst models overpredicted sediment transport by several orders of magnitude while the Rosgen and Wilcock methods (both calibrated models) were fairly accurate. Design channel dimensions resulting from the bed-load transport predictions diverged as a function of discharge. Once validated, the models developed in this section can be used by design engineers to better understand sediment transport on Hobble Creek. The models may also be applied to other Utah Lake tributaries. The third section of the thesis introduces a detailed survey data set that covers the Hobble Creek floodplain on the shifted section between Interstate 15 and Utah Lake with an approximate 10 foot resolution grid. Water surface elevations at two flows, along with invert, fence, saddles, and other points, are labeled in the survey. A comparison with a survey completed last year did not reveal any significant lateral changes caused by the 2010 spring runoff. Due to the potential importance of the side ponds to June sucker survival, this data set can be used to monitor sedimentation in the side ponds. It may also be used in a GSSHA model to determine the magnitude of flow that is required before each side pond will be connected to the main channel.

Keywords: Andrew Dutson, Hobble Creek, June sucker, particle size distribution, bed-load transport

ACKNOWLEDGMENTS

I would like to thank Dr. Rollin H. Hotchkiss for giving me the opportunity to study and develop and for providing advice, encouragement, and direction at all stages of this project. I could not have made it this far without his patience and expertise. I would also like to express appreciation to the members of my graduate committee: Dr. Alan K. Zundel, Dr. E. James Nelson, and Dr. Russell B. Rader for their support and guidance along the way. Also, many thanks goes to the entire team of graduate and undergraduate students for their arduous work in all phases of data collection and to Brigham Young University for the organization, facilities, scholarships, and equipment that have made my studies possible. Most importantly, I express gratitude to my wife, Katie, and to my son, Ryley, for their encouragement and patience throughout the duration of my studies.

TABLE OF CONTENTS

LIST OF TABLES

LIST OF FIGURES

1 A Description of the Particle Size Distribution on Hobble Creek from 400 W to Interstate 15

1.1 Chapter Abstract

The June sucker (*Chasmistes liorus*) is an endangered fish species that is native to Utah Lake and currently spawns only in the Provo River. One step that must be taken in order to delist the June sucker is to create a secondary self-sustaining spawning run. The lower portion of Hobble Creek has been selected as the best location for this run. Many parameters are required for successful recruitment to occur. These include adequate water depth, intermediate flow velocities, and proper bed material. The purpose of this study was to investigate the current condition of the bed material in Hobble Creek and the effect that crossings and diversion dams have on the spatial distribution of particle sizes. Surface and subsurface samples were collected from eleven reaches in the 1.5 mile section of interest. Particle size distributions were generated for each sample and visual observations were made of each reach. A comparison of the longitudinal distribution of the D_{50} for each sample showed that Packard Dam and the 1650 W crossing create a major division in the bed particle distribution. Armoring is also common in most of the reach, with the most notable armoring occurring upstream of the Packard Dam/1650 W division and immediately downstream of all diversion dams. Locations for June sucker spawning are poor in the reaches below Packard Dam due to the large amount of fines. The best locations for successful recruitment of June sucker are upstream where the mean particle size is

significantly larger. Unfortunately, Packard Dam makes these locations inaccessible to the June sucker.

1.2 Introduction

On April 30, 1986, the June sucker (*Chasmistes liorus*) was federally listed as an endangered species with critical habitat (JSRIP 2010; JSRT 1999). At that time, it was estimated that fewer than 1,000 adult June sucker lived in Utah Lake (JSRIP 2010). By 1998, that number had dropped to less than 300, based on counts of spawning adults (Keleher et al. 1998). Restoration efforts are being made in an attempt to save the June sucker population. For example, in 2005, 8,809 June sucker were transferred from a protected breeding site to Utah Lake (CUWCD 2005).

The June sucker population is important to Utah Lake because June sucker are considered to be an indicator species. In other words, the drop in the June sucker population indicates that the Utah Lake ecology is doing poorly (JSRIP 2010). Investment in the recovery of the June sucker population will also result in attention to the ecology of Utah Lake as a whole.

Currently the lower 4.9 miles of the Provo River is the only self-sustaining reach utilized by the June sucker for spawning (JSRIP 2010). According to a study done by Cope and Yarrow (1875), many other Utah Lake tributaries such as Hobble Creek and Spanish Fork were also used for spawning in the late 1800's. One of the steps that must be completed in order to delist the June sucker as an endangered species is to recreate a second self-sustaining spawning run (JSRT 1999). Hobble Creek has been identified as the best candidate for this restoration. Figure 1-1 shows an aerial view of the westernmost reach of Hobble Creek in June of 2010.

Figure 1-1. Aerial photo of Hobble Creek taken in June 2010.

Prior to the 2009 spring runoff season, relocation construction was completed on the quarter mile section of Hobble Creek between Interstate 15 and Utah Lake (see Figure 1-1). In addition to constructing meanders and side pools, part of the construction was to remove invasive reeds (*Phragmites australis*) that were preventing the June sucker from finding the entrance to Hobble Creek. Since the relocation effort, adult June suckers have been observed to migrate in Hobble Creek as far upstream as Packard Dam (Stamp 2010).

In order to create a self-sustaining spawning reach, stream restoration must continue upstream of Interstate 15 to sections of the creek where spawning environments are better. A new, triple barrel, fish passage friendly culvert is currently under construction at the Interstate 15 crossing. This culvert will enhance the ability of the adult June sucker to migrate upstream in Hobble Creek in order to find suitable spawning locations (Parsons 2010).

Little is known about the spawning habits of the June sucker. However, suggestions have been made that adult June sucker prefer riffles with 1-3 feet of depth and velocities ranging from 0.2 to 3.2 feet per second (JSRIP 2010; Stamp et al. 2009). In addition, preferred substrate for spawning is stated to be 100-200 mm (Stamp et al. 2009), although spawning has been observed in a wide range of substrates sizes. It may be that spawning will occur in any range of substrates, but the percentage of surviving larvae is higher in substrates that consist of gravels and cobbles (Rader 2011).

In order to continue upstream restoration efforts, the existing particle size distribution in the reach of interest had to be investigated. These data could then be used to determine which locations are currently the most suitable for spawning, and what the steady state conditions are for the substrate given the existing bridges, diversion dams, and channel geometry.

1.3 Procedure

1.3.1 Sampling Sites

Restoration efforts are currently being considered to extend as far upstream as the 400 W crossing. Therefore, the section of Hobble Creek between 400 W and Interstate 15 became the focus for this study. The 400 N crossing involves a bridge for a two lane road and a subsequent bridge for a set of two railroad tracks. Hobble Creek passes under these bridges at an approximate 45° angle. The Interstate 15 crossing contains a double-barreled box culvert that is approximately 350 feet long. There are also two intermediate crossings along the creek. The 950 W crossing involves a narrow bridge for a small two lane road. The 1650 W crossing is composed of four bridges—two small frontage road bridges with a three-track and a single track railroad bridge in between.

There are also three diversion dams in this section of Hobble Creek. The most upstream dam is located near 650 W. This diversion dam is approximately 2 feet high. Backwater from this dam is not significant. The next diversion dam is known as Packard Dam. Packard Dam is approximately 6 feet high and causes backwater that extends through the 1650 W crossing. The final diversion dam is located at 1000 N. This dam is about 4 feet tall and causes backwater that extends upstream almost 1000 feet.

In order to more precisely characterize the bed material in Hobble Creek and to facilitate investigation of spatial variability in the bed material, the section of interest was divided into the eleven reaches shown in Figure 1-2. Reaches 1-4 were located between 400 W and 1650 W, while Reaches 5-11 were located between 1650 W and Interstate 15. The bounds of Reaches 1 through 4 were set by dividing the portion of the creek between 400 W and 1650 W into eight sections of equal length. Four of the eight sections were then randomly selected to be sampled while the other four remained unsampled. The bounds for Reaches 5 through 11 were set by walking the stream and placing markers where sustained visual differences in the substrate surface were noticeable. Due to deep backwater caused by Packard Dam, the 1000 N dam, and the Interstate 15 culvert, three portions of the creek between Reach 4 and Interstate 15 were not sampled. These sections were located between Reaches 4 and 5, Reaches 10 and 11, and Reach 11 and Interstate 15. Visual inspection of these sections suggests that the bed material is comprised almost entirely of sands and silts.

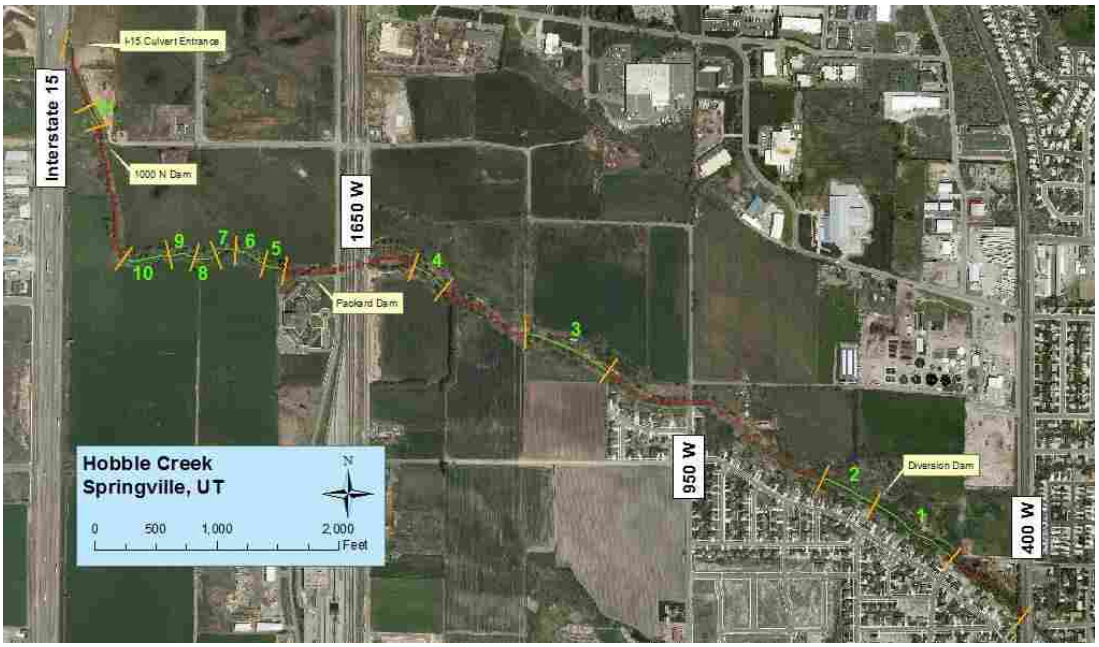

Figure 1-2. Reach numbering along Hobble Creek from 400 W to Interstate 15.

Visual observations were made about the physical appearance of each reach during the sampling process. These observations are summarized in Table 1-1.

1.3.2 Sampling Methods

A sample size that is independent of an assumed underlying particle size distribution assumption was presented by Church et al. (1987). This sample size ensures that the largest particle will not account for more than 1% of the total sample mass. For a D_{max} between 32 and 128 mm, the total sample mass is determined using Equation (1-1).

Table 1-1. Visual observations for each reach made during sampling process.

Reach Number	Observations/Comments	Size of Bed Material	Bars	Riffles/Pools	Length [ft]
1	• upstream from 2' diversion dam	• sparse boulders ø=1-1.5 ft • fines near dam		mostly riffle, no significant pools	778
2	• downstream from 2' diversion dam	• sands and small pebbles near dam • scattered boulders throughout			474
3	• fairly homogenous bed material • small drainage ditch discharge near beginning	• very few fines on surface		some deep pools	745
4	• just above 1650 W & Packard Dam backwater	• major downstream fining • cobbles upstream • sands downstream	large sandbar near end		317
5	• begins about 200 ft downstream of Packard Dam	• mostly coarse gravel and cobbles	several exposed gravel bars	alternating pools and riffles	180
6	• physical characteristics are similar to Reach 5	• fewer cobbles than Reach 5	several exposed gravel bars	alternating pools and riffles	273
7		• much finer than previous two reaches	exposed sand bars		181
8	• bed material had a lot of variation	• ranged from boulders to fines	several exposed gravel bars		181
9	• small, natural debris dam divides Reaches 9 & 10	• fines mixed with gravels	few exposed bars	70% pools	215
10	• downstream boundary is at 90° bend and beginning of backwater from 1000 N dam	• particle size increases downstream			388
11	• begins about 75 ft below 1000 N dam • ends at backwater from I-15 culvert • lots of vegetation on the streambed	• mostly sands and silts	a few exposed gravel bars		188

$$m_s = 138{,}000 D_{max}{}^3 \quad (1\text{-}1)$$

where:

m_s = total mass of sample (kg)

D_{max} = diameter of largest particle in reach (m)

This empirical relationship was first presented by Neumann-Mahlkau (1967) after he fit a regression function to a graph showing the error of the sample mass to be less than 1% due to the arbitrary presence of the D_{max} particle in the sample. D_{max} for the section of Hobble Creek between 1650 W and Interstate 15 was determined to be 76 mm by conducting a preliminary pebble count (Wolman and Union 1954). This yielded a required sampled size of at least 60 kg (133 lbs).

The method outlined by Bunte and Apt (2001) was followed to collect samples from both the surface and the subsurface. An imaginary grid was overlaid on each section from bank to bank, and a subsample was taken from a random position within each grid cell. The grid cells were sized so that there were at least 100 subsamples taken from each reach. This ensured that no single subsample could account for more than 1% of the entire sample. Because June sucker spawning occurs in riffle sections, pools were not of interest in this study. Consequently, all samples were taken from riffles. The subsamples from each grid cells were combined to create a conglomerate sample from each reach that had a weight of at least 133 pounds. This process was repeated so that a surface and a subsurface sample was collected from each reach.

Shovels were used to collect each sample. A square nosed shovel was used to scrape off and collect the surface layer at each sampling site and a standard shovel was used to collect the subsurface samples once the surface layer had been removed. In order to preserve the fines from

being washed away, a sawed off 55-gallon barrel was used in areas of relatively high velocity to shield the sample from the flow (Bunte and Abt 2001). A subsurface sample with the barrel flow shield is shown in Figure 1-3.

Figure 1-3. Subsurface sample taken from within a 55-gallon barrel flow shield.

It should be noted that samples from Reaches 1-3 were collected and analyzed about four months following those from Reaches 4-11. All reaches were sampled during a flow of approximately 20-30 cfs.

1.3.3 Sieving Methods

Due to the relatively large size of the samples that needed to be sieved, samples were split using standard methods as follows. Samples were first dumped into a small plastic

swimming pool and split into quarters. One quarter section was removed at random and split in half using a sample splitter to make the final sample size small enough to be put through the sieve machines. All samples were oven dried for 24 hours at 350°F before sieving. Both halves of the quarter sample were sieved separately and recombined after weighing.

In order to make sure the data would not be compromised by only sieving one quarter of the sample, all four quarters of the first sample were sieved separately. The particle size distribution for each quarter sample was compared to the particle size distribution of the entire combined sample as shown in Figure 1-4. Wilcoxon and equivalence statistical tests (Conover 1980) showed no significant difference between any of the parameters of any of the distributions.

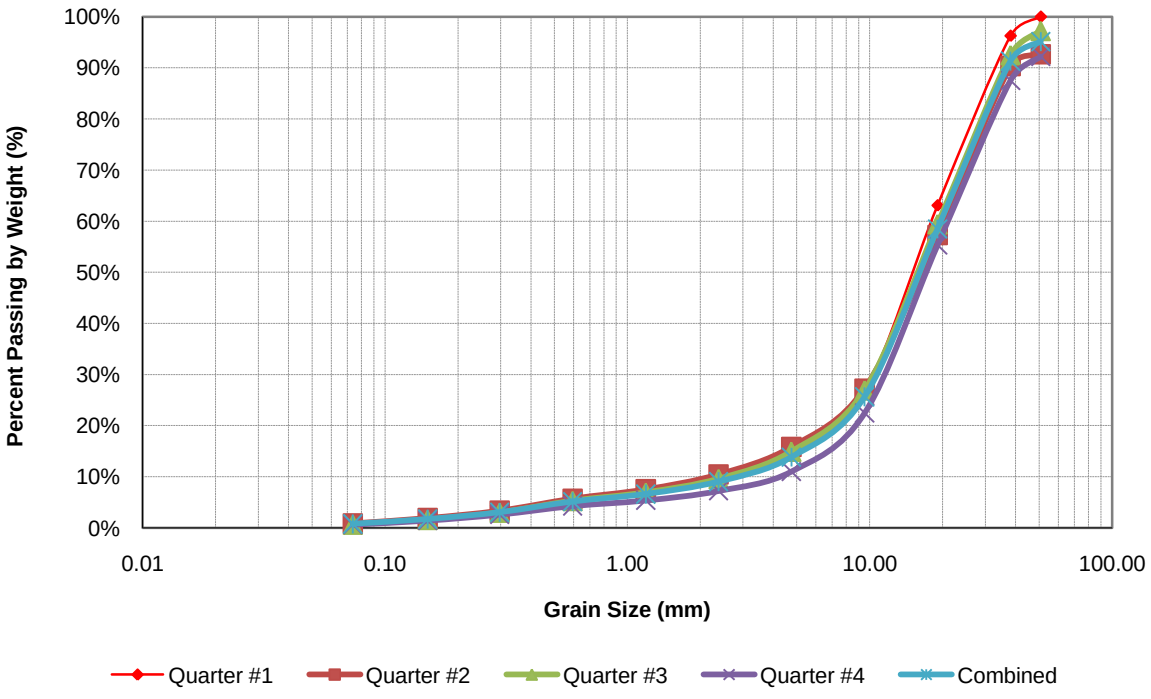

Figure 1-4. Comparison of each quarter sample PSD with combined PSD.

The stack of sieves used had sieve size increments of 1.0 phi units. A 2-inch sieve was the largest and a No. 200 (0.0029-inch) sieve was the smallest (Bunte and Abt 2001). Because many larger particles were found in the samples from Reaches 1 through 3, the particles retained for these reaches on the 2-inch sieve were sorted further using a template. Unfortunately, because this same practice was not followed for Reaches 4 through 11, data for the particles larger than 2 inches is unknown for these sections.

1.4 Particle Size Distributions

Surface and subsurface particle size distributions for each of the eleven reaches are shown in Figure 1-5 through Figure 1-15.

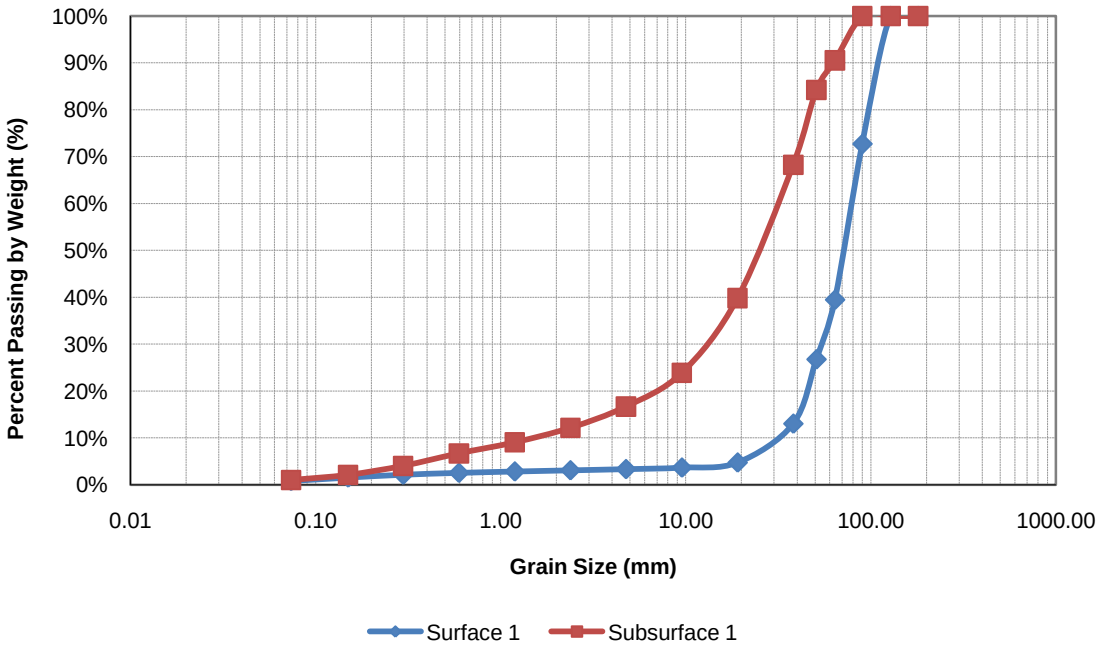

Figure 1-5. Particle size distributions for Reach 1.

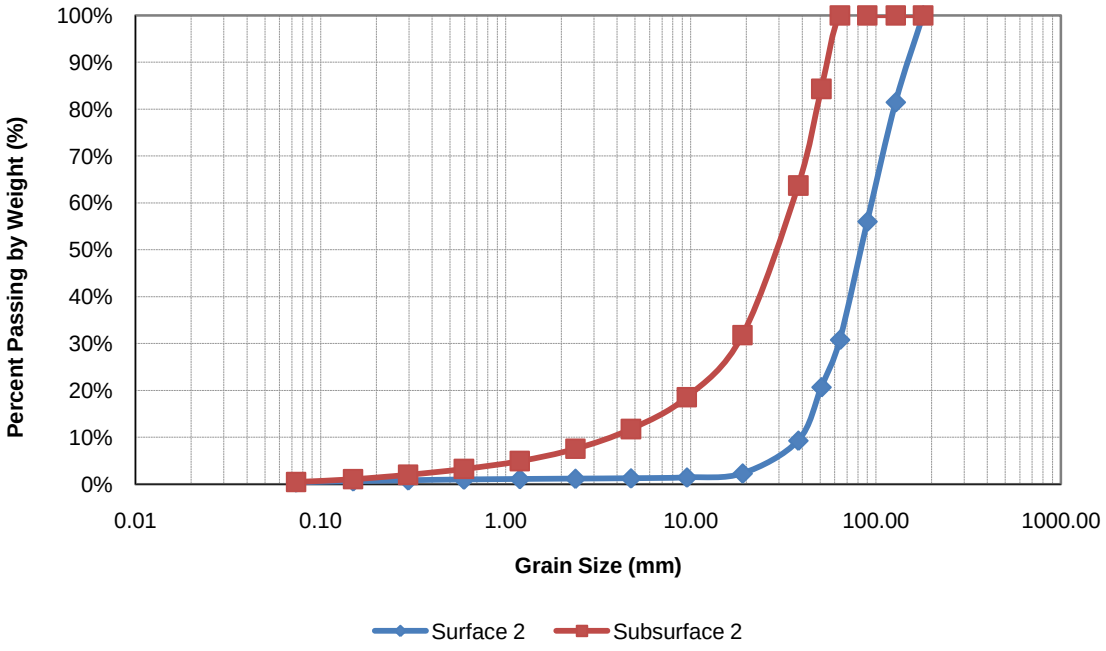

Figure 1-6. Particle size distributions for Reach 2.

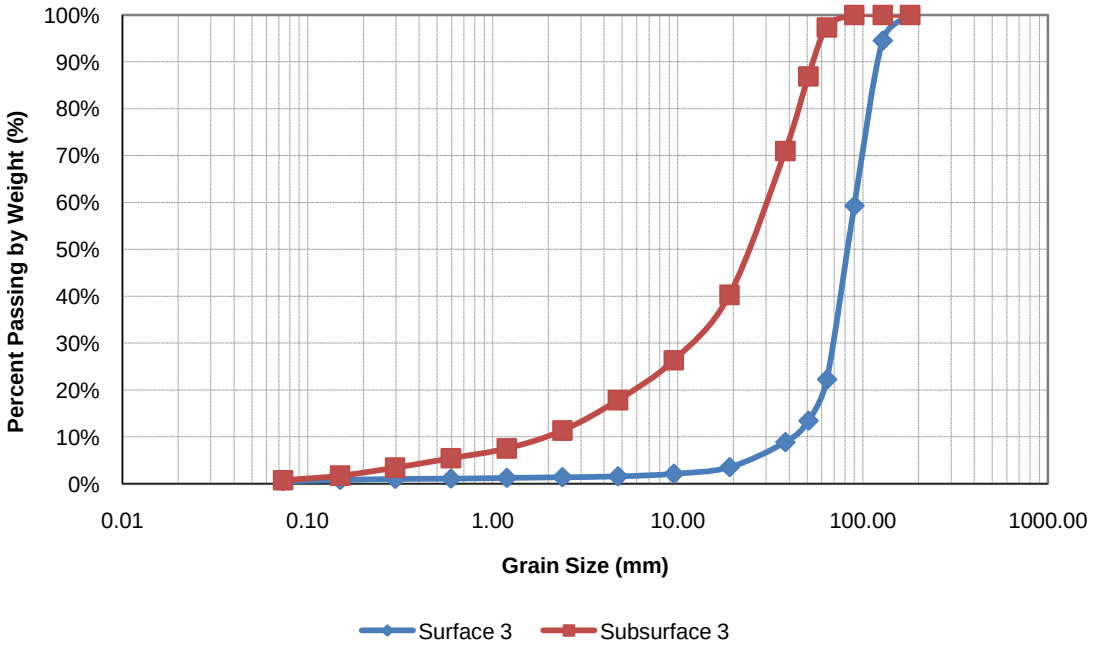

Figure 1-7. Particle size distributions for Reach 3.

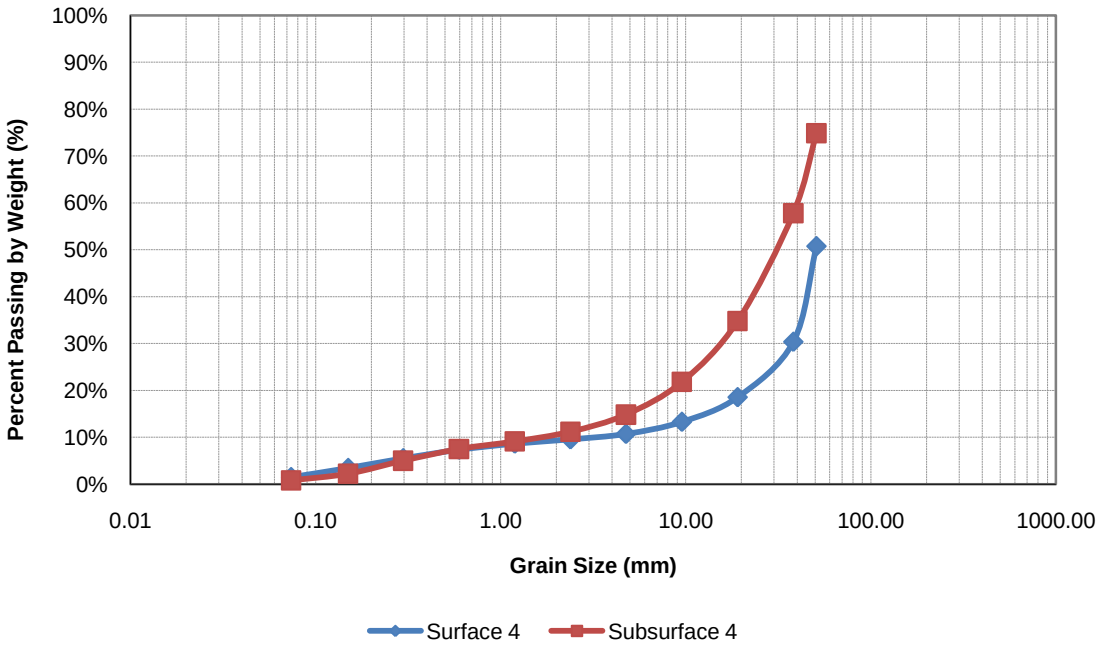

Figure 1-8. Particle size distributions for Reach 4.

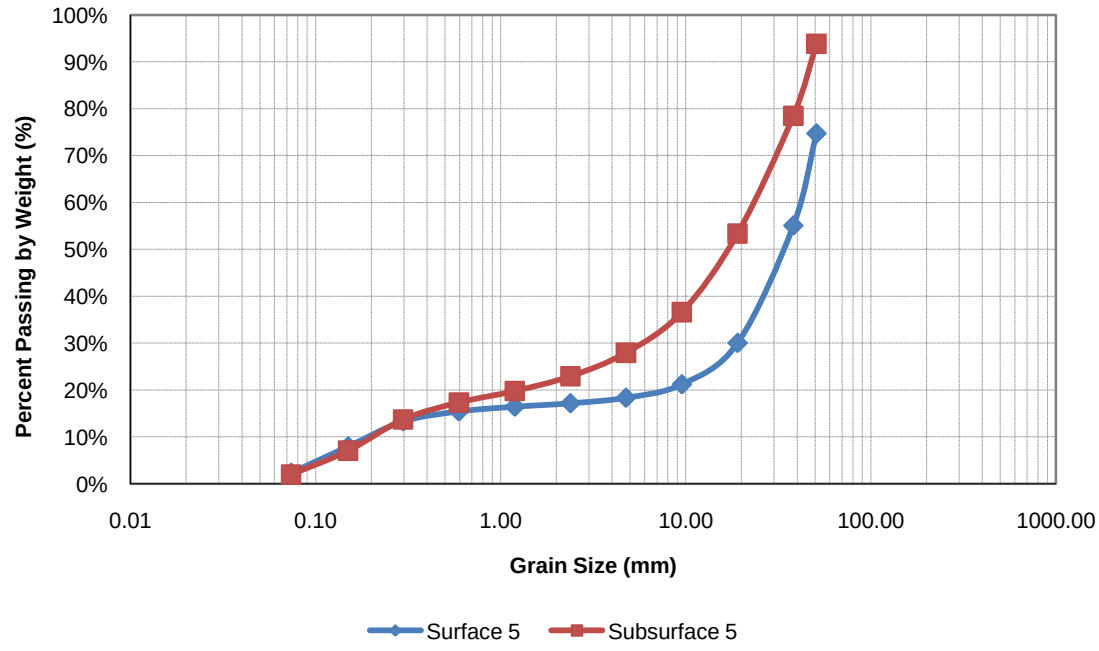

Figure 1-9. Particle size distributions for Reach 5.

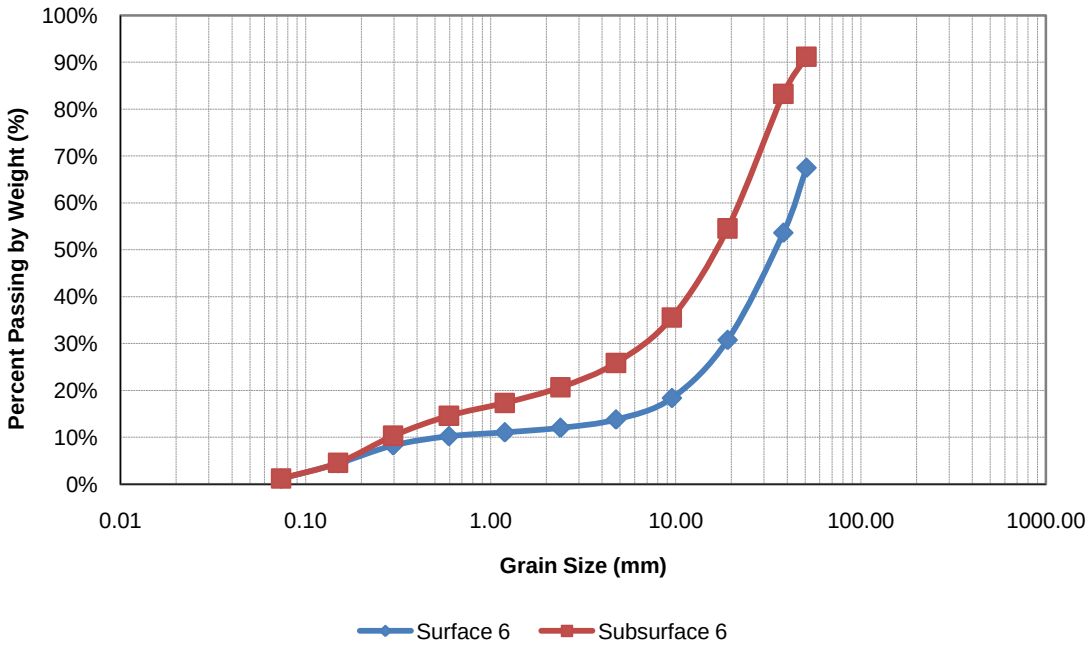

Figure 1-10. Particle size distributions for Reach 6.

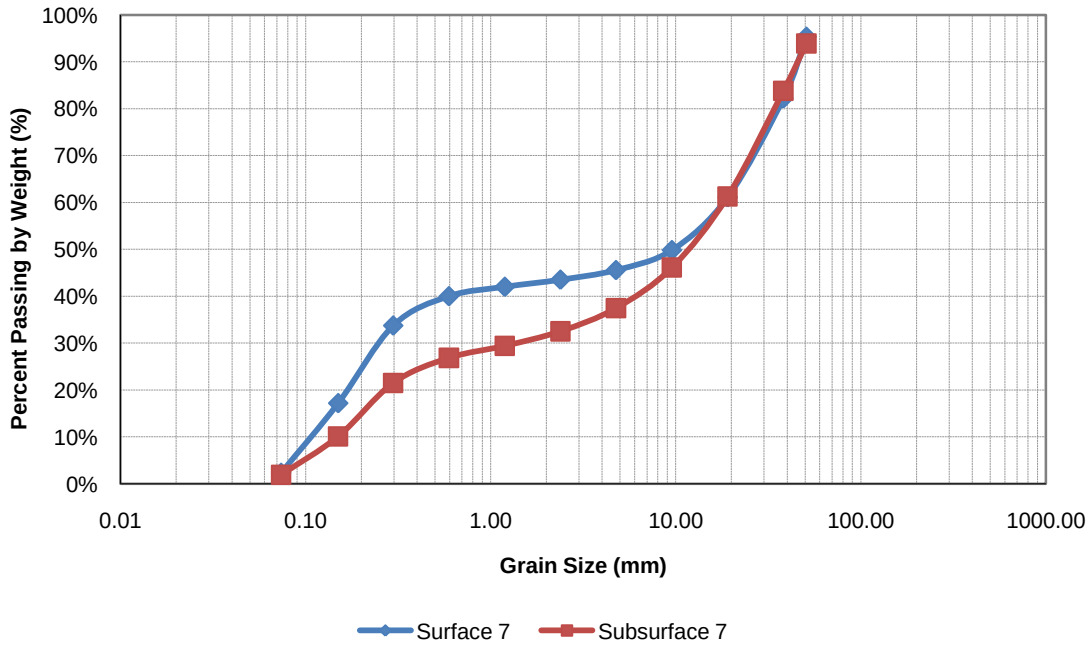

Figure 1-11. Particle size distributions for Reach 7.

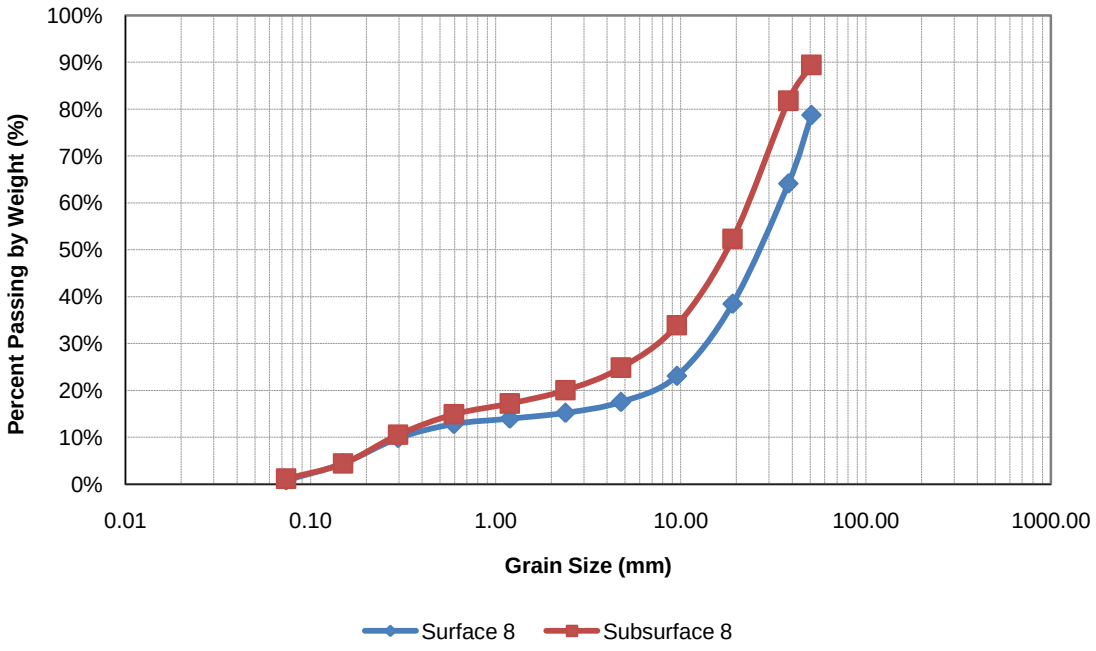

Figure 1-12. Particle size distributions for Reach 8.

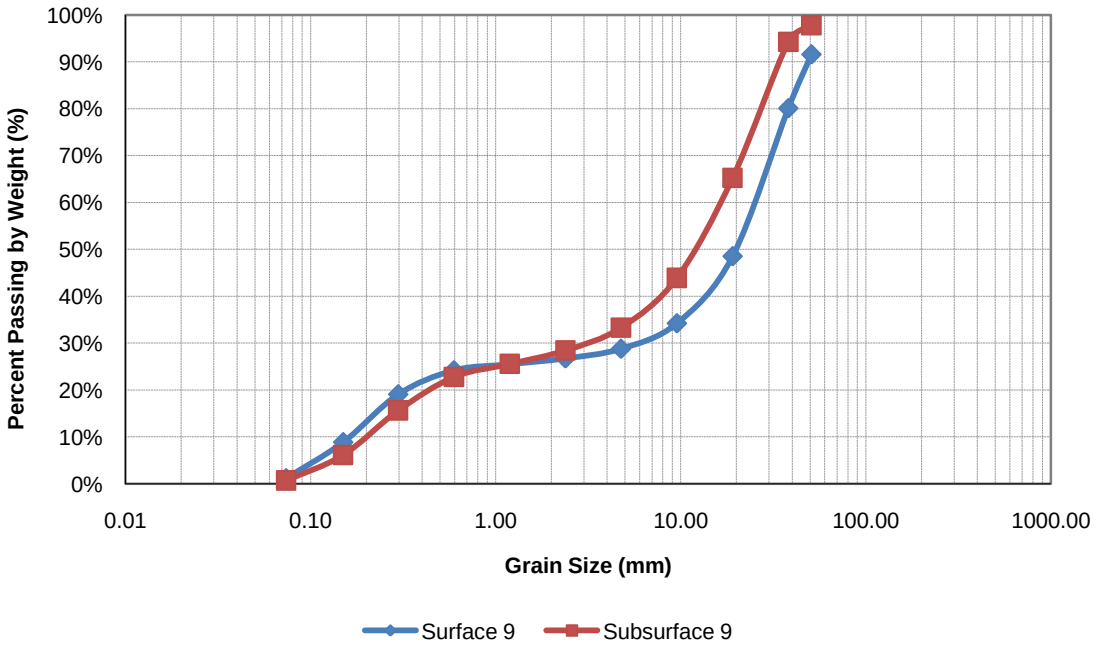

Figure 1-13. Particle size distributions for Reach 9.

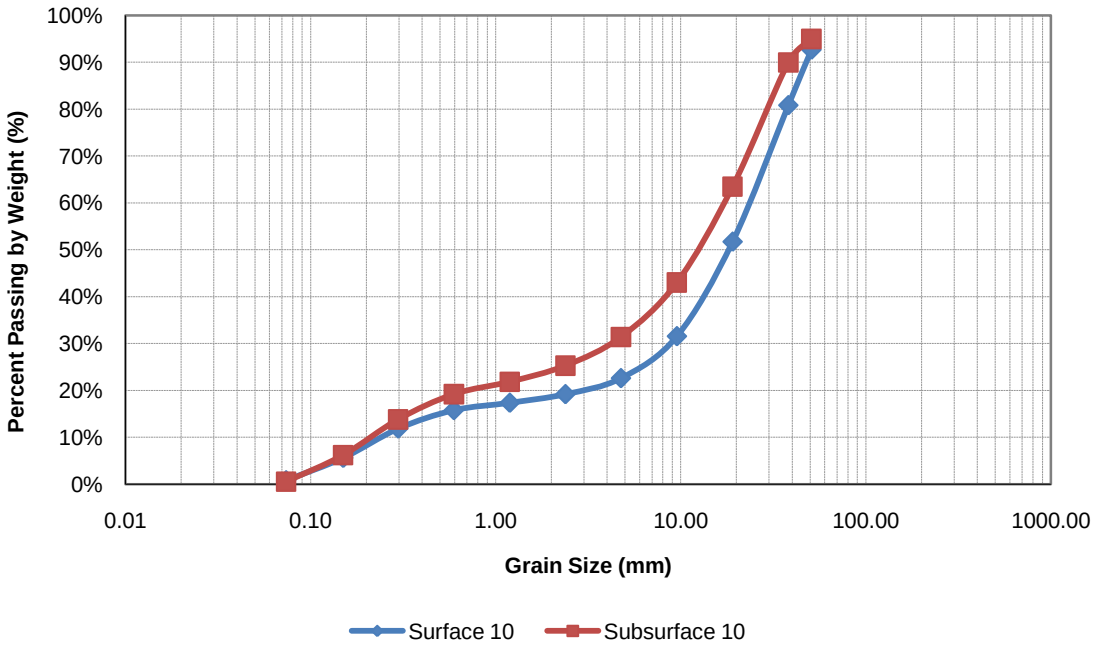

Figure 1-14. Particle size distributions for Reach 10.

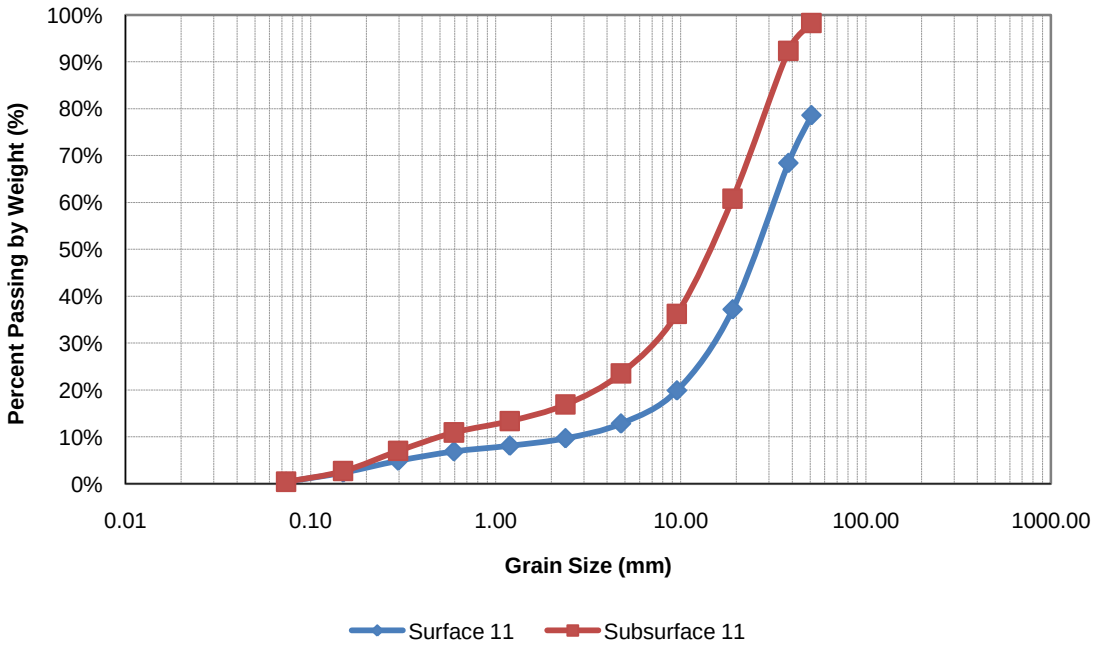

Figure 1-15. Particle size distributions for Reach 11.

Table 1-2 shows the D_{50} for the surface and subsurface of each reach. Additional parameters can be found in Table A-1 and Table A-2 of Appendix A.

Table 1-2. Surface and subsurface D_{50} for each reach.

Reach	Surface D_{50} [mm]	Subsurface D_{50} [mm]
#1	71.29	24.42
#2	82.96	28.29
#3	82.60	23.72
#4	50.26	30.13
#5	33.12	16.56
#6	34.15	16.13
#7	9.63	11.38
#8	26.02	17.46
#9	19.68	11.61
#10	17.96	12.07
#11	25.33	14.05

1.5 Discussion

In addition to the visual observations mentioned above, quantitative observations included the spatial variability of particle sizes, and bed armoring.

1.5.1 Spatial Variability of D_{50}

Information about how channel characteristics such as bridges and dams affect bed material can be discovered by plotting particle size against location. Figure 1-16 and Figure 1-17 compare D_{50} to distance upstream from the Interstate 15 culvert for surface and subsurface particles, respectively. Comparisons of D_5, D_{16}, D_{25}, D_{75}, D_{84}, and D_{95} against location all show similar results and are included in Appendix A.

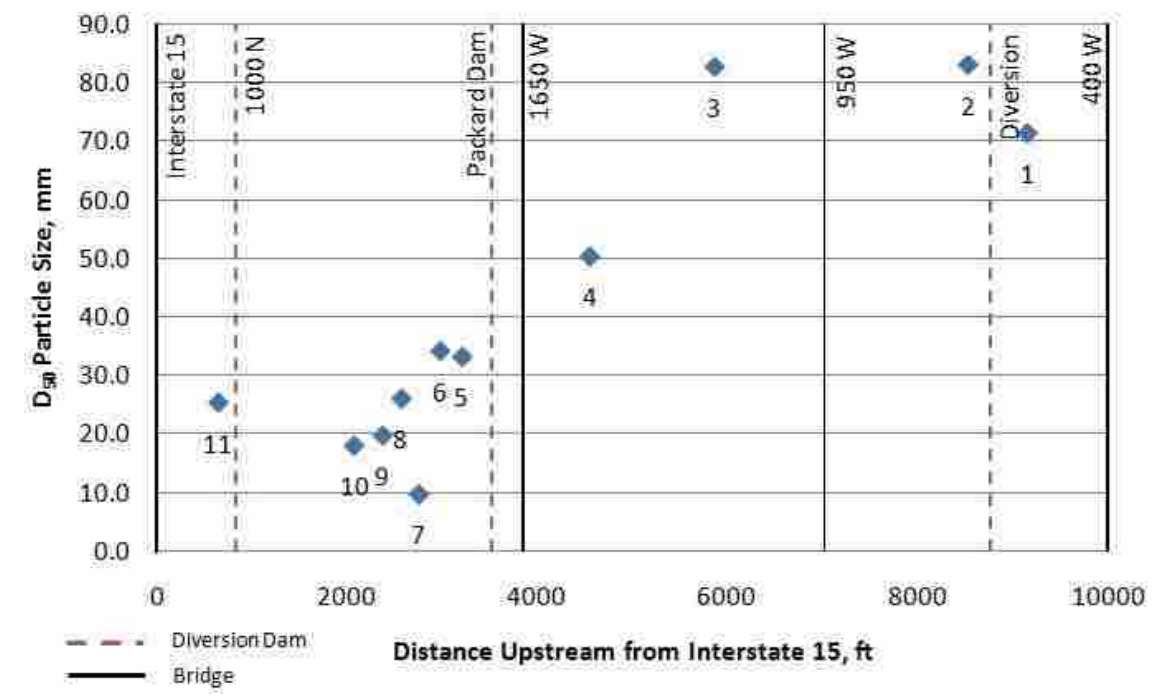

Figure 1-16. Surface D_{50} vs. distance upstream from Interstate 15.

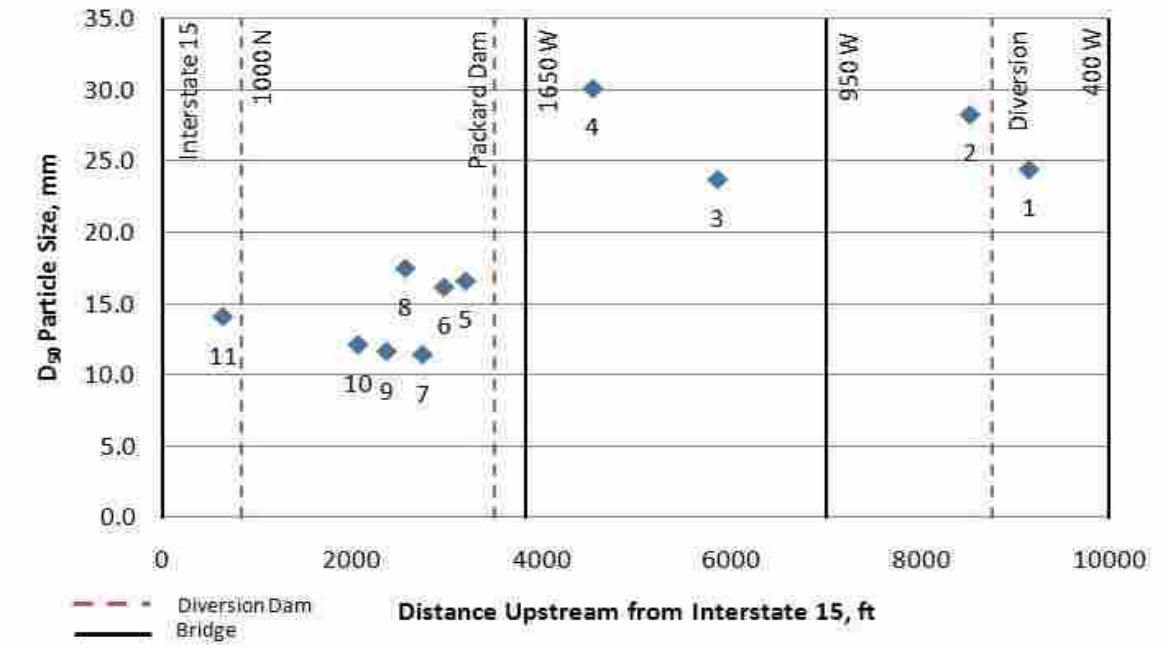

Figure 1-17. Subsurface D_{50} vs. distance upstream from Interstate 15.

The D_{50} of both the surface and subsurface particles decreases significantly in the vicinity of the Packard Dam and the 1650 W crossing. On average, the D_{50}'s are 3.0 and 1.8 times larger upstream than downstream for the surface and subsurface, respectively. The Packard diversion dam is about 200 ft upstream from the beginning of Reach 5 and has flash boards that are typically up year-round. Two frontage road bridges and two railroad bridges all span the backwater at the 1650 W crossing, just 250 feet upstream from Packard Dam. Finally, due to the dam and the bridges, backwater extends 850 feet from Packard Dam to the downstream end of Reach 4.

In backwater sections, the velocity of a stream essentially stops. This causes any sediment that is being transported by the stream to drop out. Evidence of this is seen by noting the large sand bar at the beginning of the backwater section just below Reach 4. It is also visually noted that fines make up most of the particle sizes in the backwater sections between Reach 10 and Reach 11 and between Reach 11 and the Interstate 15 culvert.

Fines dropping out of the flow and covering the stream surface is of great concern when locating potential spawning locations. In order for successful recruitment of June sucker, larvae must be exposed to an open flow of water. If the interstitial flow is choked by fines, the supply of oxygen will be restricted and deadly ammonia secretions will build up around the larvae (JSRT 1999; Shirley 1983).

Once flow passes a backwater zone, it has excess transport capacity because sediment has dropped out upstream. This excess capacity causes scour immediately downstream from dams and culverts (Kondolf 1997). This was also observed in this study. The surface D_{50}'s of Reaches 5 and 6 are larger than any other reach downstream of Packard Dam due to the fines in these sections being picked up by the excess transport capacity. By the time the flow crosses

Reach 7, the excess transport capacity has been satisfied and the transport and deposition of fines is once again in equilibrium. The same pattern is seen in Reach 11 where the D_{50} is larger than the reaches immediately upstream and the section downstream is composed mostly of fines.

1.5.2 Bed Armoring

Armoring is a term used to describe the effect of an oversized surface layer shielding flow from a smaller subsurface layer. Bed armoring is created by flows that wash away the fines from the surface without replenishing them by deposition from upstream (Andrews and Parker 1987). Bathurst (2007) uses the ratio of surface D_{50} to subsurface D_{50} to quantify bed armoring in his bed-load transport prediction equation. An armoring ratio of 1.0 indicates that armoring is not present while armoring ratios of 3-4 indicate significant armoring. The armoring ratio for each reach is plotted in Figure 1-18.

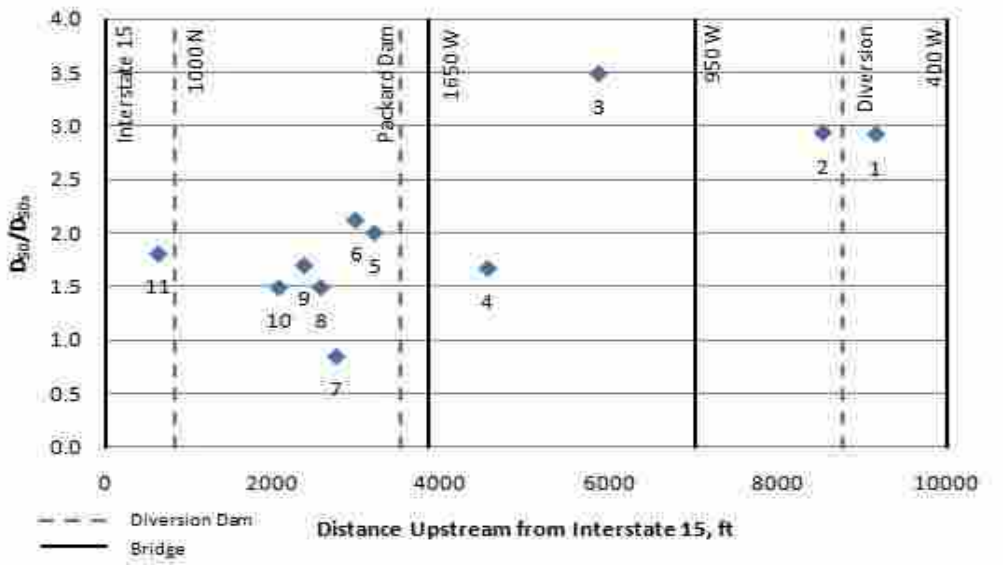

Figure 1-18. Armoring ratio vs. distance upstream from Interstate 15.

With the exception of Reach 4, all of the reaches above Packard Dam and the 1650 W crossing have an armoring ratio that averages 1.9 times larger than the armoring ratio of the reaches downstream. It is not surprising that the armoring ratio of Reach 4 is lower due to its proximity to the backwater section.

Reaches 5 and 6 have the highest armoring ratio of all the reaches downstream from Packard Dam. This is due the fact that the excess transport capacity created by Packard Dam scours the fines out of Reaches 5 and 6. Since all the fines from upstream have already settled out in the backwater section, there are no fines to replace what is scoured out in these reaches. A similar jump in armoring ratio is seen in Reach 11 immediately downstream of the 1000 N diversion dam.

Reach 7 is the only reach in which some degree of armoring does not occur (surface D_{50}/subsurface D_{50}<1). This may be attributed to the abundance of fines being carried downstream from Reaches 5 and 6.

1.6 Conclusions

The objective of this study is to provide a detailed description of the particle size distribution on the bed of the sections of Hobble Creek that are of interest to June sucker spawning restoration. Sections of Hobble Creek that are upstream from Packard Dam and the 1650 W crossing have particle sizes that are nearly twice the size of those that are downstream. As seen from the particle size distributions at each reach, some degree of bed armoring is present in most of the creek. The armoring ratio is much larger in the upstream sections and also peaks locally immediately downstream of the diversion dams.

The three backwater sections—upstream of the Interstate 15 culvert, upstream of the 1000 N diversion dam, and upstream of Packard Dam and the 1650 W crossing—have a significant impact on the spatial distribution of particle sizes. The bed of the backwater sections is made almost entirely of fines, while the bed of the sections immediately below the backwater sections contains relatively large surface particles compared to subsurface particles.

In its present condition, Hobble Creek has been observed to provide an environment that is utilized by some spawning June sucker. However, the impedance to fish passage and the spatial distribution of particle sizes caused by the diversion dams limits the number of suitable spawning environments that currently exist. It is believed that the most suitable spawning environments are found upstream of Packard Dam. It is also believed that increasing the amount of the stream that is accessible to June sucker would increase the production of larval fish.

2 A Comparison of Field Data and Predictive Equations for Sediment Transport Rate on Hobble Creek

2.1 Chapter Abstract

Bed-load transport data are both time consuming and costly to collect. Many predictive models are used to forgo the costs that physically measuring bed-load rates can add to a restoration project. The objective of this study is to compare the products of predictive equations and their resulting channel design dimensions to measured transport rates and existing channel dimensions. Bed-load data were obtained for three sites on Hobble Creek, Utah in the spring of 2006. Four predictive models were used to predict bed-load rates: the Meyer-Peter, Müller (MPM) formula, Wilcock's two parameter model, Rosgen's Pagosa reference curve, and Bathurst's Phase 2 bed-load transport equation. Observed rates were compared to predicted rates, and sediment transport at bankfull conditions was used to find stream design geometries (width, depth, and slope). The MPM formula consistently over predicted the transport rates by up to six orders of magnitude; this resulted in narrower and deeper stream designs. The Bathurst formula predictions and channel dimensions were similar to the MPM predictions on two of the three sites. Bathurst predictions for the third site, which was significantly more armored than the first two sites, were close to observed values. The Wilcock and Rosgen models generally performed better, although bed-load rates up to two orders of magnitude larger and smaller than observed rates were predicted at some sites. Design geometries based on the Wilcock and Rosgen bed-load rates were similar to those geometries designed to carry observed transport rates. It was

observed that as bed-load transport rate increased, the difference in channel design dimensions for MPM and Bathurst became increasingly large while the Wilcock and Rosgen dimensions followed observed dimensions. This indicates that simply choosing a sediment transport model without collecting any field data in hopes of reducing costs and designing restored channels for predicted rates is not likely to work, especially for alluvial channels where transport rates can be relatively large. Predictive equations that involved some sort of calibration using a few observed transport rates yield much more accurate predictions than uncalibrated models. Predictive equations may be less expensive than collecting bed-load data, but the increased risk of incorrect channel dimensions and a resulting channel failure should create a sufficient incentive for restoration engineers to seriously consider collecting enough bed-load data in the field to enable the use of calibrated models.

2.2 Explanatory Comments

During the spring runoff season of 2006, a team of BYU students lead by Jaron Brown collected bed-load data on Hobble Creek. Jaron compiled and analyzed the data and prepared a draft journal article as part of his thesis (Brown 2008). The draft journal article contained an explanation of how the data were collected, an introduction to the various equations that were used in the analysis, and a comparison of design channel dimensions.

As part of this thesis, the work of Jaron Brown was reanalyzed and the draft journal article was revised. The remainder of this chapter is the final draft of the journal article. Sections 2.3 and 2.4, which introduce the article and discuss how the data were collected, were left generally as written by Jaron Brown, with slight revisions. The remainder of the document follows Brown's outline and contains portions of his original writing, but is comprised mostly of

original analysis, results, conclusions, and commentary. The alterations came as a result of calculation corrections, additional detail, and further discussion.

2.3 Introduction

The practice of obtaining bed-load data in the field for stream restoration projects is not always used in consulting engineering firms. In fact, current literature (Doyle et al. 2007) on the subject has hinted that using predictive equations rather than field data is the norm amongst restoration firms due to economic and time constraints. This is often at the sacrifice of greater accuracy. A compromise option is to obtain minimal field data that can be used to calibrate a predictive equation (Wilcock et al. 2009). The objective of this paper is to show the relevance of obtaining field data. This will be done by comparing the differences between final channel design dimensions resulting from calibrated and uncalibrated predictive models and channel dimensions based solely on field data.

2.4 Bed-load Measurements

Bed-load transport data were collected at several locations on Hobble Creek during the spring 2006 snowmelt runoff season (see Figure 2-1). Hobble Creek is understood to be a supply limited stream, meaning that the transport capacity exceeds the sediment supply (Montgomery et al. 1996). The flow rate ultimately peaked at 13.3 m^3/s (representing approximately a 5-year flood) and decreased daily down to 2.1 m^3/s, at which point bed-load movement ceased. Bed-load traps designed by Bunte and Abt (Bunte et al. 2007) of the United States Forest Service were used to obtain bed-load samples. The total transport rate of the stream was found and correlated with the measured flow rate that occurred on each sampling day.

2.4.1 Measurement Sites

Measurement sites were selected based on two criteria. The highest priority was given to sites where uniform flow conditions existed. At the time of sampling, Hobble Creek was an ungaged stream; consequently, discharge measurements were needed with every bed-load measurement. This meant that the hydraulic characteristics at each site needed to be such that an accurate discharge measurement could be taken. The second criterion in selecting sites was proximity to roads and/or bridges—these being necessary for bed-load sampling during unwadeable conditions. Roads facilitated the delivery of several portable bridges designed and constructed to span the stream only a few feet above the water surface (Bunte et al. 2007). Data from three sites were used in this study. Figure 2-1 depicts Hobble Creek and the relative locations of these sample sites.

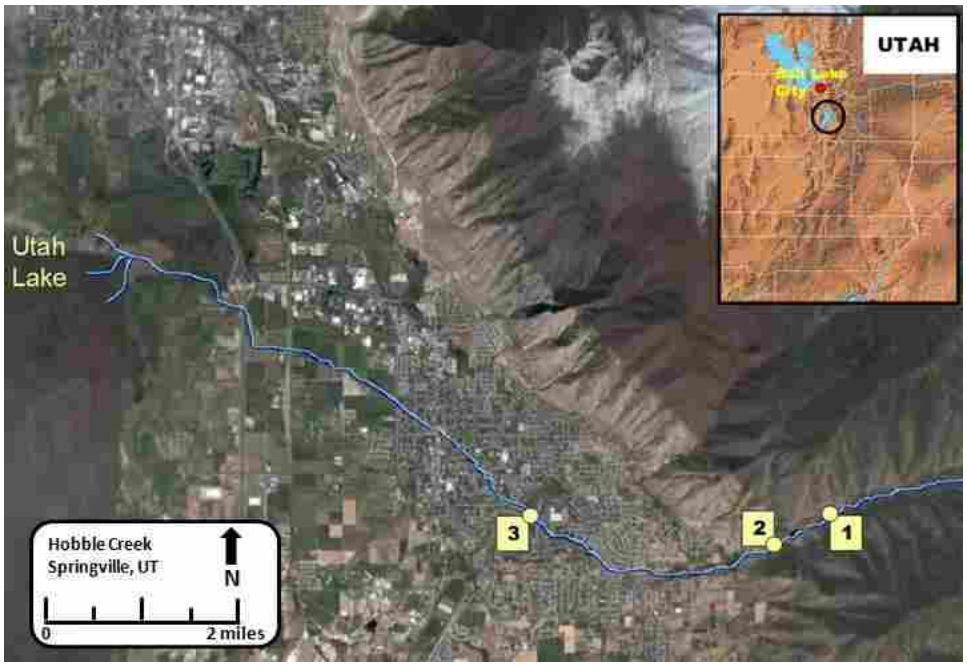

Figure 2-1. Sample sites labeled according to relative location.

Site 1 is located 30 m upstream from the backwater zone for the most upstream diversion structure on Hobble Creek. Site 2 is located near the mouth of Hobble Creek canyon, about 800 m downstream from a debris basin. Site 3 is located next to Springville High School and about 150 m downstream from a culvert. Cross sections for all sites can be seen in Appendix B.

2.4.2 Sampling Methods

Bunte/Abt traps were used to collect bed-load data (Bunte et al. 2007). These traps have an opening width of 0.30 m, a height of 0.22 m, and a 4.5 mm mesh net. A ground plate, designed to improve sampling efficiency, was staked to the streambed below each trap. Wadeable conditions are required before bed-load measurements begin in order to set up ground plates and the stakes to which the traps are attached. One of the Bunte-Abt traps is shown in Figure 2-2 as it would have appeared on the streambed.

Figure 2-2. Bunte/Abt bed-load trap as it would be deployed on the streambed.

When conditions were such that wading in the stream to set up the Bunte/Abt traps was unsafe or impossible, a hand-held variation of the Bunte/Abt traps was used. This variation, known as the "Stanley Sampler", incorporated several sections of steel pipe that, when coupled together, form a forked pole up to 12' long. This was attached to the Bunte/Abt traps using the straps normally used to fasten the trap to the ground stakes (see Figure 2-3). All sampling devices were used in a similar fashion—by measuring the width of the stream and taking samples at evenly spaced intervals across the stream. Consequently, only a percentage of the streambed width was sampled. Sample times ranged from 5 minutes to 1 hour, depending on the stream flow rate and rate at which the sampler nets would fill up. When flows and bed-load were high, sample times longer than 5 minutes resulted in nets too heavy to pull out easily. Once the flow subsided, sample times up to an hour long were required to collect bed-load. Data from bed-load sampling is summarized below in Table 2-1.

Figure 2-3. Handheld version of the Bunte-Abt trap nicknamed "Stanley Sampler".

Table 2-1. Summary of bed-load transport, hydraulic, surface, and subsurface data used in this study.

(1)	(2)	(3)	(4)	(5)	(6)	(7)	(8)	(9)	(10)	(11)	(12)	(13)	(14)	(15)
Location	Date	Measured Discharge (cfs)	Bed-load Sample Weight (g)	Sample Collection Time (min)	Bed Width (ft)	Sampling Device	Sampler Width (ft)	Number of Samples	Slope (ft/ft)	D_{84} Surface (mm)	D_{65} Surface (mm)	D_{50} Surface (mm)	D_{50} Subsurface (mm)	Average Depth (ft)
Site 1	11-May	269.5	29.2	5	19	Stanley	1	7	0.008	97.8	74.0	60.8	16.3	2.15
Site 1	18-May	284.9	1724.7	5	18	Stanley	1	11	0.008	97.8	74.0	60.8	16.3	2.07
Site 1	27-May	164.8	0.5	10	16	Stanley	1	10	0.008	97.8	74.0	60.8	16.3	1.78
Site 1	31-May	108.6	0	60	18	B/A	1	5	0.008	97.8	74.0	60.8	16.3	1.58
Site 2	23-May	214.5	4	5	23	Stanley	1	15	0.013	104	67.2	54.7	26.1	1.53
Site 2	25-May	154.1	1795.7	5	23	B/A	1	7	0.013	104	67.2	54.7	26.1	1.32
Site 2	31-May	89.2	73.94	60	23	B/A	1	7	0.013	104	67.2	54.7	26.1	0.99
Site 3	17-May	250.7	1726.4	5	22	Stanley	1	14	0.011	121.2	93.7	69.7	1.7	1.85
Site 3	19-May	258	366	5	22	Stanley	1	14	0.011	121.2	93.7	69.7	1.7	1.83
Site 3	24-May	175.9	12.55	5	22	Stanley	1	13	0.011	121.2	93.7	69.7	1.7	1.51
Site 3	30-May	114.8	626.76	60	16	B/A	1	8	0.011	121.2	93.7	69.7	1.7	0.70
Site 3	1-Jun	90.5	1.3	60	16	B/A	1	4	0.011	121.2	93.7	69.7	1.7	0.71

Notes: (6) Bed width is the width in which water was moving as opposed to being ponded near the bank.

(10) Slope was determined to be the average slope of the nearest one or two riffle heads in both the upstream and downstream directions.

(15) Average depth is cross-sectional area divided by top width.

The bed width shown in Table 2-1 corresponds to the effective width, which, as defined by Zimmerman and Church (2001), is the width within which water is moving as opposed to being ponded near the bank. The use of this bed width assumed that bed-load transport on the sides of the stream is negligible.

The slope in Table 2-1 was determined to be the average slope of the nearest one to two riffle heads both upstream and downstream. The surface particle size parameters were obtained from a pebble count done at each site. The subsurface particle size parameters were obtained from a sieve analysis of samples taken from each site. Complete survey data along with particle size distributions for each site can be seen in Appendix B.

2.4.3 Transport Rate Calculation

The following equation was used to find the calculated bed-load transport rate for the observed data:

$$Q_s = \frac{mb}{twn\rho s} \quad (2\text{-}1)$$

where:

Q_s = bed-load transport rate (m^3/s)

m = total mass caught in traps (kg)

b = streambed width (m)

t = sample time (s)

w = sampler width (m)

n = number of traps

ρ = density of water (kg/m^3, taken as 1000 kg/m^3)

s = specific gravity of sediment (taken as 2.65)

In this study bankfull flow was assumed to be equal to a 1.5 year flood (Dunne and Leopold 1978; Petit and Pauquet 1997; Rosgen et al. 2006). This assumption was made because the stream geometry of Hobble Creek has been significantly altered to prevent flooding and facilitate irrigation. The alterations make it impossible to accurately determine bankfull discharge using field indicators. A value of 5.29 m^3/s was found using 43 years of data from a discontinued stream gage that was located just upstream from Site 1. Figure 2-4 shows the flood frequency curve generated for Hobble Creek.

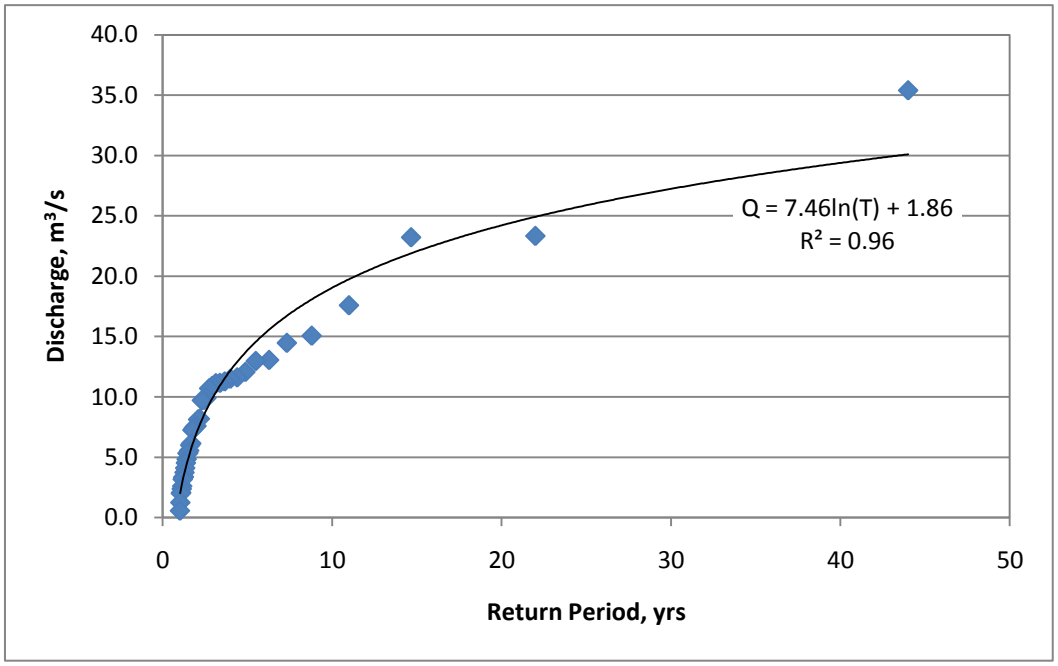

Figure 2-4. Flood frequency curve for Hobble Creek.

Because bed-load measurements were not taken at bankfull discharge, bed-load transport rate at bankfull was found to be 7.81×10^{-8} m^3/s by fitting a power trend line to a graph of measured discharge vs. measured bed-load transport (see Figure 2-5).

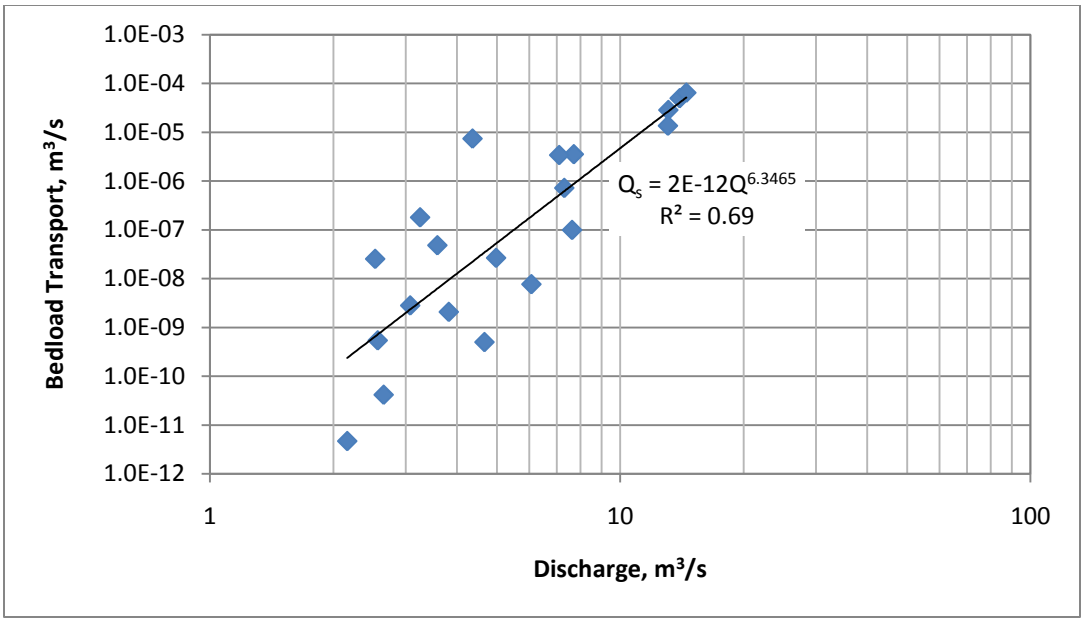

Figure 2-5. Sediment rating curve for Hobble Creek.

2.5 Predictive Equations

Engineers and geomorphologists have developed many equations for estimating sediment transport rates. In this study, field data in the form of volumetric bed-load transport (m^3/s) using Equation (2-1) are compared to estimates from four different predictive equations: the Meyer-Peter, Müller, (MPM) formula (Meyer-Peter and Müller 1948; Wong and Parker 2006), Rosgen's Pagosa reference curve (Rosgen et al. 2006), Wilcock's Two Parameter Model (Wilcock 2001), and Bathurst's Phase 2 bed-load transport equation (Bathurst 2007).

2.5.1 Meyer-Peter, Müller Equation

The Meyer-Peter and Müller equation is one of the pioneering developments in sediment transport. It is still in wide use today in research and engineering applications (Wong and Parker 2006). It was used in this study in its basic form as follows:

$$q^*_s = 8(\tau^* - \tau^*_c)^{3/2} \quad (2\text{-}2)$$

where:

q^*_s = dimensionless bed-load transport rate per unit width of streambed

τ^* = dimensionless shear stress

τ^*_c = dimensionless critical shear stress (taken to be 0.047)

In order to find the dimensionless shear stress, τ^*, the dimensional shear stress is first calculated using

$$\tau = \gamma HS \quad (2\text{-}3)$$

where:

τ = shear stress (N/m^2)

γ = specific weight of water (N/m^3)

H = depth (m)

S = slope (m/m)

This shear stress is then non-dimensionalized for use in Equation (2-2) using

$$\tau^* = \frac{\tau}{(s-1)\gamma D_{50}} \quad (2\text{-}4)$$

where:

s = specific gravity of sediment (taken as 2.65)

D_{50} = bed surface particle size for which 50% of the material is finer (m)

For the purposes of comparing predicted to observed values, the dimensionless unit transport rate q^*_s from Equation (2-2) is then re-dimensionalized to find the volumetric transport rate. A rearrangement of the Einstein equation (Einstein 1950) was used for redimensionalizing:

$$Q_s = q_s^*\left[D_{50}\sqrt{(s-1)gD}\right]b \tag{2-5}$$

where:

Q_s = bed-load transport rate (m^3/s)

g = gravitational acceleration (m/s^2, taken as 9.807 m/s^2)

b = bed width (m)

2.5.2 Rosgen's Pagosa Reference Curve

David Rosgen's Pagosa Reference Curve (Rosgen et al. 2006) is an empirical dimensionless transport equation. The rating curve relates bed-load transport (made dimensionless by dividing all bed-load transport rates by the bed-load transport rate found at bankfull flow) to flow rate (made dimensionless by dividing all flow rates by the bankfull flow rate):

$$Q_s^* = -0.0113 + 1.0139(Q^*)^{2.1929} \tag{2-6}$$

where:

Q^*_s = dimensionless bed-load transport rate

Q* = dimensionless discharge

The final results are redimensionalized in order to compare to observed rates by multiplying the dimensionless bed-load transport rate by the bed-load transport rate at bankfull flow.

2.5.3 Wilcock's Two Parameter Model

The Wilcock Two-Parameter model is based on the Meyer-Peter, Müller equation, but has the advantage of being calibrated with observed data (Wilcock 2001). Sieve analyses of the captured bed-load revealed that all bed-load was in the gravel range. Therefore, in all Wilcock equations, f_i (fraction of gravel or sand) is 100% for gravel and 0% for sand.

To use the Wilcock model, a velocity-discharge relationship was needed. In order to create this relationship, trapezoidal cross sections were approximated for each site as a simplification using actual site geometry. Manning's equation was used to generate a relationship between discharge and depth. Manning's n was calibrated using observed data within reason by adjusting the value to minimize the squared error between observed and calculated values of depth. Velocity was then calculated by dividing discharge by area and a velocity-discharge curve was created.

Shear stress was calculated using

$$\tau = 0.052\rho(gSD_{65})^{0.25}v^{1.5} \quad (2\text{-}7)$$

where:

τ = shear stress (N/m^2)

ρ = density of water (kg/m^3, taken as 1000 kg/m^3)

g = gravitational acceleration (m/s^2, taken as 9.807 m/s^2)

S = slope (m/m)

D_{65} = bed surface particle size for which 65% of the material is finer (m)

v = water velocity (m/s)

Following Wilcock (2001), a dimensionless bed-load transport per unit width was calculated according to the relationship of τ to τ_r (a reference shear stress).

$$q_b^* = 11.2\left(1 - 0.846\frac{\tau_r}{\tau}\right)^{4.5} \quad for \quad \tau \geq \tau_r \tag{2-8}$$

or

$$q_b^* = 0.0025\left(\frac{\tau}{\tau_r}\right)^{14.2} \quad for \quad \tau \leq \tau_r \tag{2-9}$$

where:

q_b^* = dimensionless bed-load transport per unit width

τ_r = reference shear stress (N/m^2)

The resulting values from both equations are equal when the shear stress equals the reference shear stress. The bed-load transport rate is then redimensionalized using

$$q_b = \frac{q_b^* \rho_s \left(\frac{\tau}{\rho}\right)^{3/2}}{(s-1)g} \tag{2-10}$$

where:

q_b = bed-load transport per unit width (kg/s/m)

ρ_s = density of sediment (kg/m^3, taken as 2650 kg/m^3)

s = specific gravity of sediment (taken as 2.65)

These calculated values of bed-load transport per unit width are then superimposed on actual measured values and τ_r is adjusted to calibrate the model with the observed data. A calibrated curve for Site 1 along with the observed data is shown in Figure 2-6.

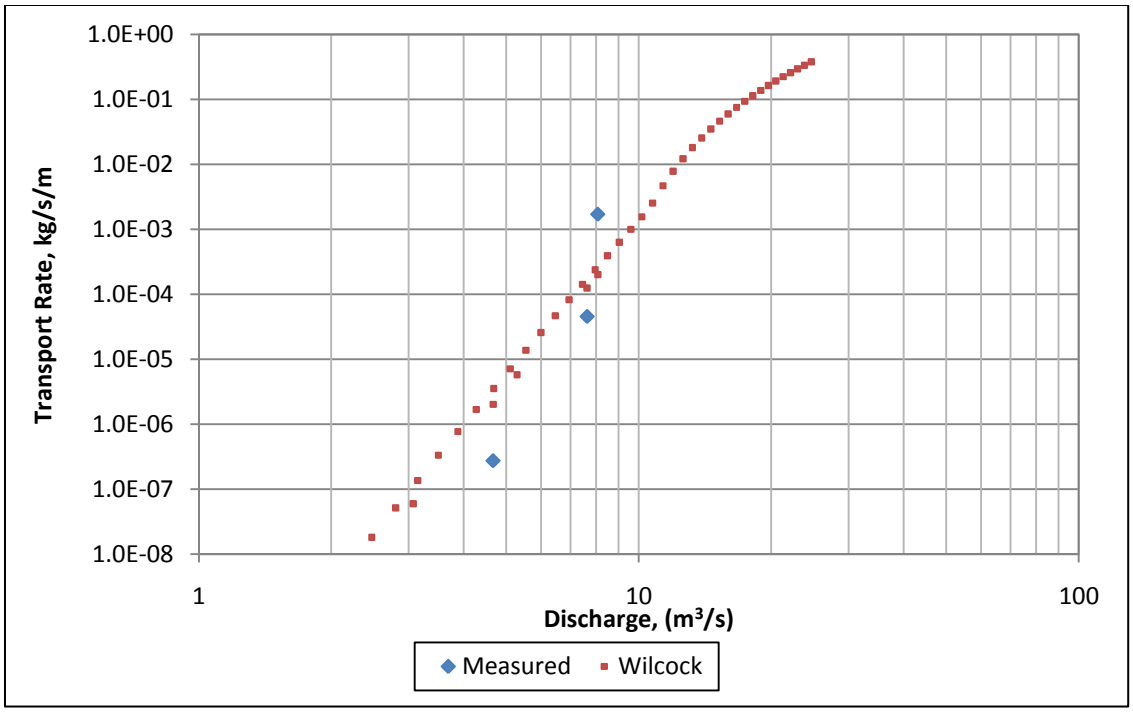

Figure 2-6. Calibrated Wilcock model curve along with measured transport rates.

2.5.4 Bathurst's Phase 2 Bed-load Transport Equation

The Bathurst method (Bathurst 2007) considers bed-load transport as supply-limited by a coarse armor layer (Phase 1), until a critical discharge, q_{c2}, is reached. When flows exceeds the critical discharge, motion of armor layer particles is initiated and a Phase 2 equation predicts bed-load rates:

$$q_s = \alpha\rho(q - q_{c2}) \tag{2-11}$$

where:

q_s = bed-load transport per unit width (kg/s/m)

α = rate of bed-load change as discharge changes

ρ = density of water (kg/m^3, taken as 1000 kg/m^3)

q = stream discharge per unit width (m^3/s/m)

q_{c2} = critical value of discharge per unit width for initiation of motion (m^3/s/m)

The armoring coefficient is found using

$$\alpha = 29.2S^{1.5}\left(D_{50}/D_{50s}\right)^{-3.30} \tag{2-12}$$

where:

S = slope (m/m)

D_{50} = bed surface particle size for which 50% of the material is finer (m)

D_{50S} = bed sub-surface particle size for which 50% of the material is finer (m)

The critical discharge, q_{c2}, for each site is calculated by averaging the results from

$$q_{c2} = 0.0513g^{0.5}D_{50}^{1.5}S^{-1.20} \tag{2-13}$$

and

$$q_{c2} = 0.0133g^{0.5}D_{84}^{1.5}S^{-1.23} \tag{2-14}$$

where:

g = gravitational acceleration (m/s^2, taken as 9.807 m/s^2)

D_{84} = bed surface particle size for which 84% of the material is finer (m)

Values for total bed-load transport rate are found for comparative purposes using:

$$Q_s = \frac{q_s b}{\rho s} \tag{2-15}$$

where:

Qs = total bed-load transport rate (m^3/s)

b = stream width (m)

s = specific gravity of sediment (taken as 2.65)

2.6 Comparative Results between Observed and Predicted Rates

Because each sample site had a different slope, depth, bed width, and substrate size, observed bed-load data were stratified by site, and predicted bed-load rates were calculated for individual sites. Figure 2-7 through Figure 2-9 show the sediment rating curves that were developed for each site based on observations and predictions. Observations and predictions that are not shown on the graphs have transport rate values of zero.

The results shown in Figure 2-7 through Figure 2-9 can be summarized by the following four observations: 1) the predicted rates from the uncalibrated Meyer-Peter, Müller equation are consistently between two and six orders of magnitude larger than observed rates; 2) the Rosgen curve predictions were generally within one or two orders of magnitude and predicted both above and below the observed rates at each site; 3) the calibrated Wilcock equation performed better than the uncalibrated MPM formula—Wilcock predictions were within an order of magnitude for Sites 1 and 3 but were consistently off by two orders of magnitude both above and below observed rates at Site 2; and 4) the Bathurst equation predicted rates were almost identical

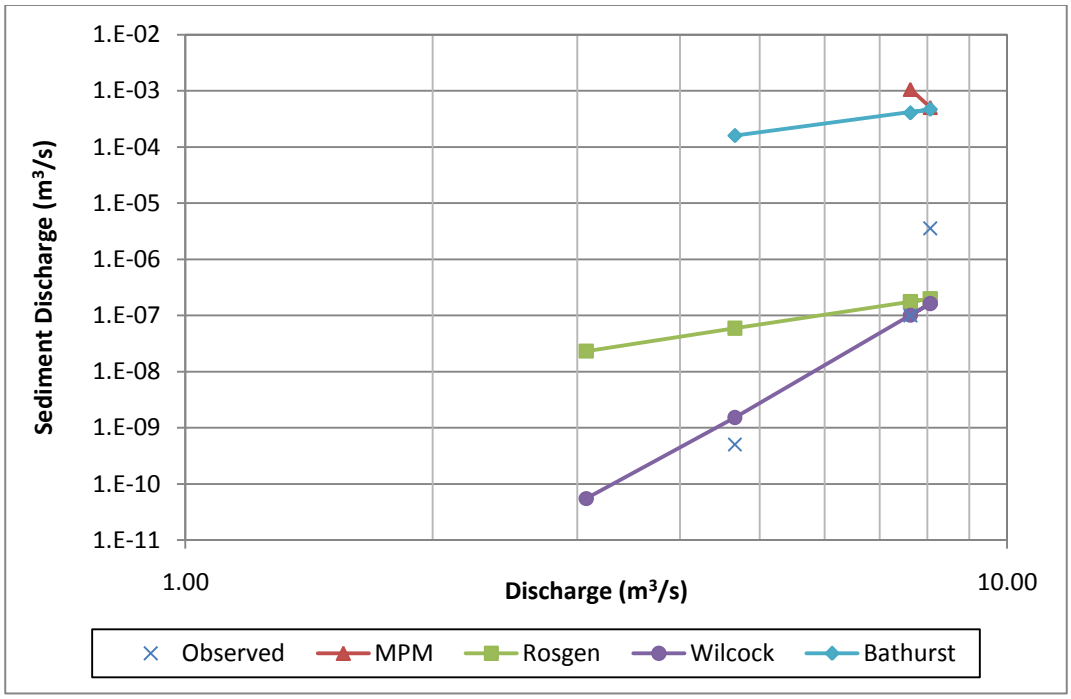

Figure 2-7. Predicted transport rates compared to observed rates at Site 1.

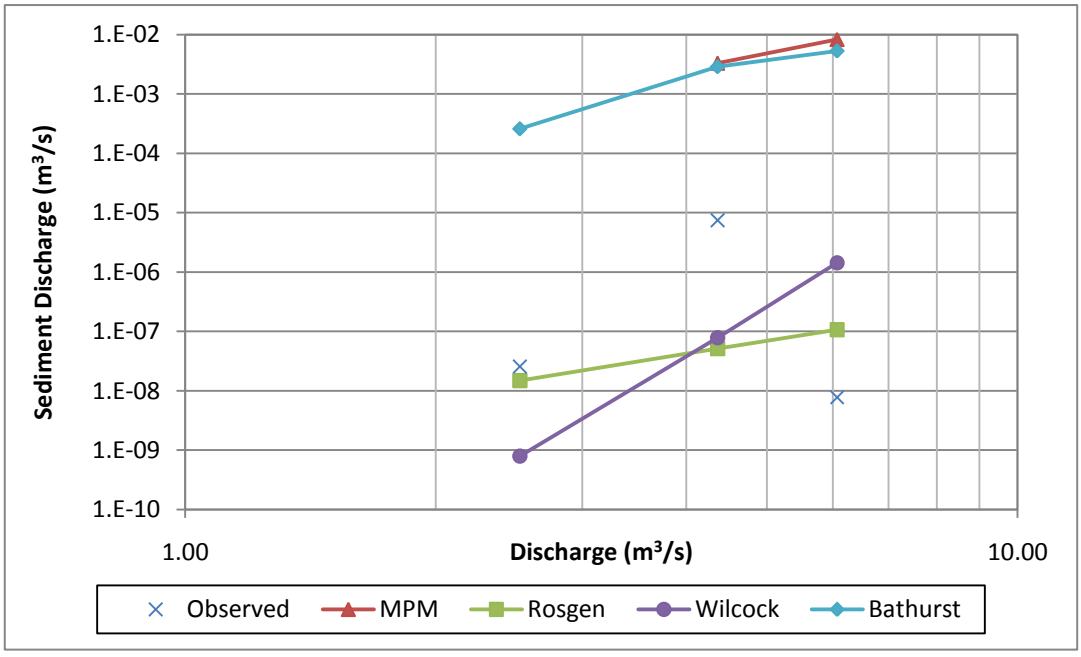

Figure 2-8. Predicted transport rates compared to observed rates at Site 2.

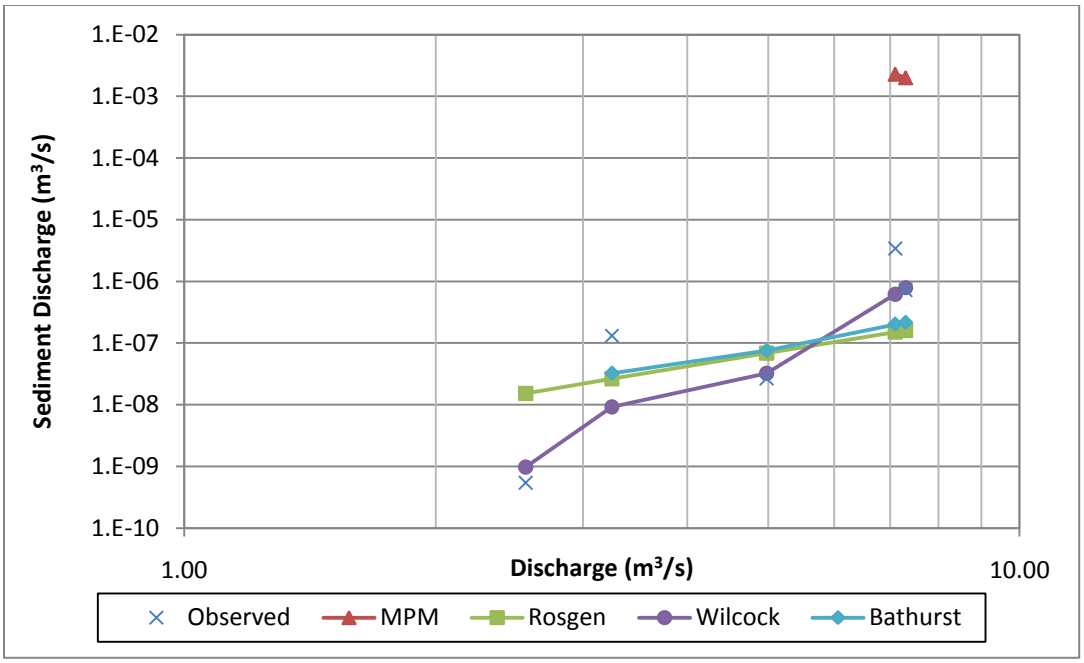

Figure 2-9. Predicted transport rates compared to observed rates at Site 3.

to the MPM predictions at Sites 1 and 2 but were within an order of magnitude at Site 3 where the armoring ratio was significantly higher than the other two sites.

It should be noted that the range of particles sizes encountered in this study at each site (2-110 mm) extend beyond the range of particle sizes (0.4-29 mm) used to develop the MPM equation (Brunner 2001). Also, Bathurst (2007) states that the armoring ratio should be between 1.52 and 11 for proper application of the Bathurst model. This assumption is violated at Site 3 which has an armoring ratio of 41. However, the high armoring ratio is the factor that makes the Site 3 prediction more accurate than the predictions at sites 1 and 2 where the assumption is not violated.

2.7 Implications of Discrepancies between Observed and Predicted Rates

Because sediment transport rates are a function of channel size, designing for different values of transport rate may result in different design channel dimensions. There are several methods for deriving channel sizes from sediment transport rate, but the general idea is to find a relationship between a transport equation and equations dealing with hydraulic geometry.

2.7.1 Method for Determining Channel Dimensions

The Stable Analytic Method (SAM) software calculates stable channel dimensions from a predetermined discharge and bed-load rate. The SAM method utilizes the MPM formula from 1948, the Limerinos equation for grain roughness, the Cowan equation for determining the total bed roughness coefficient, and Manning's equation for hydraulic calculations (Thomas et al. 2002). In this study, the Wilcock method for calculating channel dimensions from sediment transport rates was used as a simplification. This method differs slightly from the SAM software by using the Wilcock form of the Meyer-Peter, Müller equation. It assumes steady, uniform flow and all calculations are one dimensional. It also uses only rectangular channels and a single grain size (D_{50}) for the bed material.

Given discharge, bed-load transport rate, Manning's n, Shield's stress, D_{50}, and stream width, iterations are performed to solve for shear stress, slope, velocity, depth, and hydraulic radius. The iteration process begins with finding shear stress by using

$$\tau = \left[(s-1)\rho g D_{50}\right]\left[\tau_C^* + \left[\frac{Q_s}{8b\sqrt{(s-1)gD_{50}{}^3}}\right]^{2/3}\right] \quad (2\text{-}16)$$

where:

τ = shear stress (N/m^2)

s = specific gravity of sediment (taken as 2.65)

ρ = density of water (kg/m^3, taken as 1000 kg/m^3)

g = gravitational acceleration (m/s^2, taken as 9.807 m/s^2)

D_{50} = bed surface particle size for which 50% of the material is finer (m)

τ_c^* = critical Shields stress (taken as 0.047)

Q_s = bed-load transport rate (m^3/s)

b = stream width (m)

Uniform stream velocity from Manning's equation is

$$v = \frac{\sqrt{S}}{n} R^{2/3} \quad (2\text{-}17)$$

where:

v = stream velocity (m/s)

S = stream slope (m/m)

n = Manning's roughness coefficient

R = hydraulic radius (m)

Design flow depth can then be found from the continuity equation for a rectangular channel as

$$h = \frac{Q}{vb} \tag{2-18}$$

where:

h = design depth (m)

Q = discharge (m^3/s)

Hydraulic radius is found using

$$R = \frac{bh}{b + 2h} \tag{2-19}$$

Once the hydraulic radius is known, design slope can be found using the shear stress found above:

$$S = \frac{\tau}{\gamma hR} \tag{2-20}$$

where:

γ = specific weight of water (N/m^3, taken as 9800 N/m^3)

This iteration process is performed for a range of stream widths until a slope equal to the existing stream slope is found. At this point, the stream width and flow depth are recorded as representing the channel design dimensions.

Due to the iterative process, using different values of sediment transport from different predictive models will ultimately result in different design channel dimensions.

2.7.2 Comparison of Channel Dimensions

The process outlined above was used to determine hypothetical design dimensions for Hobble Creek based on the observed and predicted transport rates at bankfull conditions for each site. Based on the nature of the iterative equations, two solutions are possible for each set of input values. One solution results in a deep, narrow channel while the other solution results in a shallow, wide channel. Because the shallow, wide channel more closely represents the existing channel, this design was chosen as the solution to use for the comparisons in this study. Five different sediment transport values were used at each site to find channel dimensions—the observed transport, and each of the four predicted transport values. The five resulting design cross sections are compared to currently existing cross sections in Figure 2-10 through Figure 2-12.

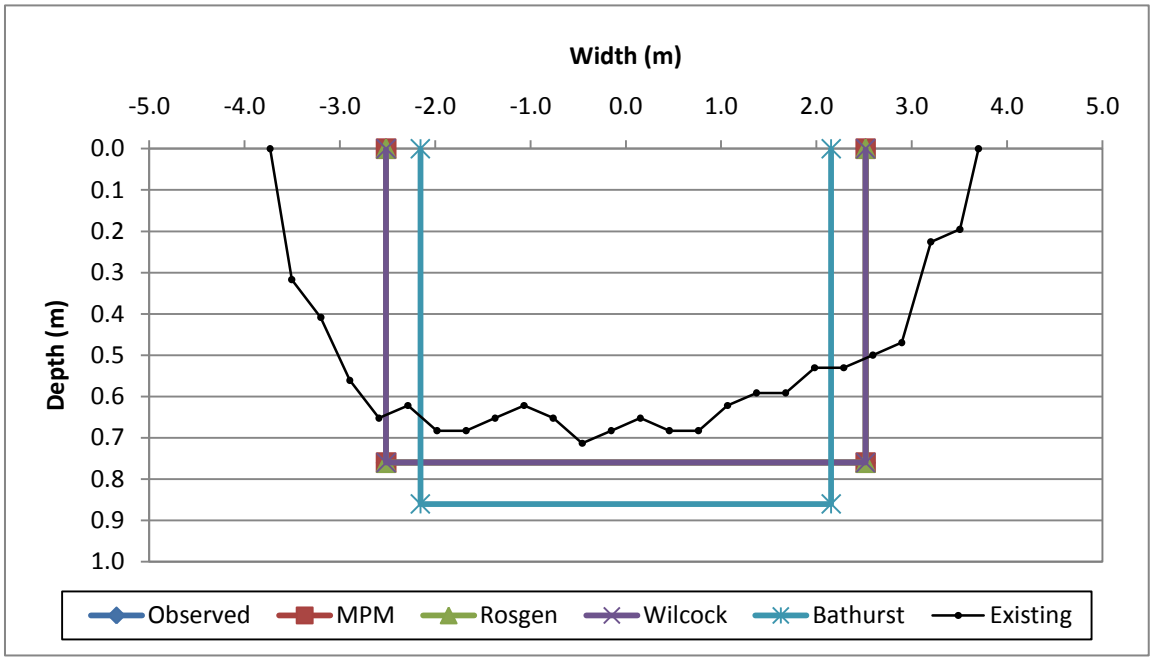

Figure 2-10. Design and existing cross sections for Site 1.

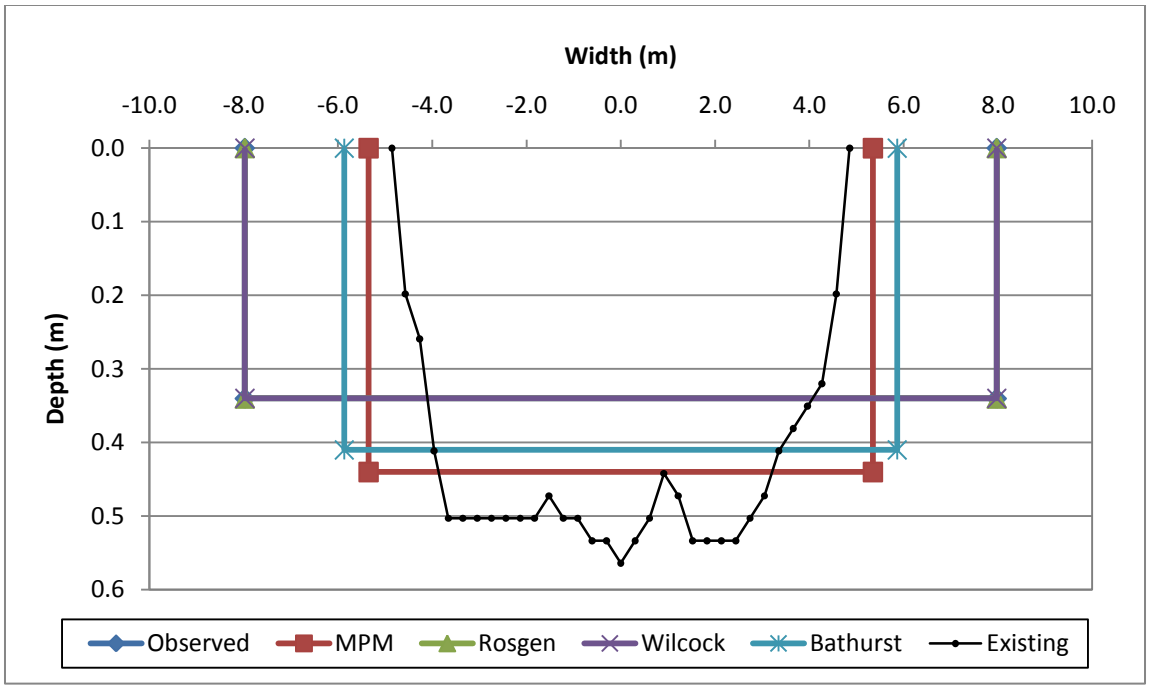

Figure 2-11. Design and existing cross sections for Site 2.

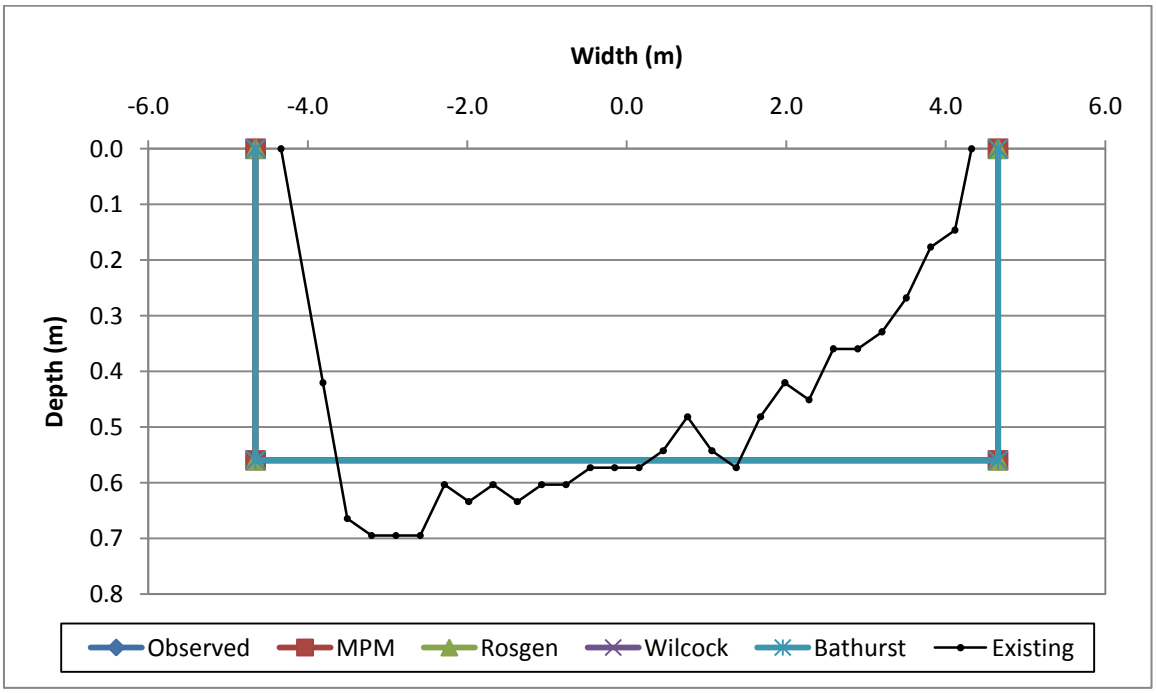

Figure 2-12. Design and existing cross sections for Site 3.

2.7.3 Discussion on Channel Dimensions

Urbanization and flood control efforts extending over the past century since the settlement of Utah Valley have considerably altered the course, shape, and hydrologic regime of Hobble Creek. Some discrepancy between the natural and constructed channel can only be expected.

Bankfull channel dimensions for all predictive equations match the channel dimensions derived using the observed transport rate at all sites with the exception of the Bathurst model at Sites 1 and 2 and the MPM model at Site 2. These exceptions correspond to the models that significantly overpredicted the transport rate at bankfull flow.

Further analysis revealed that a transport rate threshold seemed to exist in the development of channel designs. Before the transport rate reached a value of about 10^{-6} or 10^{-5} m^3/s, all channel designs remained constant. Once this threshold was reached, channel designs from different predictive models and observed rates began to show increasingly significant variation. All bankfull transport rates in this study, with the exception of the two Bathurst predictions and the MPM prediction mentioned above, were below the described threshold.

This observation is important when considering the difference between threshold and alluvial channels. Because the study sections of Hobble Creek are supply-limited, it is reasonable to assume that if the same study were to be done on an alluvial channel, observed transport rates would be higher. A theoretical adjustment of the observed transport rates in this study would result in the same predictions from the MPM and Bathurst models. However, the Rosgen model would predict higher values due to the bankfull transport rate being higher, and the Wilcock model would yield larger predictions due to the calibration process that essentially pins the predictions near observed values.

In general, models that overpredicted transport rates (MPM and Bathurst) resulted in channels that were one-third to one-half as wide and one-third to one-half deeper than the channels developed from observed rates. Variations from observed rates increased with transport rate. Calibrated models (Rosgen and Wilcock) always resulted in channel dimensions that were similar to dimensions predicted by observed rates.

2.8 Conclusions

The objective of this study was to demonstrate the importance of field data in a stream restoration effort. Bed-load and the variables that control it vary considerably between locations, and a predictive equation may not account for every possible controlling parameter. For example, the Bathurst equation accounts for a course armor layer that limits supply. This may improve the predicted rate accuracy over non-calibrated, capacity limited equations, but there may be other factors besides the armor layer in limiting bed-load on Hobble Creek and other streams. In order to capture the effects of all the influencing factors, predictive models should be calibrated using observed transport data. This is especially true in alluvial channels where bed-load transport rates are comparatively higher than in supply limited channels.

While these results are applied specifically to the Hobble Creek restoration effort, they are also generally applicable to all restoration projects involving channel design and realignment. Although some sediment transport models may predict a transport rate close to that which actually occurs, uncalibrated models may mispredict rates by several orders of magnitude, resulting in incorrect channel design dimensions. Better even than a calibrated model, bed-load transport rates obtained in the field, though expensive to obtain, are more reliable than any model, and less expensive than a project failure.

3 A Detailed Topographic Survey of the Hobble Creek Channel from Interstate 15 to Utah Lake

3.1 Chapter Abstract

Due to the endangerment of the June sucker (*Chasmistes liorus*) the lower portion of Hobble Creek has been the focus of several restoration efforts. Construction was completed near the end of 2008 and involved relocating the existing channel into a new channel that included meanders and a floodplain with side ponds. Since that time, annual surveys have been completed in order to monitor geomorphological changes. The 2010 survey contains labeled points that cover the entire property with an approximate 10 foot resolution grid. Water surface elevations were surveyed for two different discharges, 0.15 cfs and 23 cfs. A profile plot of the channel invert and a topographic map of the floodplain are also included in the 2010 data set. A comparison of the 2010 survey with the 2009 survey does not reveal any significant lateral changes. The majority of changes that occurred involved small alterations of the connections between the side ponds and the main channel. It is suggested that the annual surveys continue to be performed, especially with the introduction of the new Interstate 15 culvert upstream and the anticipated supplemental flows that will be introduced within the next few years. Future annual surveys should include an analysis of elevation changes along with lateral changes and an HEC-RAS sedimentation model should be created using the 2010 data set.

3.2 Introduction

On April 30, 1986, the June sucker (*Chasmistes liorus*) was federally listed as an endangered species with critical habitat (JSRIP 2010; JSRT 1999). At that time, it was estimated that fewer than 1,000 adult June sucker lived in Utah Lake (JSRIP 2010). By 1998, that number had dropped to less than 300, based on counts of spawning adults (Keleher et al. 1998). Restoration efforts are being made in an attempt to save the June sucker population. For example, in 2005, 8,809 June sucker were transferred from a protected breeding site to Utah Lake (CUWCD 2005).

Currently the lower 4.9 miles of the Provo River is the only self-sustaining reach utilized by the June sucker for spawning (JSRIP 2010). According to a study done by Cope and Yarrow (1875), many other Utah Lake tributaries such as Hobble Creek and Spanish Fork were also used for spawning in the late 1800's. One of the steps that must be completed in order to delist the June sucker as an endangered species is to recreate a second self-sustaining spawning run. Hobble Creek has been identified as the best candidate for this restoration. Figure 1-1 shows an aerial view of the westernmost reach of Hobble Creek in June of 2010.

As seen in Figure 3-1, restoration efforts have been completed on the quarter mile section of Hobble Creek between Interstate 15 and Utah Lake (see Figure 3-1). In addition to constructing meanders and side pools, part of the construction was to remove invasive reeds (*Phragmites australis*) that were preventing the June sucker from finding the entrance to Hobble Creek. Since the relocation effort, adult June suckers have been observed to migrate in Hobble Creek as far upstream as Packard Dam (Stamp 2010).

Figure 3-1. Aerial photo of Hobble Creek taken in June 2010.

Yearly topographic surveys have been performed since construction was completed. The purpose of these surveys is to discover and monitor geomorphological changes such as channel widening, incision, and sedimentation. In addition, these surveys provide topographic data for other studies that are performed on this section of Hobble Creek.

A major purpose of this paper is to describe the topographic data set that was collected during the 2010 survey so that it can be utilized in future studies. Another purpose is to provide an annual report on observed changes that have occurred since construction, and particularly since the 2009 survey.

3.3 Survey Methods

The 2010 survey was completed during October 2010. All survey points were acquired using a Topcon GR-3 GPS that transmitted to a handheld data collector. Points were adjusted

using the Spanish Fork base station. Several methods were employed while collecting points. All points that were either submerged, at the water's edge, or of particular importance such as a fence or other structure, were taken by mounting the GPS unit to a survey rod as seen in Figure 3-2. Discharge during the survey was determined from the USGS stream gage located about 3,500 ft upstream. Because the 1000 N diversion dam is located between the gage station and the survey reach, the actual discharge may be slightly lower than reported.

Figure 3-2. Survey rod with GPS unit and data collector.

Channel definition points were taken at the water's edge, the invert, and any grade changes in between. Cross sections in the channel were spaced at intervals of 20-30 feet.

Because the survey was conducted at the end of the irrigation season, water surface points were able to be collected for two flow levels—one at 0.15 cfs while water was still being diverted, and one at 23 cfs after the diversions were closed. Side pond points were taken at water's edge and along transects of approximately 20 foot spacing.

For submerged points where the ground was particularly soft, a 1 foot diameter plastic dinner plate was mounted to the bottom of the survey rod (see Figure 3-3) to keep the tip of the rod from sinking into the mud.

Figure 3-3. Dinner plate used to keep tip from sinking into the mud.

For all other general topographic points (i.e. points that were not submerged or at the water's edge), the GPS was set to automatically collect a point every 5 feet while the operators walked transects spaced about 10 feet over the entire floodplain. In order to collect these points,

the GPS unit was either mounted on top of a survey rod that was held firm against the operators body while he was walking or it was mounted on a backpack that was worn by the operator (see Figure 3-4).

Figure 3-4. GPS mounted on backpack for automatic point reading.

Existing control points that were used to establish common points in each annual survey were destroyed during the construction of the new Interstate 15 culvert. However, replacement control points were available by using the fence posts that outline the small parking area in the southeast corner of the property along with the fence posts that cut across the western edge of the property. Using this method the 2010 survey was able to be matched to the 2009 and 2008 surveys.

3.4 Description of Survey Data Set

The survey data set that was collected in 2010 covers the entire 21-acre lot that encloses the Hobble Creek restoration site. It also extends west about 1,700 feet beyond the fence line towards Utah Lake. This extension of the survey was possible due to the relatively low level of Utah Lake at the time of the survey. The data set contains over 29,000 points that cover the area in a quasi-grid with a resolution of approximately 10 feet. It is hoped that this data set will be used in future studies of this area. Figure 3-5 shows the outline of the property with the location of all survey points.

Figure 3-5. Restoration property with survey points.

The data set is divided into points that describe the location of: the water surface at two different flows (0.15 cfs and 23 cfs), the channel invert, grade control structures, ponds, fence posts, the new Interstate 15 culvert, the natural grade, and saddle points on natural grade between ponds and the main channel.

Once the survey was complete, the data were imported into Civil 3D and a surface was created. A topographic map of the surface is shown in Figure 3-6 with 1 foot contours.

Figure 3-6. 2010 Topographic map with 1 foot contours.

Figure 3-7 shows the 3-dimensional surface overlaid with an image of the property obtained from Google Earth. Figure 3-8 shows the surface with the z-axis magnified by 10x. The view is from the southeast in both figures.

Figure 3-7. 3D surface with Google Earth image overlay.

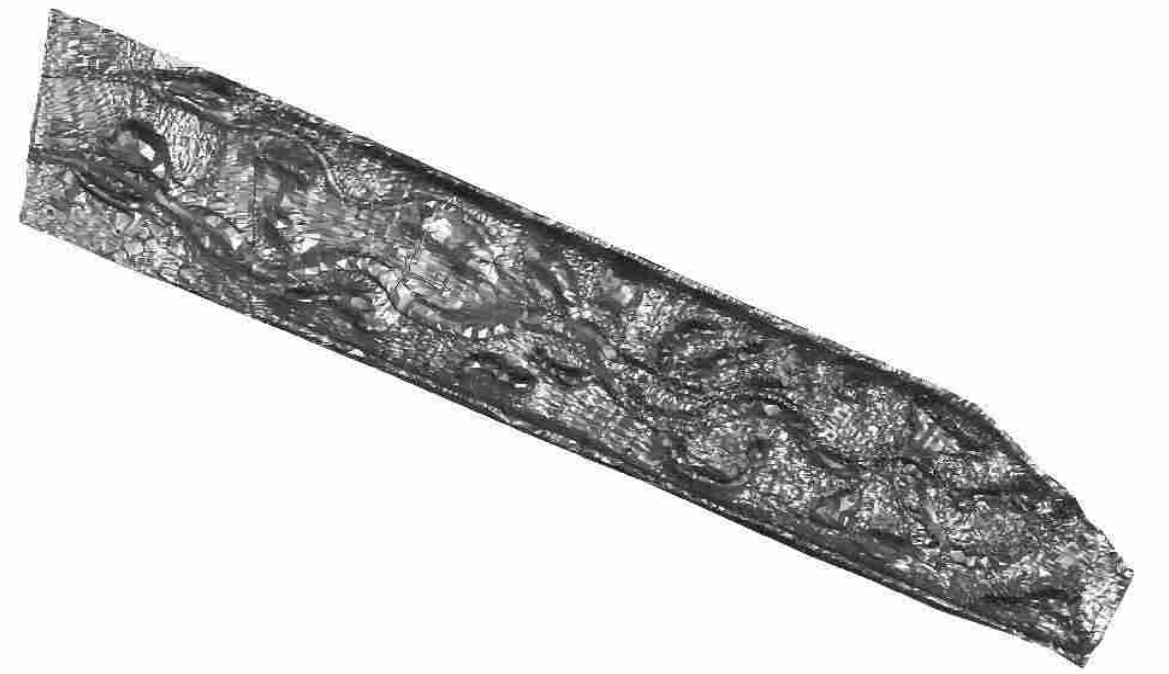

Figure 3-8. 3D surface with elevation magnified by 10x.

3.5 Profile Plot

Using the invert elevations and stationing along the main channel starting from the most upstream fence, a profile plot was generated. The profile splits at the separation of the north and south branches. The north branch profile is shown by the dashed line while the south branch profile is shown with a dotted line.

The beginning of the north branch consists of a series of pools, thus the dramatic rising and falling of the profile plot at that point. The south branch is the preferred flow path during low flows. This is due to the relatively high elevation right after the first pond on the north branch, which restricts flow in that direction. In order for the north branch to be connected, the water surface elevation must exceed this elevation of about 4,434 feet.

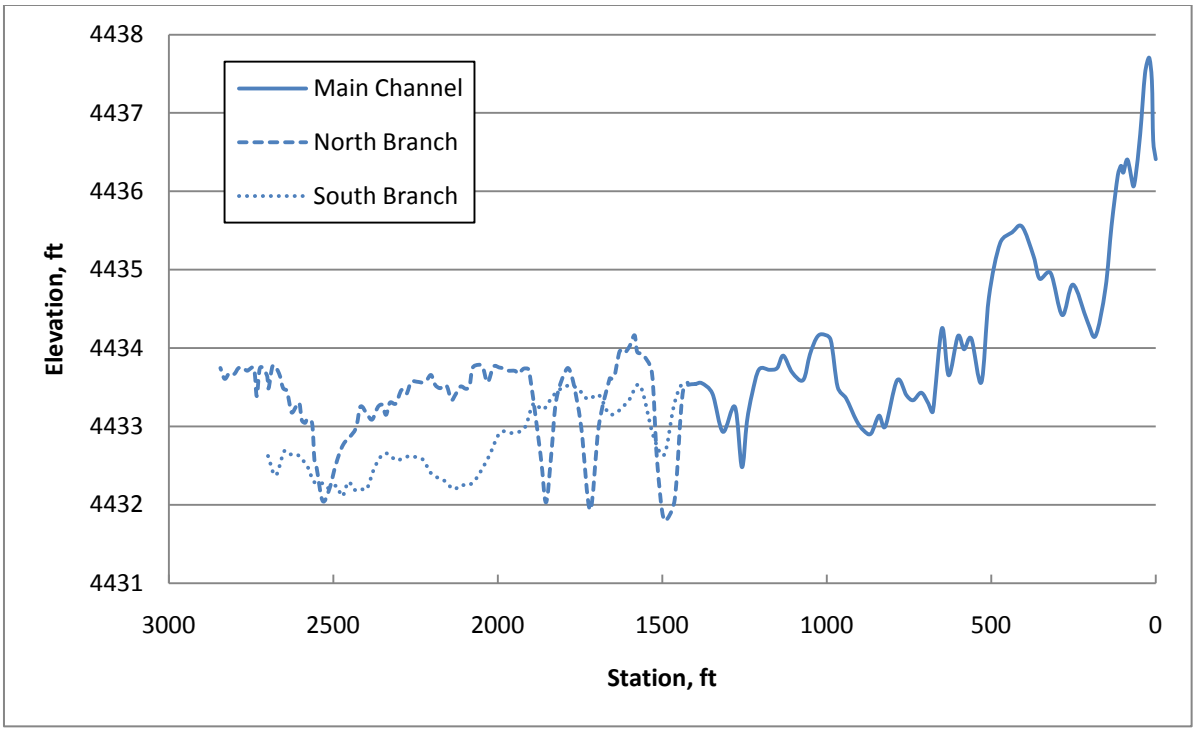

Figure 3-9. Profile plot of Hobble Creek restoration showing north and south branches.

The profile plot also shows that most of the elevation drop is completed in the first 600 feet of the channel. The remainder of the channel is mostly flat allowing Utah Lake to rise and inundate the floodplain. This is how the restoration was designed to function.

3.6 Multiple Discharge Comparison

As was previously mentioned, the timing of the 2010 survey worked out so that the water surface was able to be mapped at two different discharges—0.15 cfs and 23 cfs. This was possible due to the end of the irrigation season which meant that the upstream diversions were closed, causing more flow to be directed down Hobble Creek. Figure 3-10 shows the 0.15 cfs survey superimposed onto the 23 cfs survey.

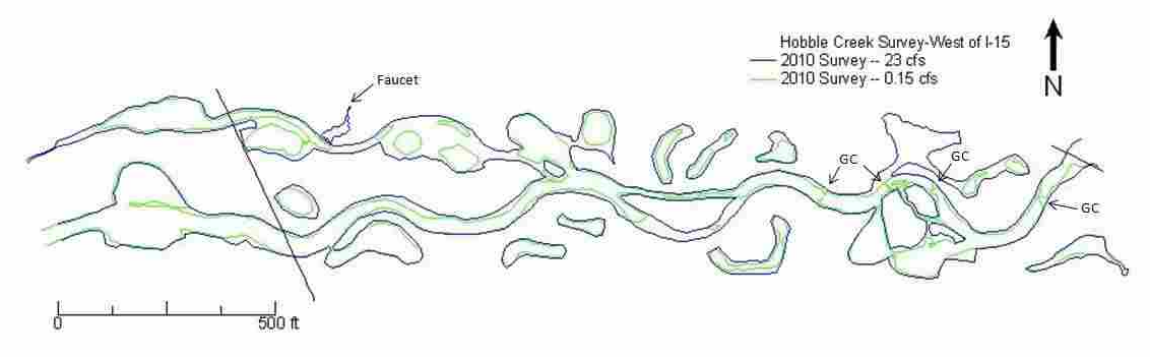

Figure 3-10. Overlay of 2010 surveys at 0.15 cfs and 23 cfs.

Four separate grade control structures are visible on the first 800 feet of the main channel in the 0.15 cfs survey and are shown where the channel seems to be temporarily pinched together.

Several observations can be made from the comparison of these surveys. The main difference is that the 0.15 cfs flow is directed entirely down the south branch of the main channel. The north branch is not connected. It should be noted that much of the water that was ponding in the last 500 feet of the north branch came from a leaky faucet near the north fence. Consequently, this portion of the survey may not be entirely representative of discharge solely from Hobble Creek.

Another significant observation is the effect that the change in discharge had on the ponds. Several of the ponds had water levels low enough to split into multiple smaller ponds. The second pond on the north side did not have any water in it at all during the low discharge. In addition, the southern branch of the temporary split in the middle of the property was not completely connected.

3.7 Annual Comparison

The peak discharge for the 2010 runoff season was 100 cfs (USGS 2010). This represents slightly more than the one year flood. The 2010 survey is the third annual survey to be performed on the restoration reach. The 2008 survey was completed as a baseline before any water was diverted into the reach. That survey simply outlined the channel banks and the channel centerline and provided a rough topographic map of the area. The 2009 survey was performed in October of 2009 during an average flow of 21 cfs, and showed the changes that occurred after the first runoff season. The 2009 survey included 5-point cross sections that were taken at 5-10 foot intervals along the main channel and additional points that mapped the perimeter and depth of the side ponds (Parsons 2010). As a reference, an overlay map of the water surface for the 2008 and 2009 surveys has been included as Figure 3-11. The darker lines are the 2009 survey while the lighter lines are the 2008 survey.

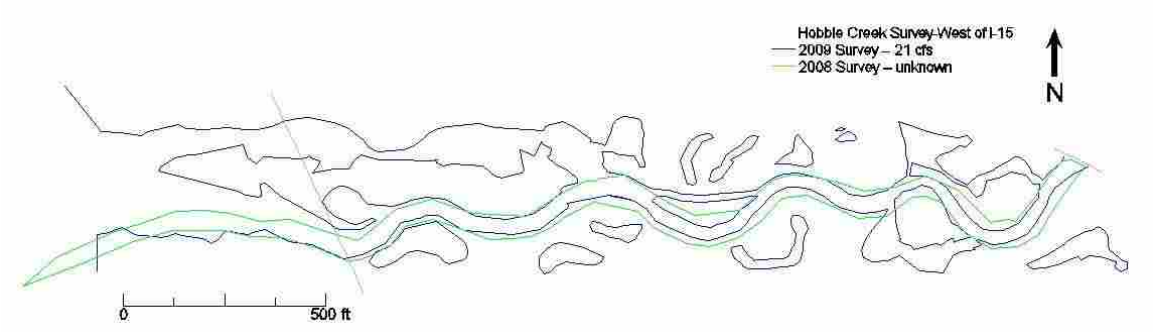

Figure 3-11. Overlay of 2008 and 2009 surveys.

Figure 3-12 shows the 2010 survey superimposed on the 2009 survey. The darker lines depict the 2010 survey while the lighter lines show the 2009 survey. The diagonal line at the west end of Figure 3-11 and Figure 3-12 is the property fence that cuts across the restoration.

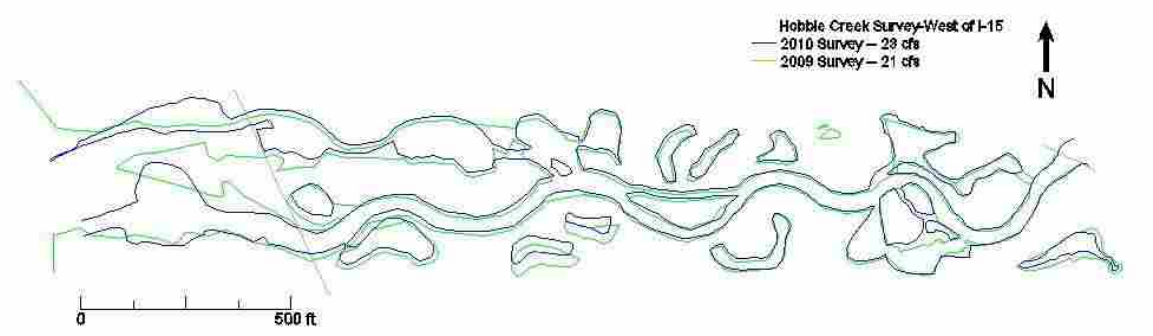

Figure 3-12. Overlay of 2010 and 2009 surveys.

Many of the observations made in 2009 were once again seen in the 2010 survey. A few of these observations, along with some additional observations, will be pointed out in greater detail. Figure 3-13 shows 10 areas of interest that will be discussed.

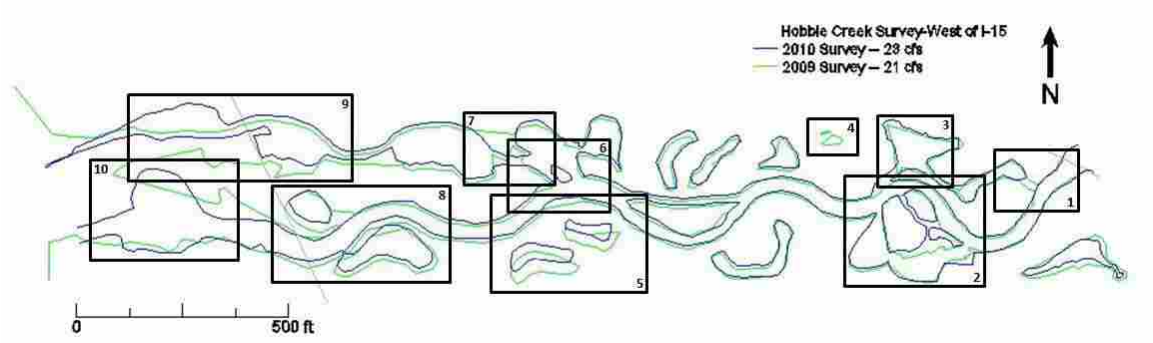

Figure 3-13. Areas of interest in 2009 and 2010 survey comparison.

The first area of interest (see Figure 3-14) was noted in 2009. The first two ponds on the north side of the channel interconnect with each other and the channel and form an alternate flow path. At the time this section of the channel was surveyed, the connection had not yet appeared. It was observed later in the month.

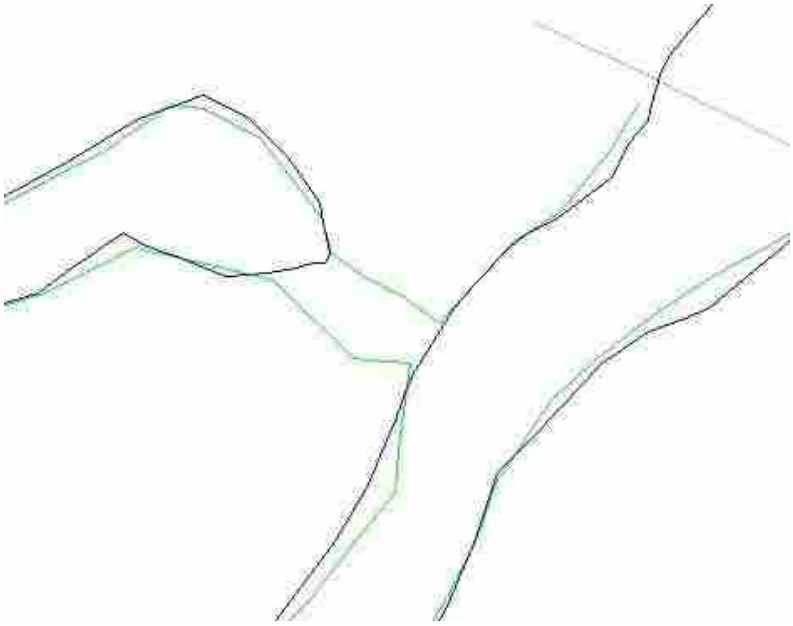

Figure 3-14. Connection of first side pond on north side.

The next area interest is the island formed by the connection with the main channel by two of the side ponds on the south side of the creek (see Figure 3-15). During the 2010 survey, a small forked stream was observed to flow from southeast to northwest across the island. This stream was not noted in the 2009 survey.

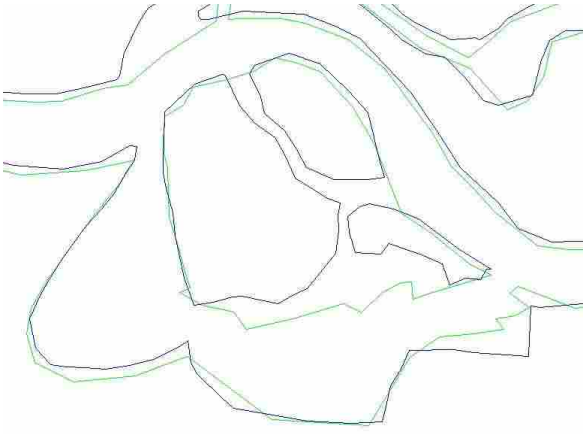

Figure 3-15. Streams flowing across island formed by side pond connection.

The third observation is the location where the alternate route mentioned in the first observation reconnects with the main channel. In the 2009 survey, this connection occurred in a narrow, north-south channel. It was observed in the 2010 survey that the connection flowed westward over relatively flat ground before slowly dumping back into the main channel over a ledge about one foot high.

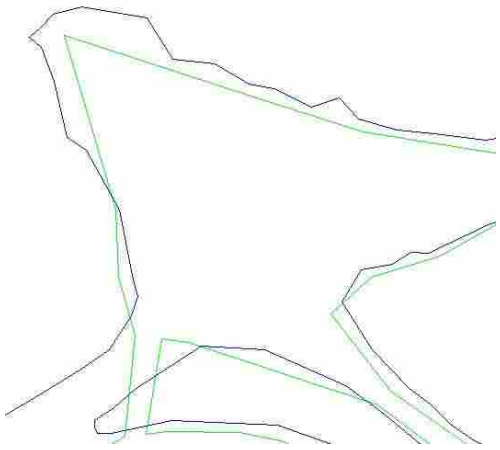

Figure 3-16. Reconnection of second side pond on north side.

Two small side ponds on the north side of the channel appeared in the 2009 survey, but not in the 2010 survey. This is likely due to the groundwater table being lower during the 2010 survey than it was during the 2009 survey. The lower groundwater level was evident by noting that the level of Utah Lake was lower during the 2010 survey.

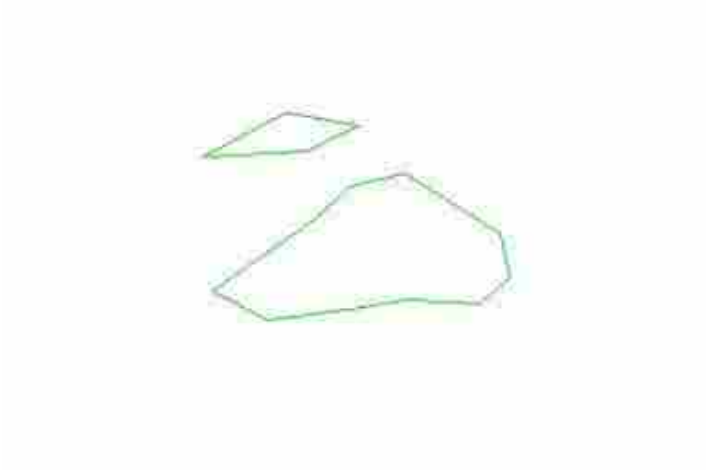

Figure 3-17. Two side ponds appearing in 2009 but not in 2010.

Once the process of overlaying the annual survey was complete, it was noticed that two side ponds on the south side of the channel did not overlap very well. It is not likely that these ponds migrated over such a distance, especially while retaining their shape. The offset is probably due to a data processing error. It is believed that the location of the ponds in the 2010 survey is correct.

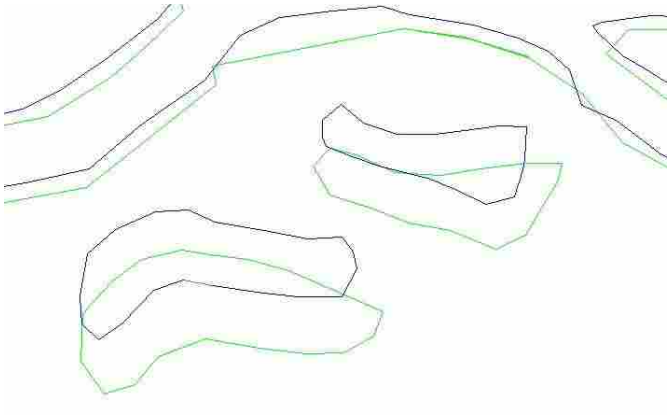

Figure 3-18. Offset of two side ponds on the south side is probably a data error.

The fifth major observation that was noticed is a small island that is forming in the entrance to the north branch. During low flows, the island is connected to the natural grade on the west, while all flow goes to the east. However, during high flows, water is free to move around both sides. The island is made up sediment that is being caught by tree branches and other debris, likely placed there during construction.

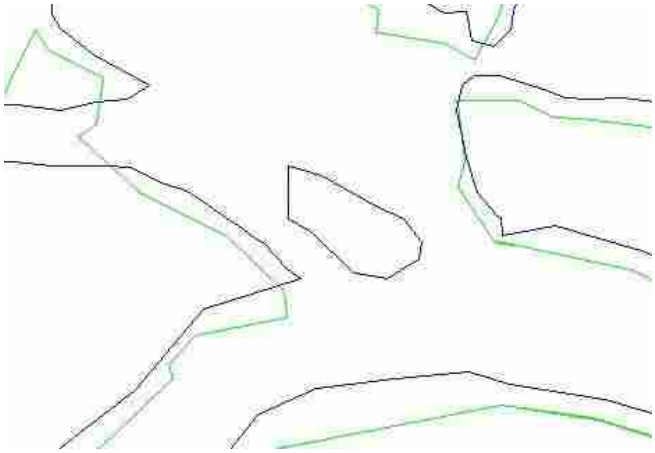

Figure 3-19. Small island forming in entrance to north branch.

The natural grade between the first two ponds in the north branch of the channel is relatively flat. In 2009, the connection between these two ponds was observed to be further north than it was in 2010.

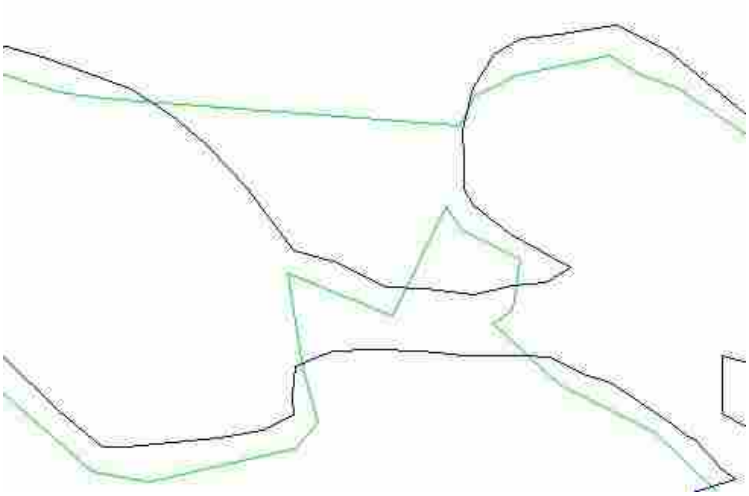

Figure 3-20. Alternate connection of ponds in north branch.

In 2009, it was observed that the side pond just east of the fence on the north side of the south branch of the main channel was connected at a flow of 21 cfs. At this same flow, the pond opposite that pond was disconnected. In 2010, just the opposite was observed. The pond on the south side was observed to be connected, even at a flow as low as 0.15 cfs. The pond on the north side was still not connected during a flow of 23 cfs.

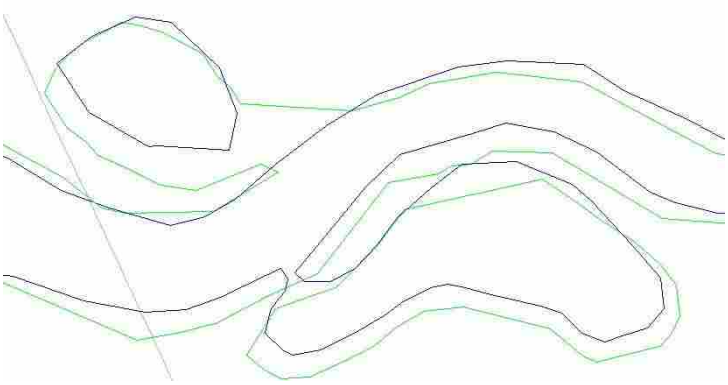

Figure 3-21. Connection and disconnection of side ponds on south branch.

Due to differing lake levels during both annual surveys, it is difficult to accurately compare the location of the channel surveys near Utah Lake. Figure 3-22 and Figure 3-23 show the north and south branches, respectively, as they approach the lake. The north branch seems to have expanded to the north, rather than the south, once the flow passes the fence. The south branch seems to have mostly maintained its position.

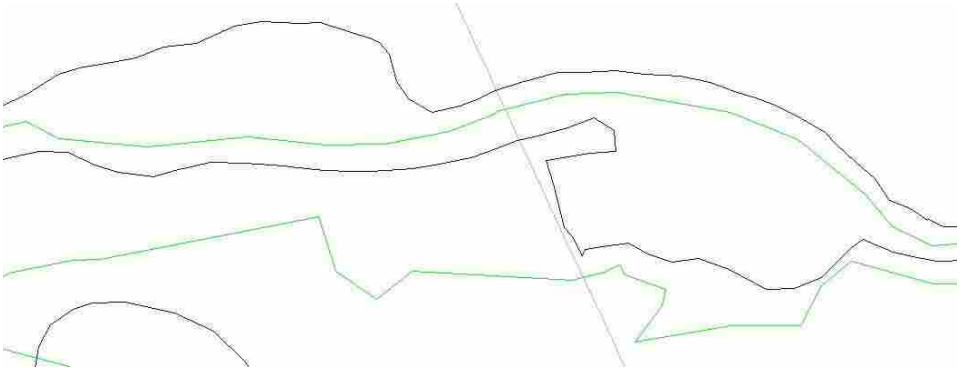

Figure 3-22. Alternate water surface location near lake on north branch.

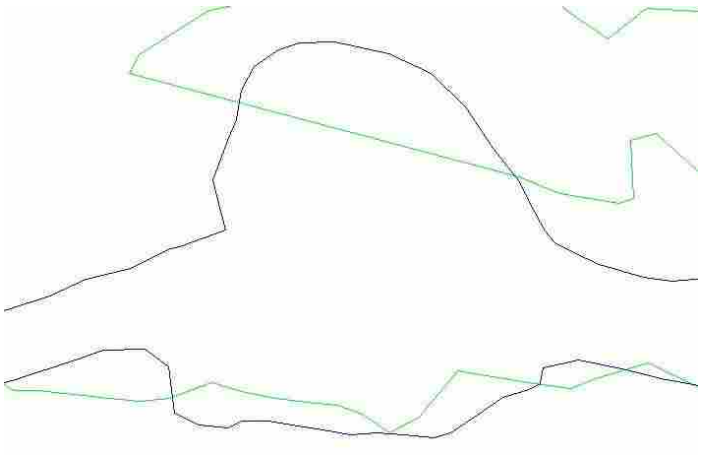

Figure 3-23. Alternate water surface location near lake on south branch.

3.8 Summary

Detailed topographic data for the Hobble Creek restoration site were obtained following the 2010 spring runoff season. The data set covers the entire property with an approximate 10 foot resolution. The data set also contains water surface elevation data for two different flows (0.15 cfs and 23 cfs) and features other points such as the channel invert, saddle points, and fence lines. A profile plot of the channel invert is also included.

A comparison of the 2010 survey with the 2009 survey showed minimal lateral change. This was largely due to a relatively low peak discharge for the 2010 runoff season and a stable channel design. Most changes that did occur during the 2010 runoff included small alterations of the connections of side ponds with the main channel.

3.9 Suggested Further Research

Although the same level of detail is not always required, it is suggested that basic annual surveys continue to be done in order to monitor changes that occur. This is especially important

with the introduction of the new Interstate 15 culvert that will open prior to the 2012 runoff season and the supplemental flows that will be added within the next few years.

In addition to lateral changes in the channel and side ponds, future surveys should include profile plots that allow the comparison of elevation changes caused by aggradation and degradation. To ensure accurate annual comparison of profile plots, permanent station markers should be installed along the channel as reference points that can be used to adjust the overlay of each survey.

Elevations changes should also be monitored in each side pond in order to understand the amount of sedimentation that is occurring in those locations. Sediment deposition is especially important on the entire floodplain of the lower 2,500 feet of the property due to the annual inundation by Utah Lake. All sedimentation may be better understood by developing an HEC-RAS sedimentation model. The 2010 survey data set provides a lot of the information necessary for this model to be set up and calibrated.

4 Relevance and Application of Findings to June Sucker

The data sets and observations that have resulted from this work are beneficial to the restoration efforts that are being made on Hobble Creek. Some of the ideas presented here, such as the development and comparison of bed-load transport models, can also be applicable in other locations that possess characteristics similar to those of Hobble Creek.

The particle size distribution data set can be used to determine where the bed material that is suitable for June sucker spawning is currently located along the creek. It can also be used to identify what the stable state conditions are for the channel in its present form (existing diversion dams, crossings, alignment, and geometry). An understanding of the stable state conditions will help channel design engineers ensure that the designed substrate material will not be washed out or filled in with finer sediment just a few years after restoration construction is completed.

Physical Habitat Simulation System (PHABSIM) software enables users to determine the suitability of a habitat for a specific species based on inputs such as flow, cross sections, bed material, and coordinate data. When coupled with survey and flow data, the data collected in this study can be used in a 1-D PHABSIM model to determine the impacts of channel alterations and stream flow augmentation on June sucker habitat. The PHABSIM software also facilitates analysis of different flow regimes by integrating the results with various discharge time series data. Using this process, normal and dry year conditions can be simulated to determine the

impact on June sucker spawning habitat. Water delivery schedules can also be created to ensure that sufficient flow is present to sustain adequate habitat.

The bed-load transport data are another tool that can be used by engineers to design the substrate material and associated channel dimensions that facilitate a stable channel. Although the data set is still too small to validate any of the sediment rating curves for Hobble Creek, this work provides an important step towards a better understanding of bed-load transport on Hobble Creek. Once additional data are able to be collected and the models can be validated, design engineers will be able to better predict sediment movement rates in Hobble Creek. Furthermore, because of the similarities that exist between most of the tributaries that drain westward from the Wasatch Mountains into Utah Lake (geographic location, urbanization, soil type, land use, etc.), the transport models developed for Hobble Creek may be reasonably applied to other rivers such Provo and Spanish Fork.

When combined with data from previous years, the topographic survey data are used to monitor changes in the portion of Hobble Creek that lies west of Interstate 15. The changes that affect June sucker the most involve sedimentation in the side ponds. Because the side ponds are only connected to the main channel (and thus to Utah Lake) for a few weeks out of the year, it is currently being investigated whether or not the side ponds can be used as a refuge where juvenile June sucker can develop for a season before being exposed to Utah Lake predators (Rader 2011). Too much sedimentation in the side ponds will not allow sufficient habitat to develop and will eventually fill in the ponds.

The topographic data can also be used to determine what channel flow is required before each pond will be connected to the main channel. This would supplement the work of Parsons (2010) which describes how long each pond is connected during an average water year.

In order to determine what flow is required, a variable stage Gridded Surface Subsurface Hydrologic Analysis (GSSHA) model should be set up that models flow over the entire property. As stage increases, the GSSHA output allows the user to visually note at what flow each pond becomes connected to the main channel.

Another method of determining connectivity would be to use measured data from the USGS stream gage located about 3000 feet upstream from the property. Individual storm hydrographs or seasonal hydrographs can be input into the GSSHA model to determine which ponds were connected at what times.

REFERENCES

Andrews, E., and Parker, G. (1987). "Formation of a coarse surface layer as the response to gravel mobility." *Sediment Transfer in Gravel-Bed Rivers. John Wiley & Sons New York. 1987. p 269-300, 13 fig, 37 ref. U. S. E. P. A. Grant*.

Bathurst, J. C. (2007). "Effect of coarse surface layer on bed-load transport." *Journal of Hydraulic Engineering*, 133, 1192.

Brown, J. M. (2008). "Sedimentological and biological analyses on Hobble Creek prior to restoration," Brigham Young University.

Brunner, G. (2001). "HEC-RAS River Analysis System: Hydraulic Reference Manual, Version 3.0." *US Army Corps of Engineers: Davis, California*.

Bunte, K., and Abt, S. R. (2001). "Sampling surface and subsurface particle-size distributions in wadable gravel-and cobble-bed streams for analyses in sediment transport, hydraulics, and streambed monitoring." 2001.

Bunte, K., Swingle, K. W., and Abt, S. R. (2007). *Guidelines for using bedload traps in coarse-bedded mountain streams: Construction, installation, operation, and sample processing*, US Dept. of Agriculture, Forest Service, Rocky Mountain Research Station.

Church, M., McLean, D., and Wolcott, J. (1987). "River bed gravels: sampling and analysis." *Sediment Transport in Gravel-Bed Rivers. John Wiley and Sons New York. 1987. p 43-88, 17 fig, 3 tab, 50 ref.*

Conover, W. (1980). "Practical nonparametric statistics John Wiley & Sons." *New York*, 493.

Cope, E., and Yarrow, H. (1875). "Report upon the collections of fishes made in portions of Nevada, Utah, California, Colorado, New Mexico, and Arizona during the years 1871-1874." *Chapter*, 6, 645-703.

CUWCD. (2005). "Red Butte Dam Rehabilitation Project."

Doyle, M. W., Shields, D., Boyd, K. F., Skidmore, P. B., and Dominick, D. W. (2007). "Channel-forming discharge selection in river restoration design." *Journal of Hydraulic Engineering*, 133, 831.

Dunne, T., and Leopold, L. B. (1978). *Water in environmental planning*, WH Freeman & Co.

Einstein, H. A. (1950). "The bed-load function for sediment transportation in open channel flows." *WATER RESOURCES BUILDING*, 43.

JSRIP. (2010). "June Sucker Recovery Implementation Program."

JSRT. (1999). "June Sucker (Chasmistes liorus) Recovery Plan."

Keleher, C. J., Lentsch, L. D., Thompson, C. W., and Resources, U. D. o. W. (1998). *Evaluation of Flow Requirements for June Sucker (Chasmistes Liorus) in the Provo River: An Empirical Approach: Final Report*, Utah Division of Wildlife Resources.

Kondolf, G. M. (1997). "Hungry water: effects of dams and gravel mining on river channels." *ENVIRONMENTAL MANAGEMENT-NEW YORK-*, 21, 533-552.

Meyer-Peter, E., and Müller, R. (1948). "Formulas for bed-load transport." 39–64.

Montgomery, D. R., Abbe, T. B., Buffington, J. M., Peterson, N. P., Schmidt, K. M., and Stock, J. D. (1996). "Distribution of bedrock and alluvial channels in forested mountain drainage basins." *Nature*, 381(6583), 587-589.

Neumann-Mahlkau, P. (1967). "Korngrössenanalyse grobklastischer Sedimente mit Hilfe von Aufschluss-Photographien." *Sedimentology*, 9(3), 245-261.

Parsons, J. R. (2010). "Changes in the Restored Reach of Hobble Creek from 2008-09, Frequency and Duration of Side Pool Connection, and Evaluation of the Interstate 15 Culvert for Fish Passage." Brigham Young University, Provo, Utah.

Petit, F., and Pauquet, A. (1997). "Bankfull discharge recurrence interval in gravel-bed rivers." *Earth Surface Processes and Landforms*, 22(7), 685-693.

Rader, R. (2011). "Personal Communication." A. Dutson, ed., Provo, Utah.

Rosgen, D. L., Silvey, H. L., and Frantila, D. (2006). *Watershed assessment of river stability and sediment supply (WARSSS)*, Wildland Hydrology.

Shirley, D. (1983). "Spawning ecology and larval development of the June sucker." 18-36.

Stamp, M. (2010). "Personal Communication." A. Dutson, ed., Provo, Utah.

Stamp, M., Eddie, T., Olsen, D., and Allred, T. (2009). "Lower Hobble Creek Ecosystem Flow Recommendations." Submitted to: Utah Reclamation Mitigation and Conservation Commission, Logan, Utah.

Thomas, W. A., Copeland, R. R., McComas, D. N., and Raphelt, N. K. (2002). "User's manual for the hydraulic design package for channels (SAM)." *US Army Engineer Research and Development Center, Vicksburg, MS*.

USGS. (2010). "USGS Surface-Water Daily Statistics for the Nation." USGS 10153100 HOBBLE CREEK AT 1650 WEST AT SPRINGVILLE, UTAH.

Wilcock, P. R. (2001). "Toward a practical method for estimating sediment transport rates in gravel bed rivers." *Earth Surface Processes and Landforms*, 26(13), 1395-1408.

Wilcock, P. R., Pitlick, J., Cui, Y., and Station, R. M. R. (2009). *Sediment transport primer: estimating bed-material transport in gravel-bed rivers*, US Dept. of Agriculture, Forest Service, Rocky Mountain Research Station.

Wolman, M. G., and Union, A. G. (1954). "A method of sampling coarse river-bed material."

Wong, M., and Parker, G. (2006). "Reanalysis and correction of bed-load relation of Meyer-Peter and Müller using their own database." *Journal of Hydraulic Engineering*, 132, 1159.

Zimmermann, A., and Church, M. (2001). "Channel morphology, gradient profiles and bed stresses during flood in a step-pool channel." *Geomorphology*, 40(3-4), 311-327.

Appendix A. Supplemental Material for "A Description of the Particle Size Distribution on Hobble Creek from 400 W to Interstate 15"

During the sampling process, photos were taken of the temporary diversion between Reaches 1 and 2, the 1650 W crossing, and the 1000 N diversion dam. These photos are shown in Figure A-1 through Figure A-3.

Figure A-1. Temporary diversion separating Reaches 1 and 2.

Figure A-2. Looking downstream at 1650 W crossing with backwater section.

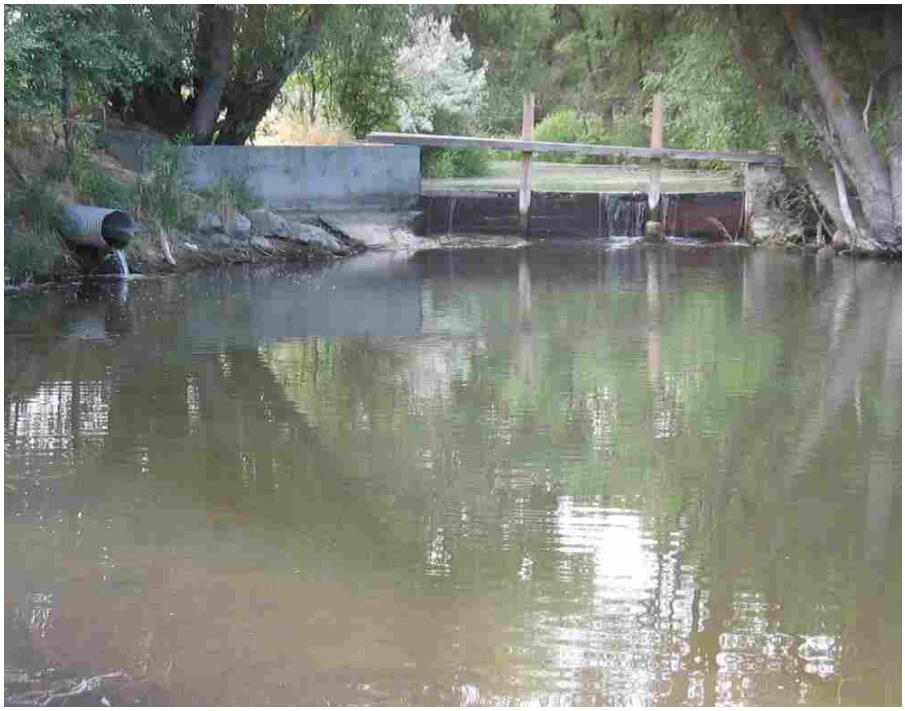

Figure A-3. Diversion dam at 1000 N.

Comparisons were also made for particle size parameters other than D_{50} during the study. They were excluded from the report because the concluding results from all parameters were the same. Table A-1 and Table A-2 show the surface and subsurface values for D_5, D_{16}, D_{25}, D_{50} D_{75}, D_{84}, and D_{95} for each of the reaches. Due to poor sieving techniques, values for D_{75}, D_{84}, and D_{95} could not be determined for every reach.

Table A-1. Parameters for surface particle size distributions.

Reach Number	D_5 [mm]	D_{16} [mm]	D_{25} [mm]	D_{50} [mm]	D_{75} [mm]	D_{84} [mm]	D_{95} [mm]
1	19.44	40.54	48.95	71.29	92.68	104.10	119.99
2	24.92	45.14	56.06	82.96	117.02	134.08	164.17
3	23.04	54.32	65.63	82.60	105.28	115.19	131.65
4	0.25	13.60	27.81	50.26			
5	0.10	0.89	12.84	33.12			
6	0.17	6.65	13.81	34.15			
7	0.08	0.14	0.21	9.63	30.09	39.65	50.43
8	0.16	3.02	10.39	26.02	47.18		
9	0.11	0.24	0.92	19.68	34.08	42.04	
10	0.14	0.65	5.72	17.96	33.17	41.16	
11	0.31	6.49	11.69	25.33	45.92		

Table A-2. Parameters for subsurface particle size distributions.

Reach Number	D_5 [mm]	D_{16} [mm]	D_{25} [mm]	D_{50} [mm]	D_{75} [mm]	D_{84} [mm]	D_{95} [mm]
1	0.38	4.28	10.01	24.42	43.03	50.63	75.20
2	1.21	7.33	13.34	28.29	44.61	50.58	59.46
3	0.51	3.91	8.54	23.72	40.98	48.23	60.81
4	0.30	5.33	11.30	30.13			
5	0.11	0.46	3.16	16.56	34.60	42.25	
6	0.16	0.85	4.23	16.13	31.22	39.16	
7	0.10	0.21	0.47	11.38	29.06	38.33	
8	0.16	0.82	4.80	17.46	32.48	41.42	
9	0.13	0.31	1.04	11.61	24.06	29.82	40.47
10	0.13	0.39	2.25	12.07	25.77	32.62	
11	0.22	2.00	5.14	14.05	26.03	31.73	43.35

Figure A-4 through Figure A-15 show comparisons of location against surface and subsurface D_5, D_{16}, D_{25}, D_{75}, D_{84}, and D_{95}.

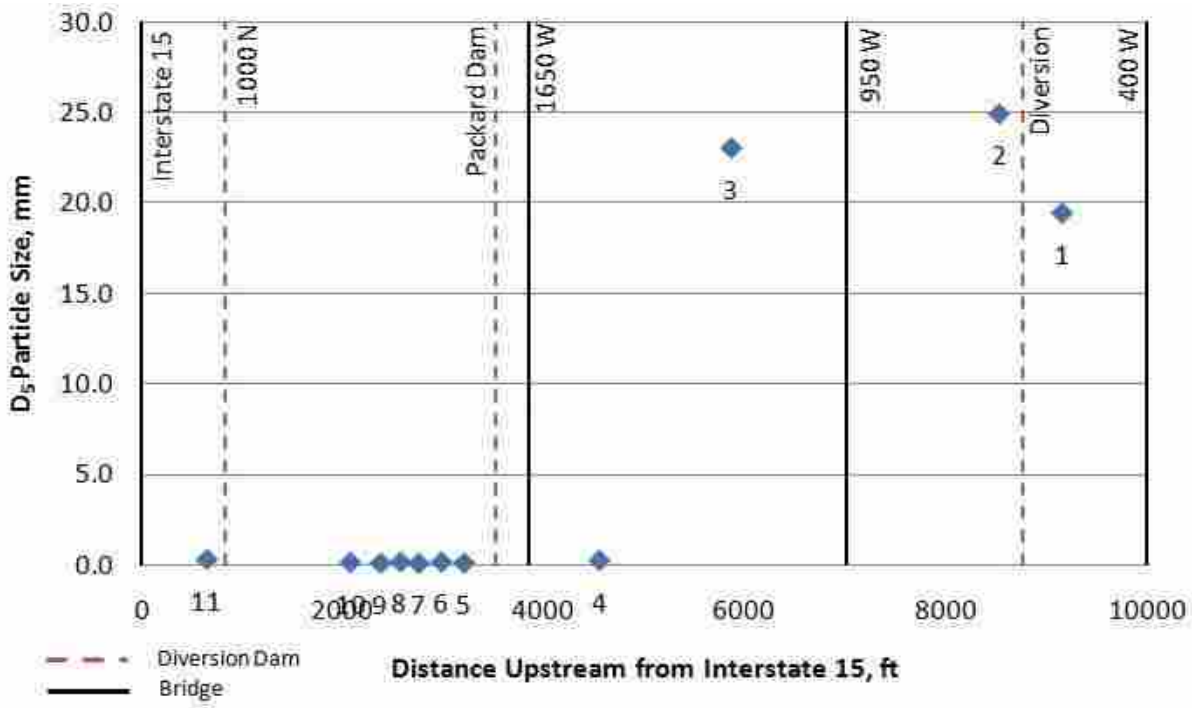

Figure A-4. Surface D_5 vs. distance upstream from Interstate 15 culvert.

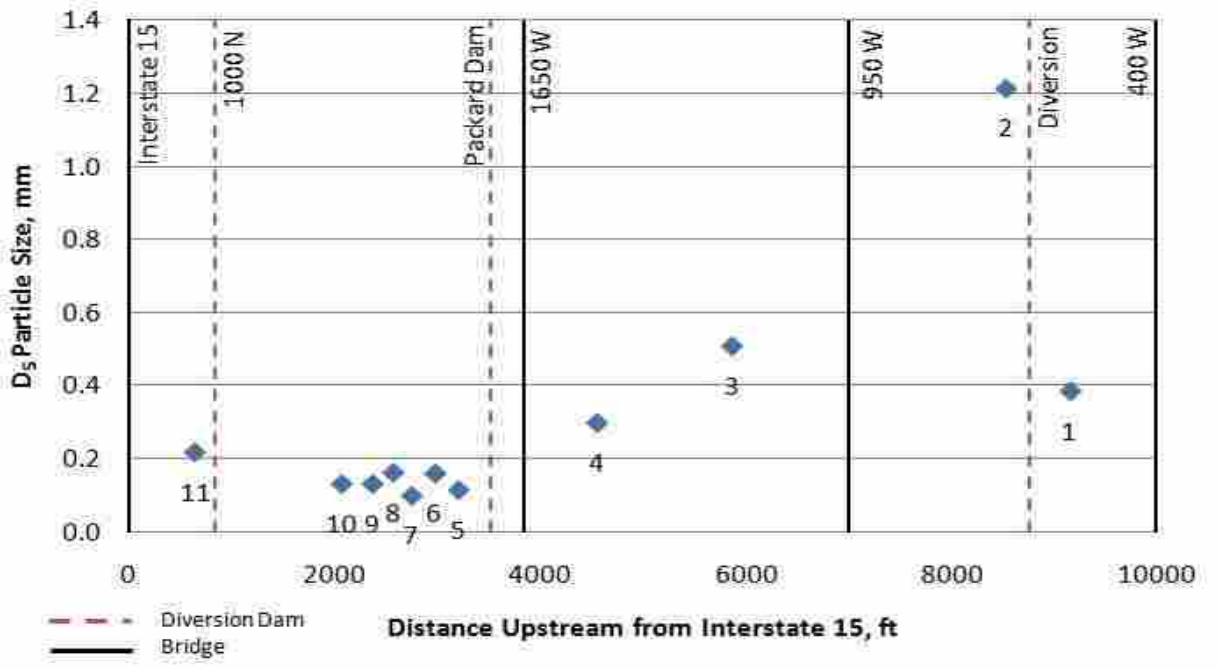

Figure A-5. Subsurface D_5 vs. distance upstream from Interstate 15 culvert.

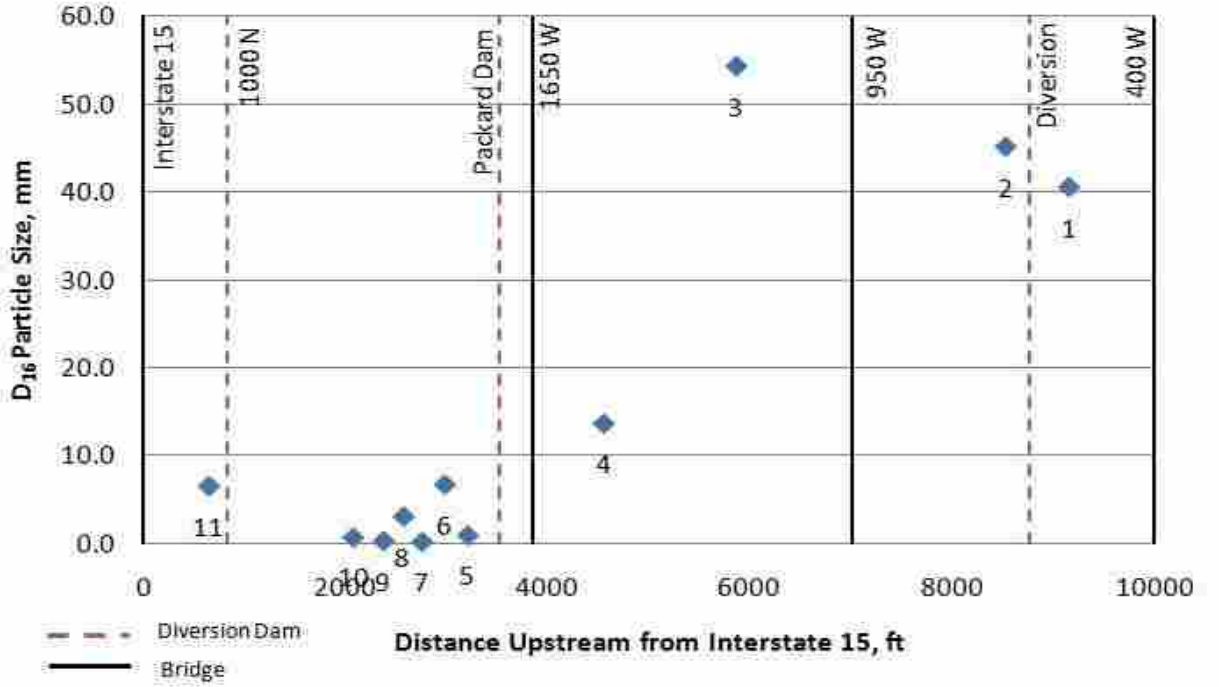

Figure A-6. Surface D_{16} vs. distance upstream from Interstate 15 culvert.

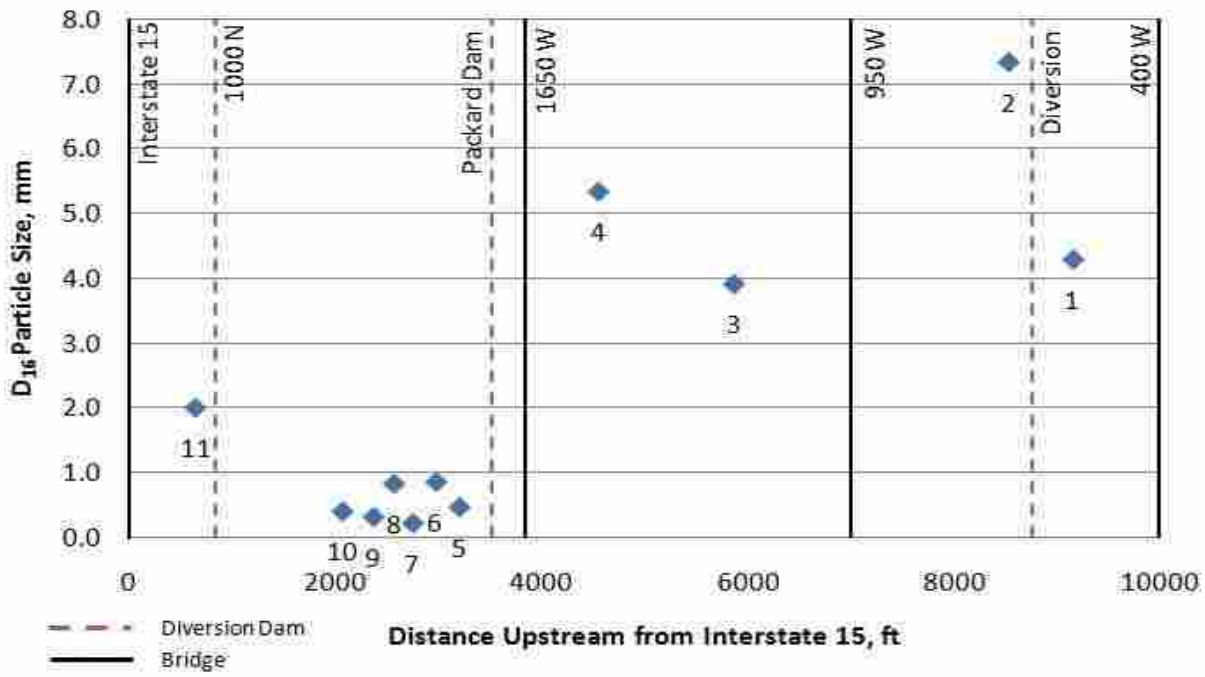

Figure A-7. Subsurface D_{16} vs. distance upstream from Interstate 15 culvert.

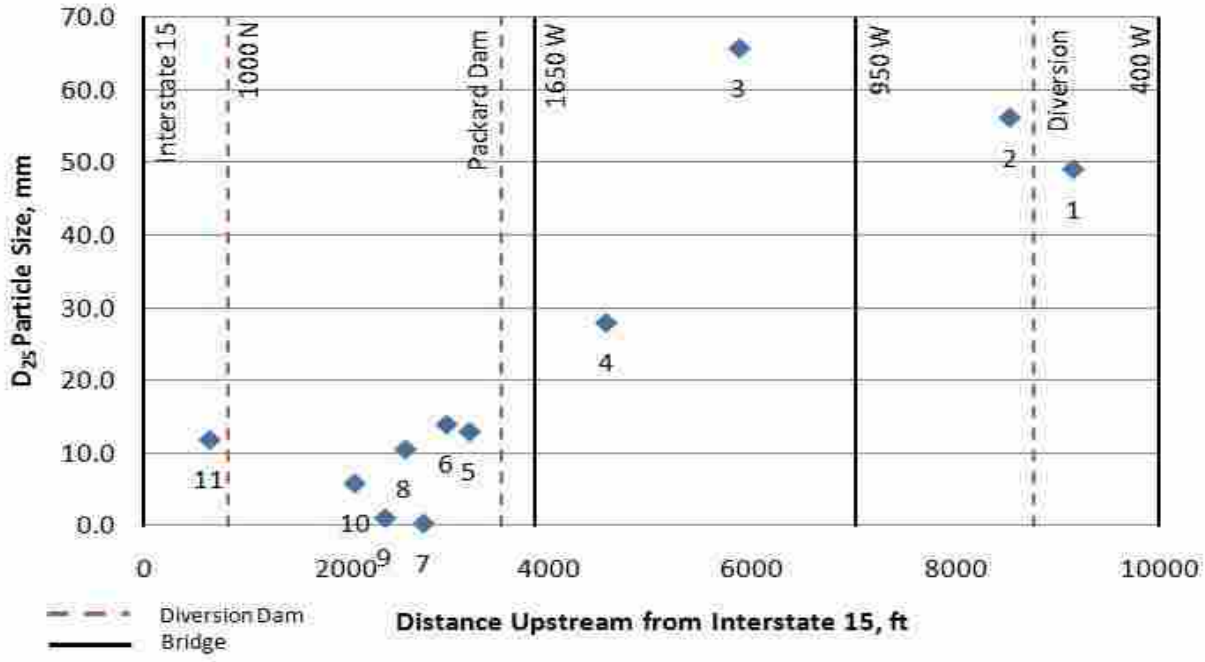

Figure A-8. Surface D_{25} vs. distance upstream from Interstate 15 culvert.

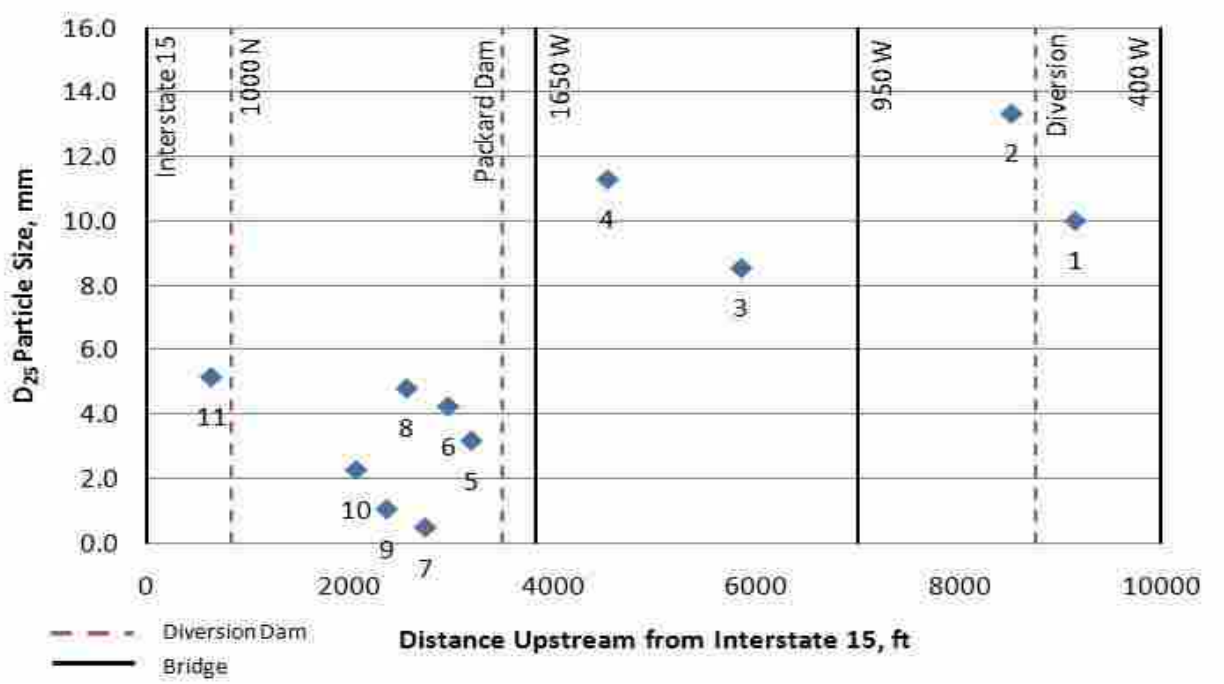

Figure A-9. Subsurface D_{25} vs. distance upstream from Interstate 15 culvert.

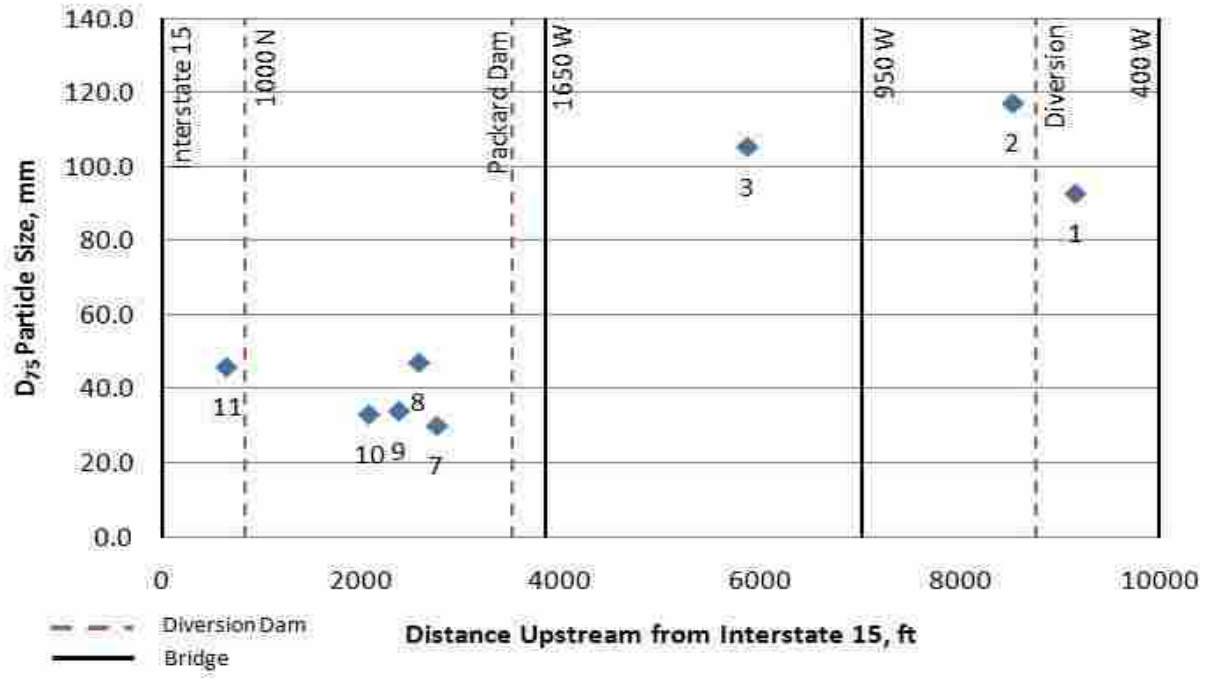

Figure A-10. Surface D_{75} vs. distance upstream from Interstate 15 culvert.

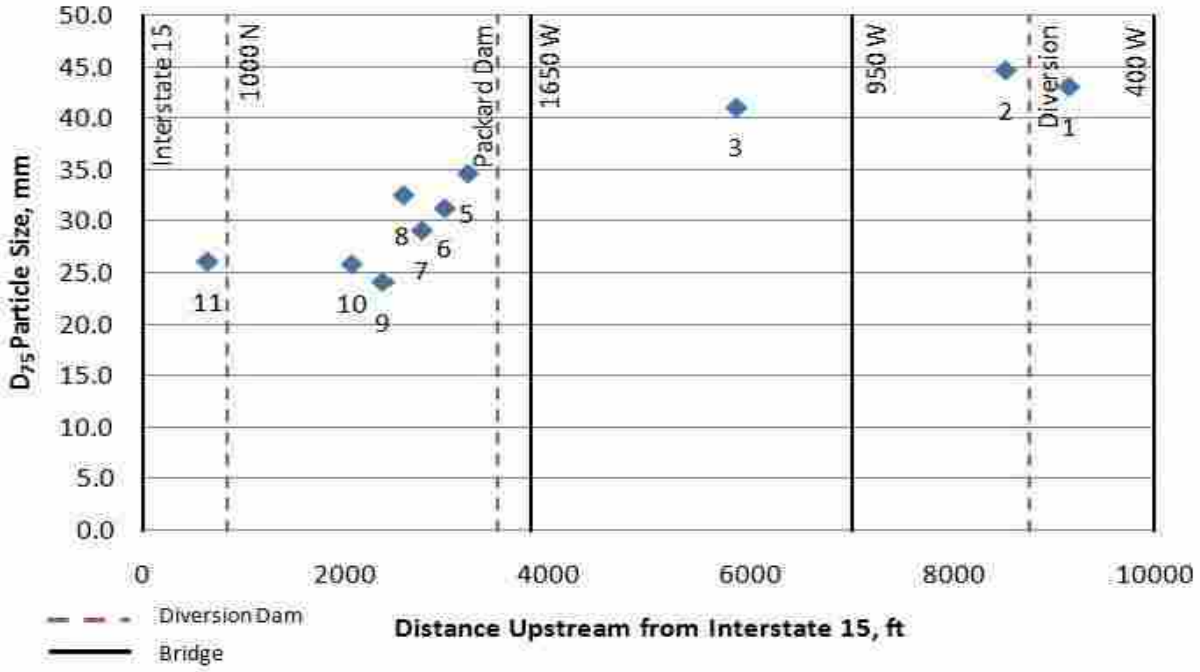

Figure A-11. Subsurface D_{75} vs. distance upstream from Interstate 15 culvert.

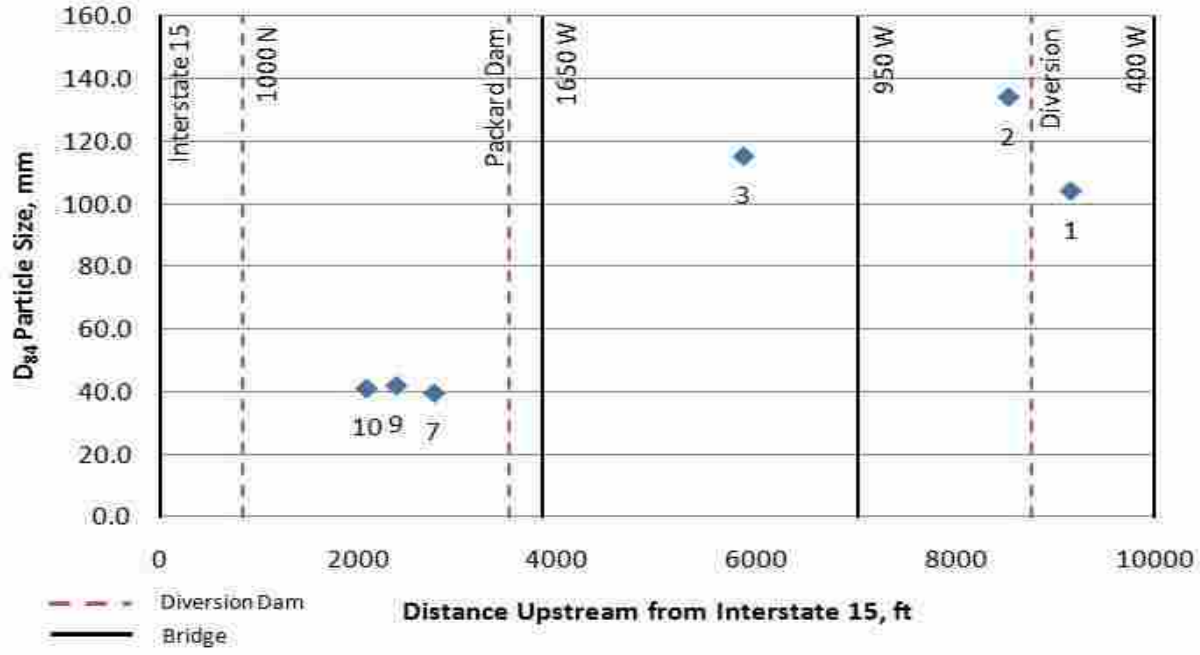

Figure A-12. Surface D_{84} vs. distance upstream from Interstate 15 culvert.

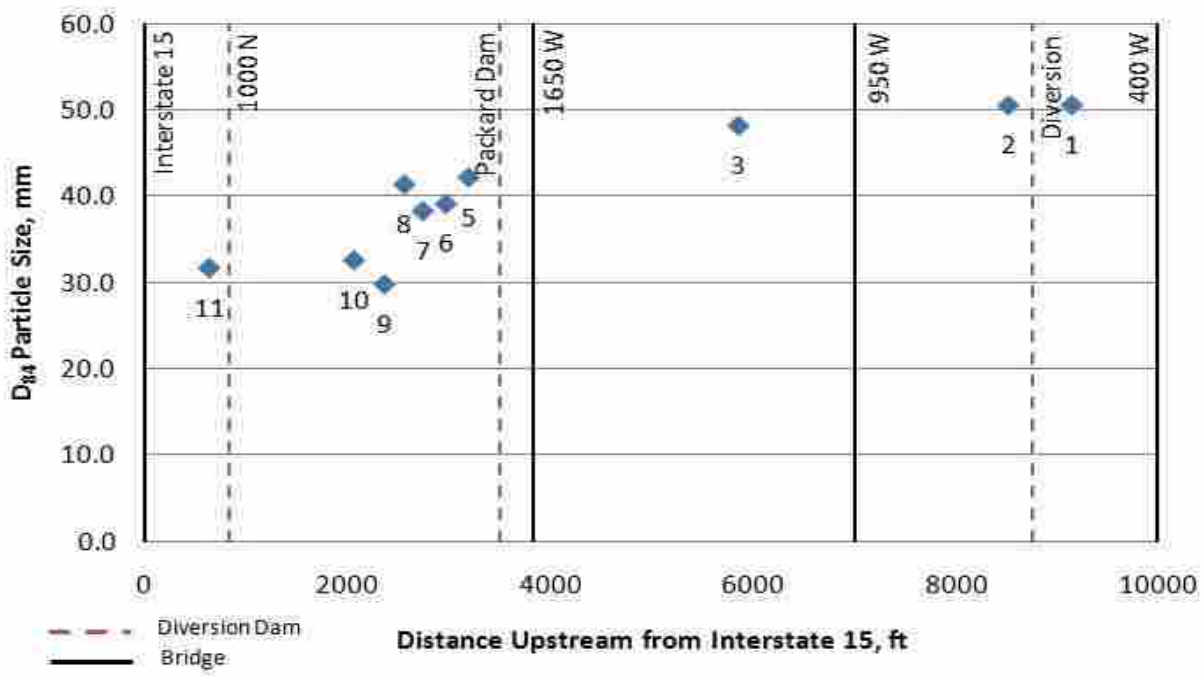

Figure A-13. Subsurface D_{84} vs. distance upstream from Interstate 15 culvert.

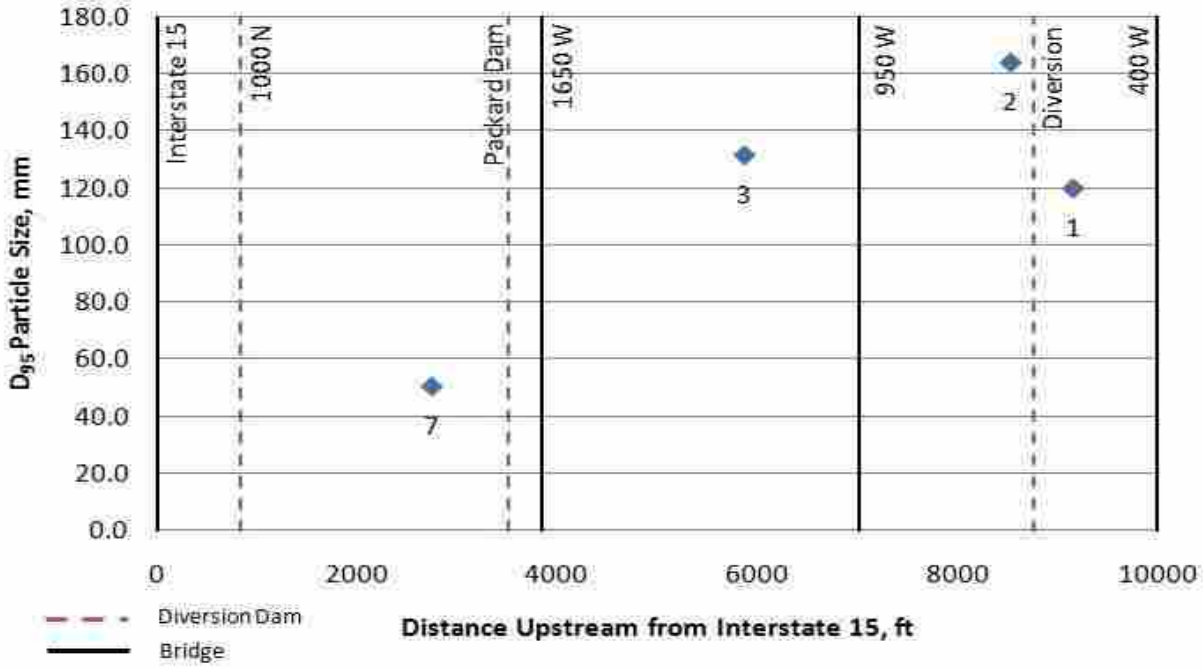

Figure A-14. Surface D_{95} vs. distance upstream from Interstate 15 culvert.

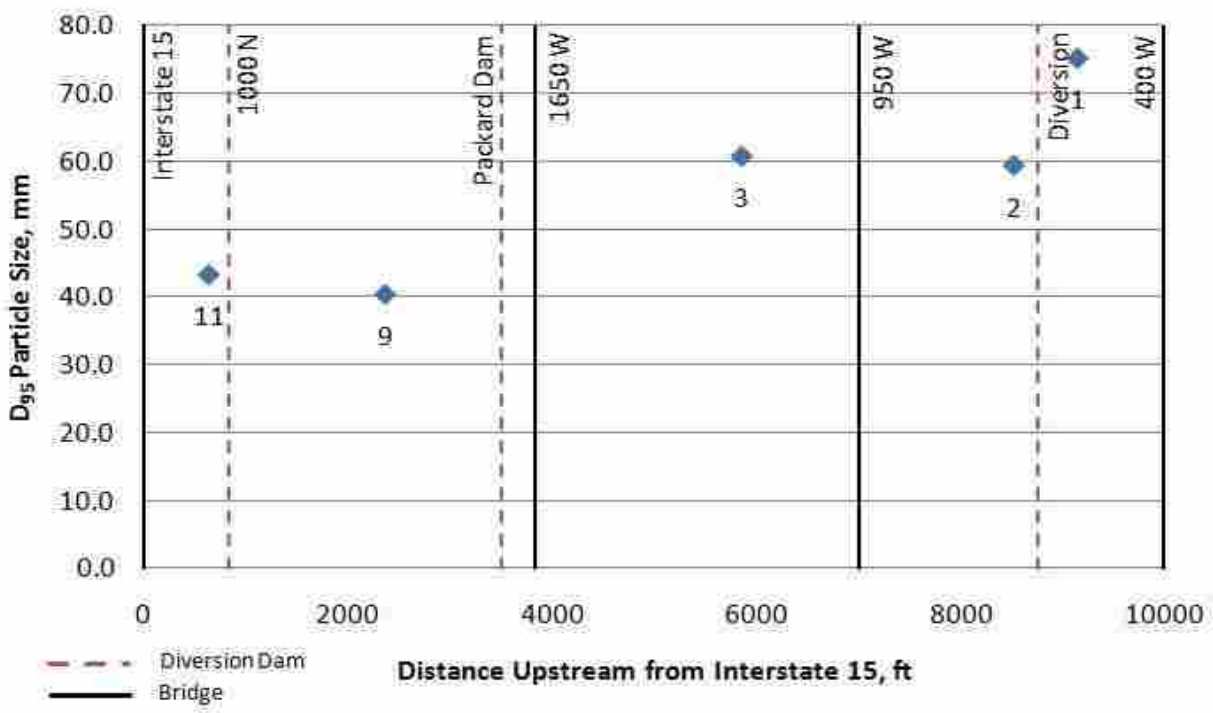

Figure A-15. Subsurface D_{95} vs. distance upstream from Interstate 15 culvert.

Appendix B. Supplemental Material for "A Comparison of Field Data and Predictive Equations for Sediment Transport Rate on Hobble Creek"

Data used for the computations in "A Comparison of Field Data and Predictive Equations for Sediment Transport Rate on Hobble Creek" is summarized in Table 2-1. A more complete set of data that was collected for the study, including cross sections, profile surveys, and particle size distributions, can be found here.

Cross sections for each site were obtained during discharge gaging and are shown here in Figure B-1 through Figure B-3.

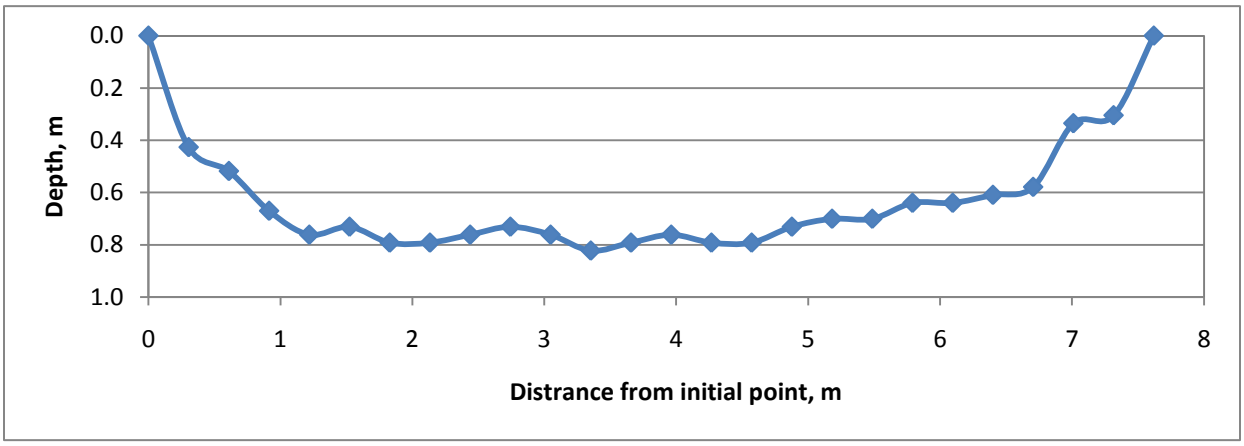

Figure B-1. Site 1 cross section.

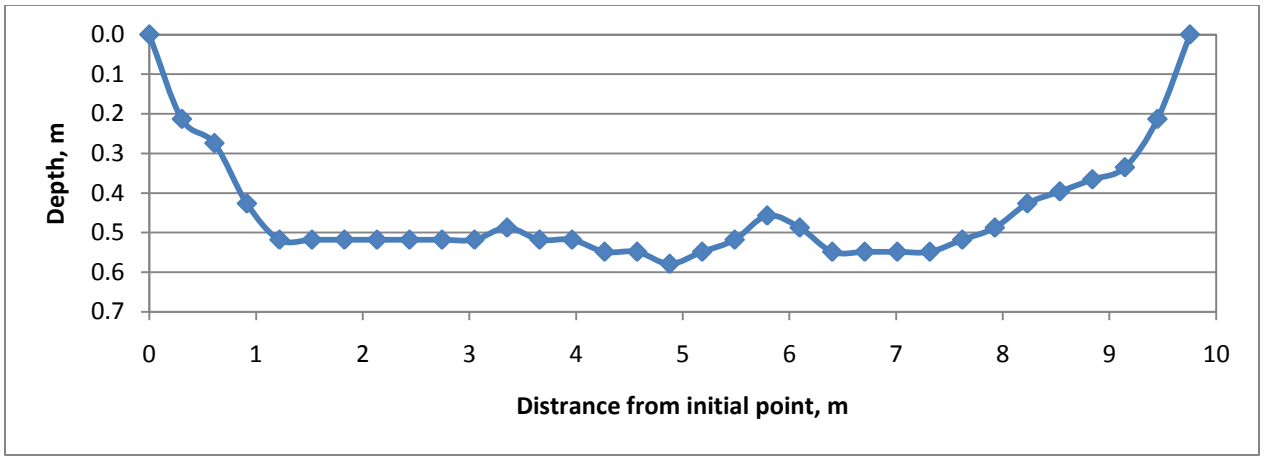

Figure B-2. Site 2 cross section.

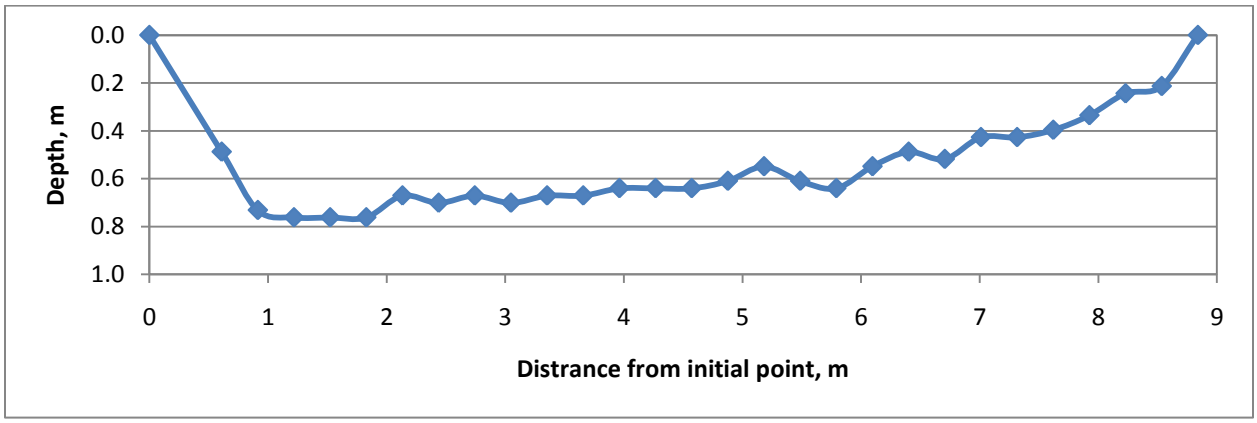

Figure B-3. Site 3 cross section.

A profile survey for the vicinity of each site is shown in Figure B-4 through Figure B-6. Riffle tops, diversions, culverts, and site locations are shown on each profile as well as a line representing the slope used for each site.

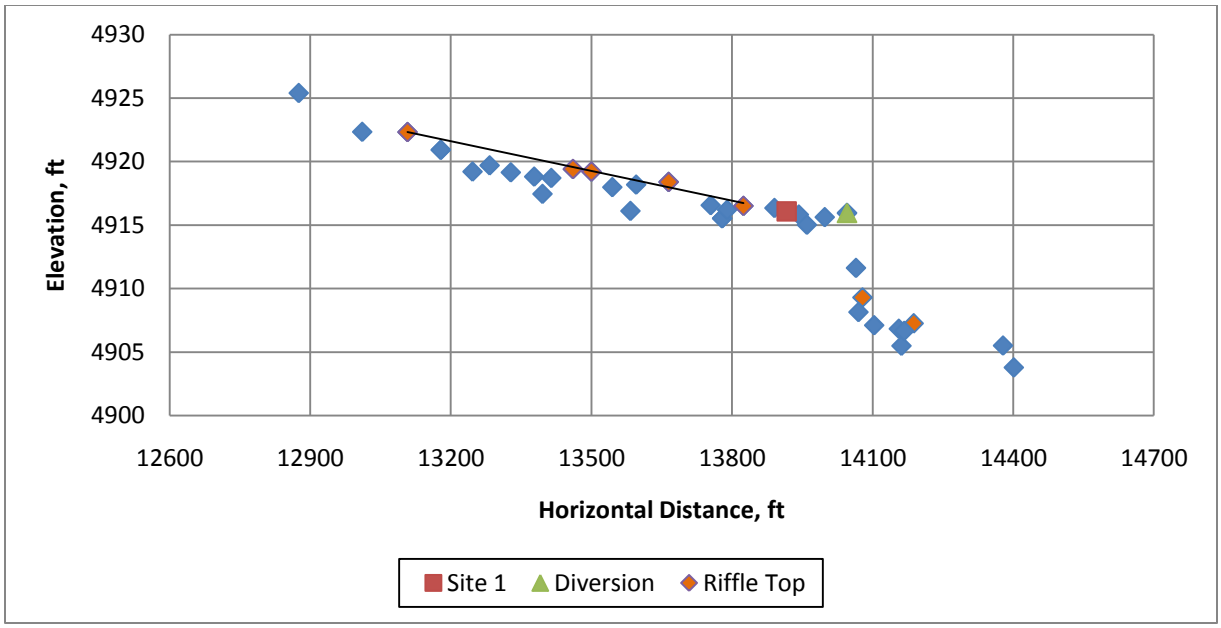

Figure B-4. Profile survey of Site 1.

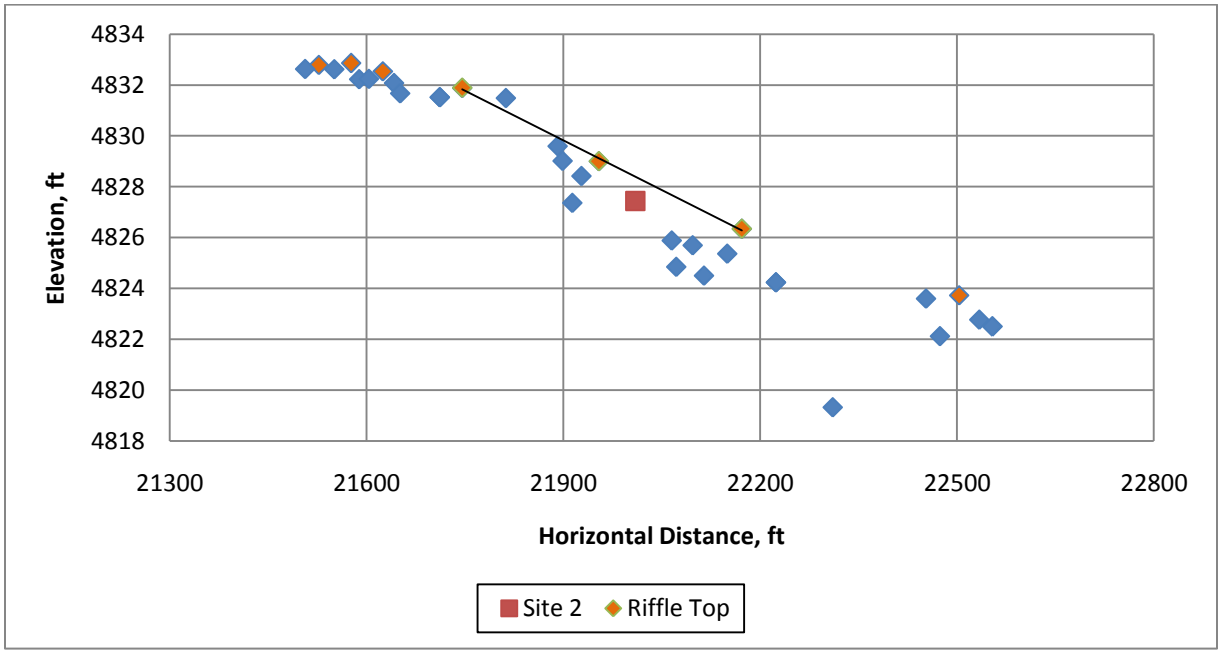

Figure B-5. Profile survey of Site 2.

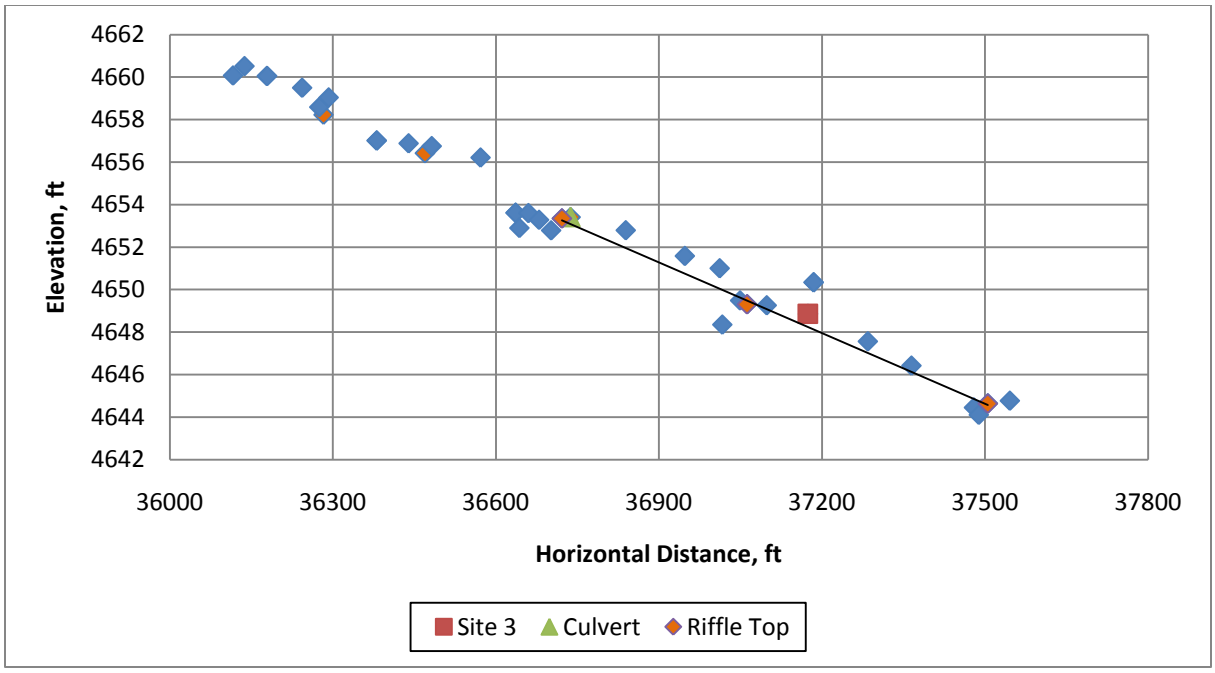

Figure B-6. Profile survey of Site 3.

Particle size parameters were required for the MPM, Wilcock, and Bathurst models. Surface particle size distributions were created from pebbles counts done at each site. Methods for the pebble counts came from Bunte and Abt (2001). Subsurface particle size distributions were created from volumetric samples obtained at each site. Figure B-7 through Figure B-12 show the surface and subsurface particle size distributions for each site. Figure B-13 through Figure B-15 are photographs of the surface and exposed subsurface at each site where subsurface volumetric samples were obtained.

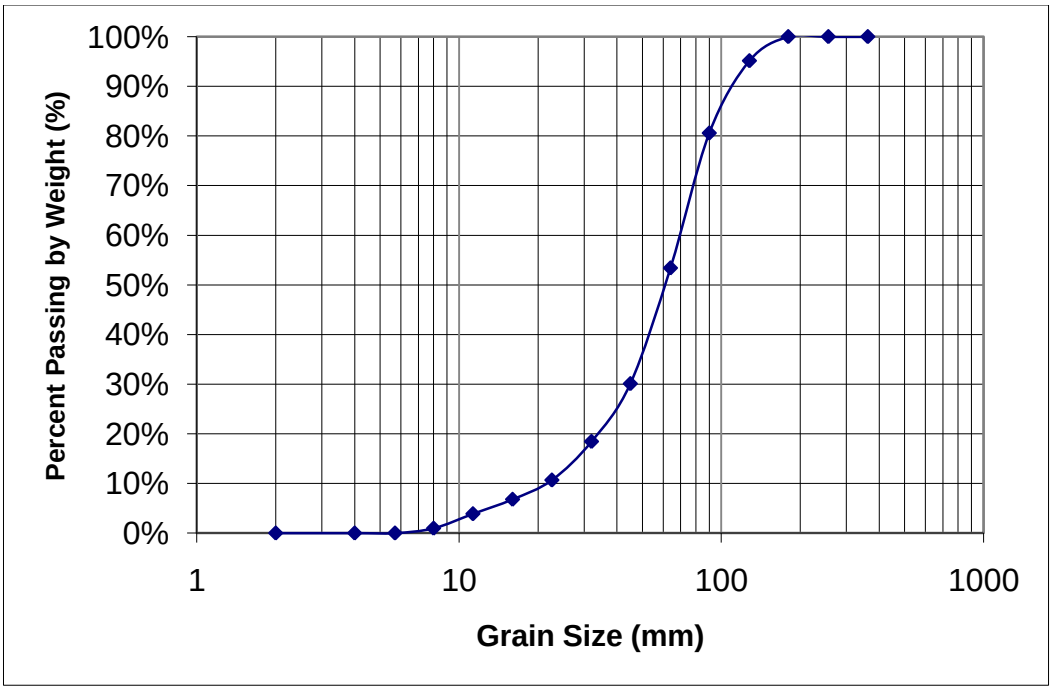

Figure B-7. Surface particle size distribution for Site 1.

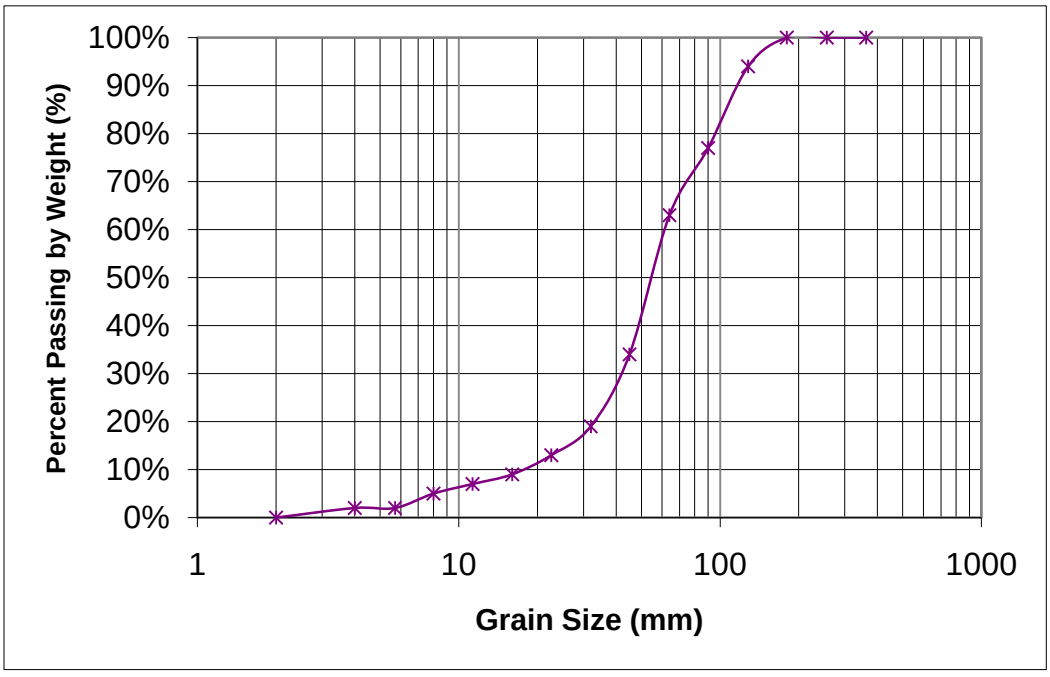

Figure B-8. Surface particle size distribution for Site 2.

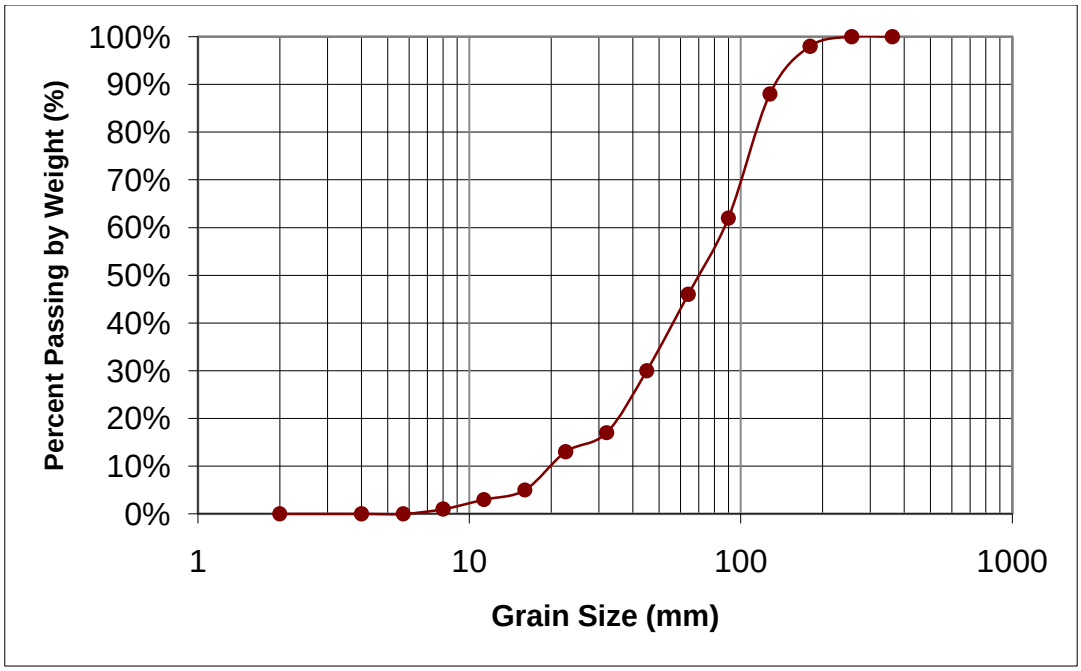

Figure B-9. Surface particle size distribution for Site 3.

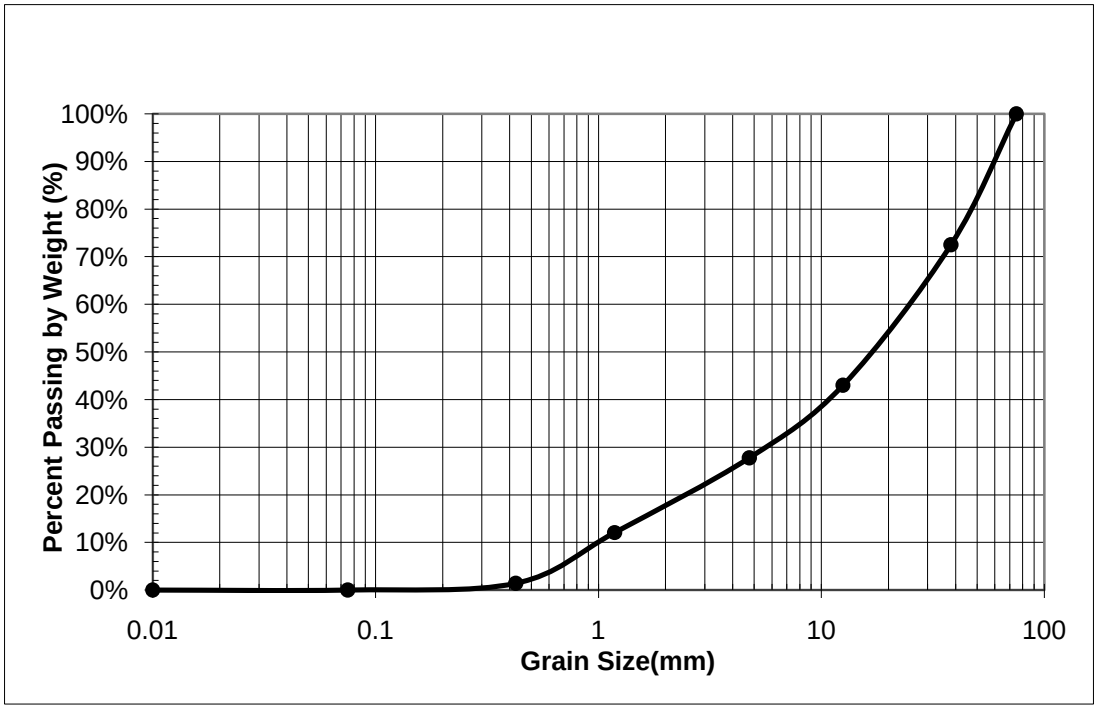

Figure B-10. Subsurface particle size distribution for Site 1.

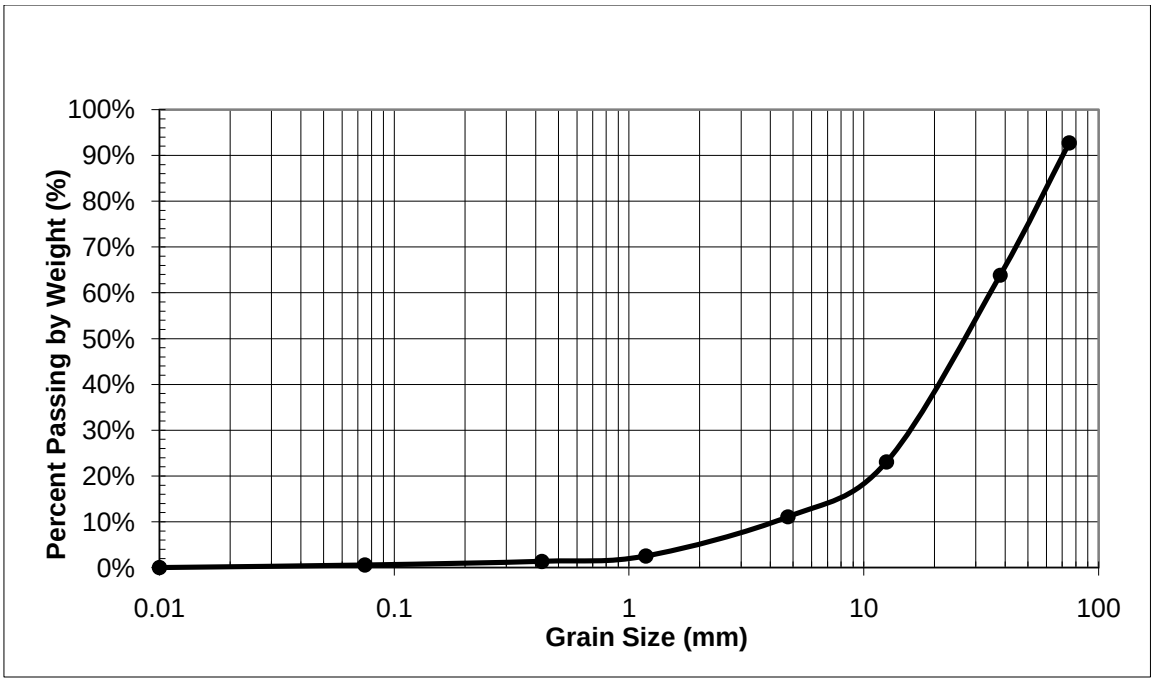

Figure B-11. Subsurface particle size distribution for Site 2.

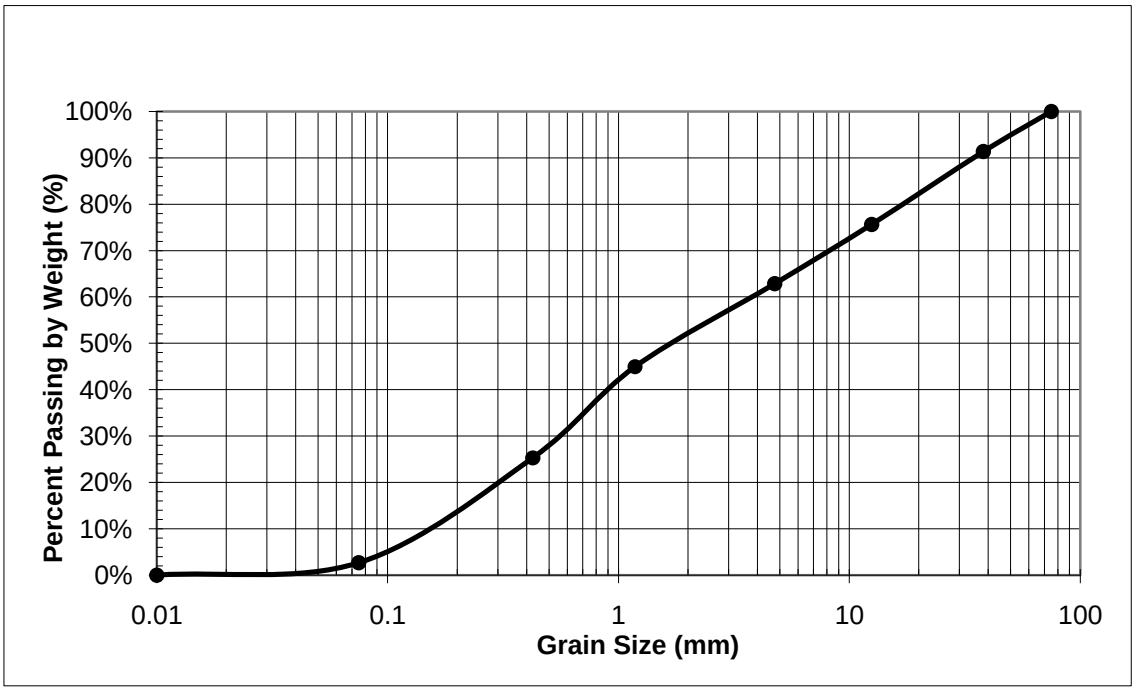

Figure B-12. Subsurface particle size distribution for Site 3.

Figure B-13. Surface and subsurface bed material at Site 1.

Figure B-14. Surface and subsurface bed material at Site 2.

Figure B-15. Surface and subsurface bed material at Site 3.